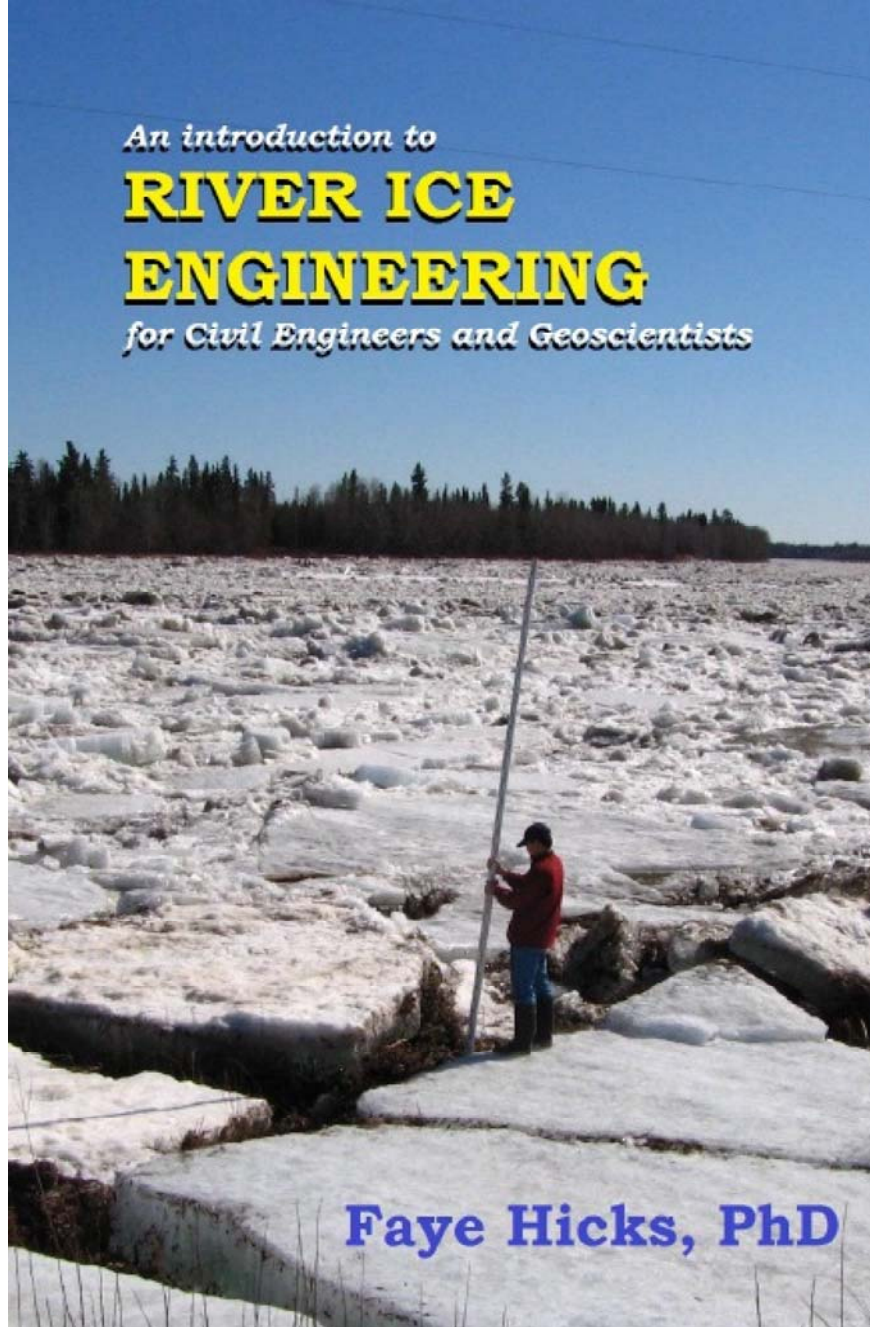


An introduction to
RIVER ICE
ENGINEERING
for Civil Engineers and Geoscientists



Faye Hicks, PhD

An Introduction to
River Ice Engineering
for Civil Engineers and Geoscientists

Faye Hicks, PhD

Copyright © Faye Hicks, 2016

All rights reserved.
ISBN 9781492788638

Cover photo courtesy of Robyn Andrishak

Also by Faye Hicks:
The Weird and Wonderful World of River Ice

Read more by Faye Hicks at:
www.fayehicks.wordpress.com



This book is dedicated to the late Dr. R. (Larry) Gerard, whose enthusiasm for river ice was an inspiration to all who had the honor to know him and to work with him.



Photos courtesy of Martin Jasek.

Author's Notes

River ice affects most rivers in the northern hemisphere for several months each winter and is often responsible for severe floods and infrastructure damage. Consequently, an understanding of river ice processes and hydraulics is essential for civil engineers, and professionals in related disciplines, who work in and around rivers. Despite the fact that ice can occupy our rivers for six months or more each year, very few undergraduate engineering programs offer much instruction on this topic and only a small number of graduate programs offer specialized river ice engineering courses. To help fill that knowledge gap, this book is designed both to provide a supplementary technical reference for senior undergraduate courses related to river engineering and to be used as the basis for the introductory portions of a specialized graduate course in river ice engineering. It is also hoped that practicing professionals will find it a useful reference text.

I'd like to extend my sincere gratitude to the many friends, students, and colleagues who so generously contributed photos and figures for this book. I'd also like to thank my friends and colleagues who kindly agreed to review and edit this book: Dr. Steve Daly, Dr. Brian Morse, Dr. Shawn Clark, Dr. Karen Dow, Dr. Yuntong She, Dr. Vincent McFarlane, Ms. Julia Blackburn, Mr. Cody Kupferschmidt, and Ms. Marsha Cooke. Your time and efforts are greatly appreciated, and your critiques and suggestions improved the book immensely. Thanks also to my dear husband, Leslie Hicks, who gave up several lovely summer afternoons to proof-read the final manuscript. If you find a typo, it's because I missed fixing something, not because he didn't find it. ☺

Finally, thanks to you – the readers. I'd love to hear what you think of this book and/or about your interesting experiences with river ice. You can email me at fayehicks.athor@gmail.com.

I hope you enjoy learning about river ice!

Faye Hicks

August 2016

Table of Contents

1. INTRODUCTION.....	1
2. FREEZE-UP AND WINTER ICE PROCESSES	3
Water Cooling	3
Border Ice Formation	4
Frazil Formation, Flocculation and Floatation	5
Anchor Ice	12
Bridging of Frazil Pans.....	18
Juxtaposed Ice Covers and Frontal Progression	19
Hummocky Ice Covers and Freeze-up Ice Jams	20
Ice Cover Growth and Snow Ice	21
Other Ice Formation Processes	24
Aufeis	24
Hanging Dams	27
Granular Ice	28
Ice Discs	28
Effects of Streamflow Regulation of River Ice	31
Persistent Open Water Downstream of the Dam	31
Effects of Fluctuating Water Levels	32
Summary	33
3. RIVER BREAKUP PROCESSES	34
Thermal Breakup Processes	35
Stage 1 – Snowmelt on the Ice Cover.....	35
Stage 2 – Development of Open Leads	35
Stage 3 – Ice Melt.....	37
Dynamic Breakup Processes	37
Stages 1 and 2 – Snowmelt and Open Lead Development	37
Stage 3 – Overflow from Open Leads	38
Stage 4 –Hinge Cracks and Shorefast Ice Inundation.....	38
Stage 5 – Formation of Transverse Cracks.....	40
Stage 6 – Sheet Ice Accumulations	42
Stage 7 – Ice Clearing.....	42
Stage 8 – Ice Jams	42
Stage 9 – Ice Jam Release and Ice Runs.....	44
Summary	47
4. RIVER ICE PROPERTIES	48
Physical Properties of Frazil Ice.....	48
Frazil Particle Shape and Size	48
Suspended Concentrations of Frazil Ice	49

Frazil Rise Velocity	51
Frazil Pan Thickness and Frazil Slush Porosity	51
Physical Properties of Polycrystalline Ice	53
Sizes of Ice Grains.....	53
Air Bubbles and Impurities	53
Relative Density of Ice	53
Thermal Properties of Ice.....	56
Latent Heat of Melting	56
Specific Heat	56
Thermal Conductivity.....	56
Thermal Diffusivity	57
Summary	57
5. HYDRAULICS OF ICE COVERED CHANNELS.....	58
Velocity Distribution Under a Simple Ice Cover	59
Hydraulic Analyses	60
Steady Gradually Varied Flow Hydraulics.....	60
Composite Roughness Equations	61
Ice Roughness from Velocity Profiles.....	64
Typical Values for Ice Underside Roughness	65
Special Considerations	68
Summary	71
6. QUANTIFYING THERMAL ICE PROCESSES.....	72
Energy Budget Approach	72
Solar Radiation	73
Longwave Radiation.....	75
Evaporation.....	76
Convective Heat Transfer.....	77
Heat Transfer from Other Sources.....	78
Linear Heat Transfer Approach.....	78
Cumulative Degree-Day Approach	80
Comparison of Methods	82
Summary	84
7. ICE JAM FORMATION AND RELEASE.....	85
Ice Jam Formation.....	85
Ice Jam Classification.....	85
Calculating Ice Jam Profiles	89
Equilibrium Ice Jams	95
Ice Jam Release	98
Ice Jam Release Mechanisms	99
Hydraulics of Ice Jam Release Events.....	102
Summary	104

8. ICE JAM FLOOD MITIGATION	106
Non-Structural Flood Mitigation Techniques	106
Floodplain Management and Flood Proofing	106
Flood Forecasting	107
Ice Cutting, Breaking, and Blasting	110
Structural Flood Mitigation Techniques.....	114
Dikes and Floodwalls	114
Channel Modifications	115
Ice Control Structures (ICS).....	115
Reactive Flood Mitigation Techniques	117
Summary	118
9. DESIGNING AND IMPLEMENTING A SAFE FIELD PROGRAM	
.....	119
Basic Data Needs.....	120
Geomorphological Data.....	120
Meteorological Data	120
Hydrometric Data	123
Ice Process Data.....	129
Summary.....	140
List of Variables	141
Cited References.....	145
Index.....	157

Chapter 1

INTRODUCTION

River ice is an important aspect of winter hydrology. Ice affects the hydraulics of the river flow and its presence can also have important implications for water quality. Perhaps most important though, the formation and release of ice floe accumulations, known as ‘ice jams’, can severely obstruct river flow, often causing floods (e.g. Figure 1.1).



Figure 1.1 Ice jam flood during 2008 breakup on the Hay River, NWT. This photo was taken looking upstream along the ice jam and shows the flooding in the adjacent old village of the Kátl'odeeche First Nation. (*Photo by F. Hicks.*)

Ice can be beneficial as well; for example, ice bridges across rivers provide a means of winter crossing where bridges are not economically viable. This is an especially important means of transportation in Canada's north. Figure 1.2 shows an example of an ice bridge crossing on the Mackenzie River in northern Canada.



Figure 1.2 Example of an ice bridge crossing. (*Photo by F. Hicks.*)

The first step in understanding river ice is to become familiar with the various processes and ice types that occur as ice forms on natural rivers in early winter, then later melts and clears away when spring arrives. These topics are covered in Chapters 2 and 3. It is also important to understand and to be able to quantify the various properties of ice that are of engineering relevance and this is the subject of Chapter 4. Even a simple, continuous ice cover has an important influence on flow velocities and water levels; Chapter 5 presents the basic hydraulics of this simple case. In order to predict the formation and decay of ice, we must be able to quantify these thermal processes; Chapter 6 presents and compares the three most common approaches to this problem. Changing flow rates and water levels can precipitate dynamic ice processes such as ice breaking, ice runs, and ice jams; Chapter 7 introduces this topic and details the methodology used to calculate ice jam profiles. Ice jam flood mitigation techniques are presented in Chapter 8. Finally, Chapter 9 presents information on how to design, and safely implement, a field monitoring program. The mechanical aspects of river ice (e.g. load bearing capacity of ice and ice forces on structures) are not covered in this book. Ashton (1986) presents an excellent introduction to the former.

Although it is not absolutely essential to read the chapters in sequence, they are intended to form a logical progression in building this basic knowledge of river ice. At the least, it is strongly recommended that you read Chapters 2 and 3 before any other chapters. Also, it will be very useful to read the chapter on hydraulics (Chapter 5) before getting into the details of ice jam profile calculations in Chapter 7. So, let's go ahead and get started!

Chapter 2

FREEZE-UP AND WINTER ICE PROCESSES

The process by which an ice cover in a river forms and evolves is substantially different from that on lakes in most aspects. The reason for this is that, away from the banks, rivers typically involve non-negligible flow velocities and substantial fluid turbulence. Consequently, flow hydraulics play a significant role in river ice cover formation, as do meteorological conditions, resulting in a plethora of strange and wonderful phenomena. This chapter provides an introduction to the various stages of ice cover development, as well as descriptions of the various types of ice observed in natural rivers.

Water Cooling

Before ice can form in a river, the river water must first cool to 0°C. The rate at which water cools is dependent upon its 'specific heat', defined as the amount of energy required to heat a unit mass of water (for example 1 kg) by 1°C. For the cooling process, the primary cause of heat loss is typically heat transfer from the water to cooler air above. Snow falling directly on the water surface can also contribute significantly to its cooling, as can heat loss to the cold ground at the river banks. The emission of long-wave radiation from the river water also causes a net loss of heat energy, while groundwater influx to the river can sometimes be a significant contributor of heat, mitigating the cooling process. Net incoming solar radiation can be efficiently absorbed by the water, because of water's low reflectance. However, during the freeze-up period, the heat contribution of the sun is typically quite small in comparison to the cooling effect of cold air temperatures.

Except for the very shallow slow moving portions of the flow near the banks, or tidal reaches, most river flows are relatively well mixed throughout their depth because of fluid turbulence. Consequently, the water temperature tends to be uniform through the flow depth and across the turbulent portion of the river channel.

Border Ice Formation

Skim ice is typically the first ice seen on northern rivers each winter (Figure 2.1). It forms on the surface of the relatively calm, slow-moving, shallow water along the river banks and around the edges of islands. Skim ice can also form around the edges of sand and gravel bars.



Figure 2.1 Skim ice observed on the Kananaskis River in Alberta.
(Photo courtesy of S. Emmer, J. Nafziger, and V. McFarlane.)

Skim ice coverage increases in extent, growing out from the banks to form border ice (Figure 2.2). Subsequent ice growth is predominantly thermal in nature, continuing in two ways. Ice grows laterally out into the flow, primarily as a result of heat loss through the ice and into the banks. The border ice also thickens, due to heat loss through the ice cover to the cold overlying air. The resulting border ice thickness is therefore typically greatest at the bank. The rate of thickness decrease out from the bank depends upon the relative rates of growth (laterally and vertically).



Figure 2.2 Border ice is typically the first type of ice that forms on a river.
(Photo courtesy of T. Ghobrial.)

To date, there have been relatively few studies documenting border ice growth rates and, consequently, the available models for predicting border ice growth rates are relatively approximate and typically require site specific calibration. Clark (2013) provides an excellent review of these earlier studies, noting that the two most significant parameters affecting the lateral growth rate of border ice are the rate of heat loss and the flow velocity adjacent to the border ice. Lateral growth rates have been found to be directly proportional to the rate of heat loss (almost linear in some cases) and inversely proportional to flow velocity. Lateral growth rates have been found to diminish noticeably for velocities in excess of about 1.2 m/s (Newbury 1968, Clark 2013).

Frazil Formation, Flocculation and Floatation

In the turbulent, faster moving portion of the river, where the flow is well mixed, ice is created in the form of *frazil ice* particles. These are small discs of ice ranging in size from less than 0.1 mm up to a few mm in diameter. The photograph in Figure 2.3 shows examples of frazil particles photographed in the lab.

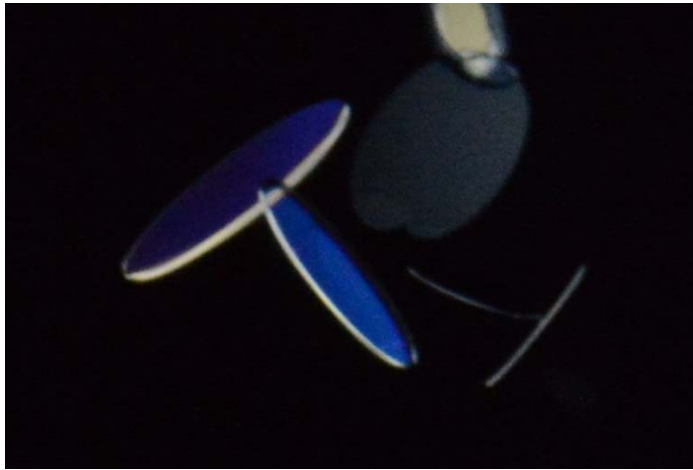


Figure 2.3 Examples of frazil ice particles grown in a lab; the largest one shown is 2.5 mm in diameter and the typical diameter to thickness ratio is ~ 11 .
(Photo courtesy of V. McFarlane.)

The formation (or primary nucleation) of ice particles can occur in two ways, by homogeneous nucleation in pure water and by heterogeneous nucleation on impurities in the water (such as tiny particles of dust, sediment, or organic material). However, homogeneous nucleation requires water supercooling of -30°C to -40°C (Michel 1978). Heterogeneous nucleation on suspended solids (such as clay or organic particles) has been observed to require supercooling in the order of -1°C to -2°C in the lab (Roberts 1979, as reported by Ashton 1986). However, these levels of supercooling are not observed in natural rivers. Frazil ice is typically observed to form at supercooling levels of about -0.06°C or less (often only a few one-hundredths of a degree below zero). According to Daly (2013) the only feasible explanation for this is that frazil particle formation in natural rivers occurs as a result of secondary nucleation on existing ice particles. The source of this ice is generally believed to be *seed crystals* falling into the water, for example from snow and sleet, crystallization of water vapor rising from the river, or from frozen droplets of water created as a result of breaking waves or splashing (Daly 2013a). Once these seed crystals have been introduced to the river and begin to grow in size, they can be fractured by collisions, multiplying the number of ice particles in the flow, and creating additional secondary nucleation particles. Because turbulence increases the likelihood of these collisions, the number of frazil particles produced is generally observed to be greater when turbulence is higher.

Figure 2.4 shows an example of a typical water supercooling curve from a laboratory experiment. In this example, the temperature initially decreases linearly because the cold room in which the experiment was conducted was held at a constant (sub-zero) temperature. In this case, the water actually supercooled to almost -0.1°C , during which period frazil particles started forming. The phase change from water to ice releases the latent heat of fusion which in turn warms the water slightly, as seen by the brief period of increasing water temperature. Eventually, the rate of heat production due to ice formation balances the rate of heat loss (due to the sub-zero temperatures in the cold room) and a consistent residual (supercooled) water temperature is seen after this time.

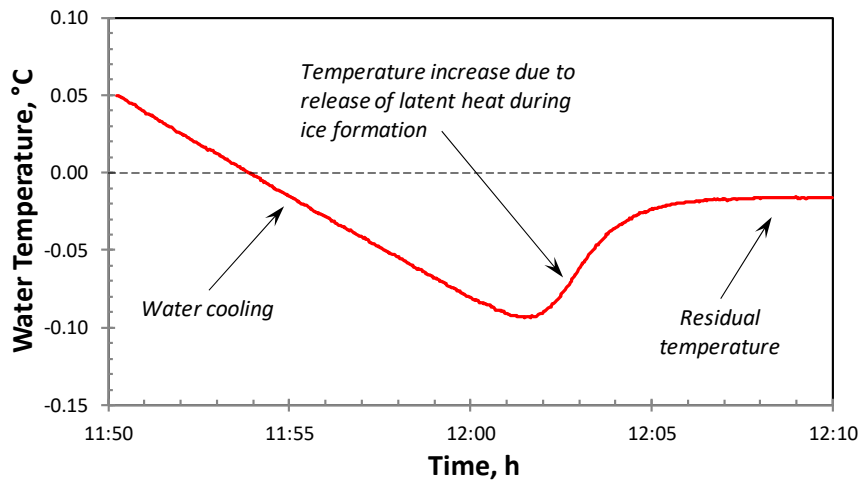


Figure 2.4 Example supercooling curve measured during frazil formation in the laboratory. (Figure courtesy of V. McFarlane.)

Frazil particles demonstrate a very adhesive-like behavior in supercooled water¹, in that they readily freeze to each other. As a result, frazil particles tend to flocculate in supercooled water (Figures 2.5 and 2.6). Frazil ice in this state is termed *active frazil* and it readily attaches to bed sediments, underwater vegetation, and screens and trash racks, as well.

¹ Daly (2013a) provides an excellent explanation of why this occurs.



Figure 2.5 Frazil floc observed in the laboratory.
(*Photo courtesy of T. Ghobrial.*)

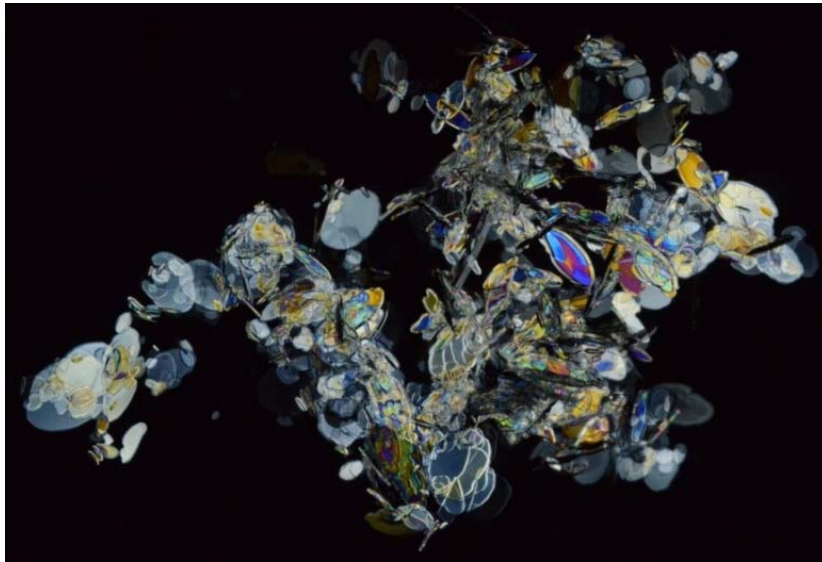


Figure 2.6 Frazil floc photographed under polarized light, exposing the individual frazil particles – vertical dimension of image is ~2.5 cm.
(*Photo courtesy of V. McFarlane.*)

Freeze-up and Winter Ice Processes

Figure 2.7 illustrates these various stages in the freeze-up process in turbulent river flow, as the water first cools, then forms frazil particles, and flocculates into balls of slush. Once these balls of frazil slush are large enough for their buoyancy to overcome the entraining effects of fluid turbulence, they rise to the water surface (Figure 2.8) where the exposed portion freezes to form *frazil pans*, also known as *pancake ice* or *pan ice* (Figure 2.9).

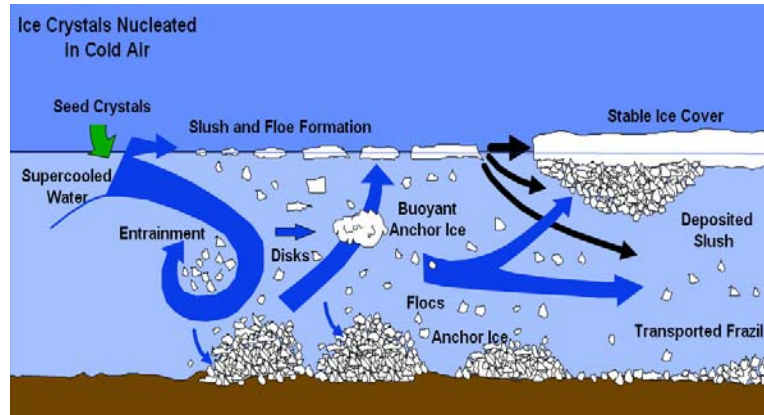


Figure 2.7 Stages in the formation and evolution of frazil ice.
(Figure courtesy of S. Daly).



Figure 2.8 Frazil slush observed on the Bow River in Alberta.
(Photo courtesy of M. Loewen.)



Figure 2.9 Frazil pans observed on the North Saskatchewan River in Alberta.
(Photo by F. Hicks.)

Frazil pans drift downstream with the flow, and tend to collide with each other, particularly as the surface concentrations of frazil pans increase. This creates the rough (bright white) upturned edges seen in Figure 2.9. Frazil pans may also freeze together edge to edge, or when they slide under/over each other, particularly in river bends where centrifugal forces push them towards the outside bank. These groupings of frazil pans are called *frazil rafts* (Figure 2.10). Collisions can also tip the frazil pans and rafts, allowing them to take on surface water that later freezes (Figure 2.11).



Figure 2.10 Frazil pans and rafts observed on the North Saskatchewan River in Alberta. (Photo courtesy of T. Ghobrial.)



Figure 2.11 Frazil raft after tipping and taking on surface water.
(Photo courtesy of T. Ghobrial.)

Some of the frazil particles or pans may also collect along the border ice. This increases the border ice encroachment on the channel, and is termed *buttering*. The lateral extent of border ice can be increased substantially by this process (Figure 2.12), but there is a limit, as appreciable surface concentrations of frazil pans also tend to wear away at the stationary ice.

Daly (2013a) provides an excellent, comprehensive analytical explanation of frazil ice formation and evolution processes for those wanting a more in-depth review of this topic.

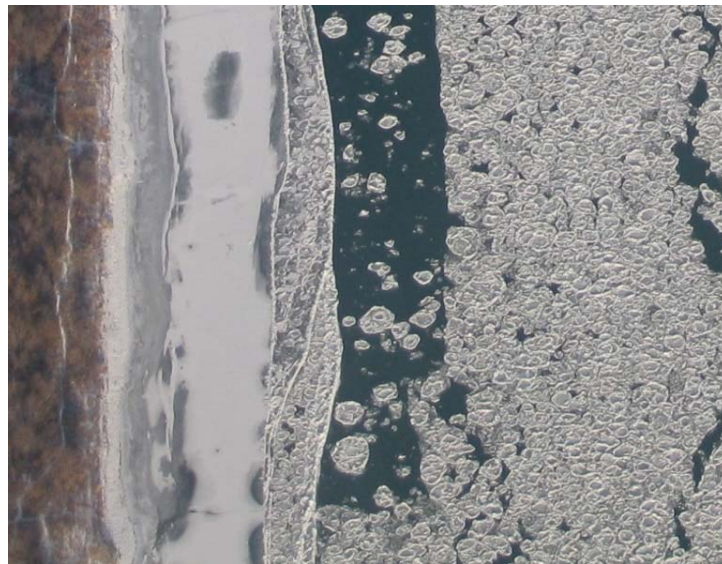


Figure 2.12 Frazil pans frozen to the border ice on the North Saskatchewan River in Alberta. (Photo courtesy of T. Ghobrial and M. Loewen.)

Anchor Ice

In some cases, frazil ice may adhere to rocks on the river bed and, if the rocks are sufficiently large to resist the ice buoyancy, the ice will be held (or anchored) on the bed, forming *anchor ice* (Figures 2.13 and 2.14). Anchor ice deposits can increase in size as a result of additional frazil ice accumulation as well as by the growth of frazil particles in-situ.



Figure 2.13 Anchor ice observed on the Kananaskis River in Alberta.
(*Photo courtesy of S. Emmer.*)



Figure 2.14 Underwater view of anchor ice observed on the Kananaskis River in Alberta. (*Photos courtesy of S. Emmer.*)

Freeze-up and Winter Ice Processes

Anchor ice always starts by deposition. Once deposited, the crystals can grow in size through heat transfer from the supercooled water. The form of anchor ice when deposited is influenced by the water velocity. Kempema et al. (e.g. 2001, 2008a, 2009) have documented anchor ice forming on bed material over a complete range in sizes from sand (Figure 2.15) to boulders, and in relatively calm water. Large crystals (up to 150 mm in diameter) have been observed (Figure 2.16).

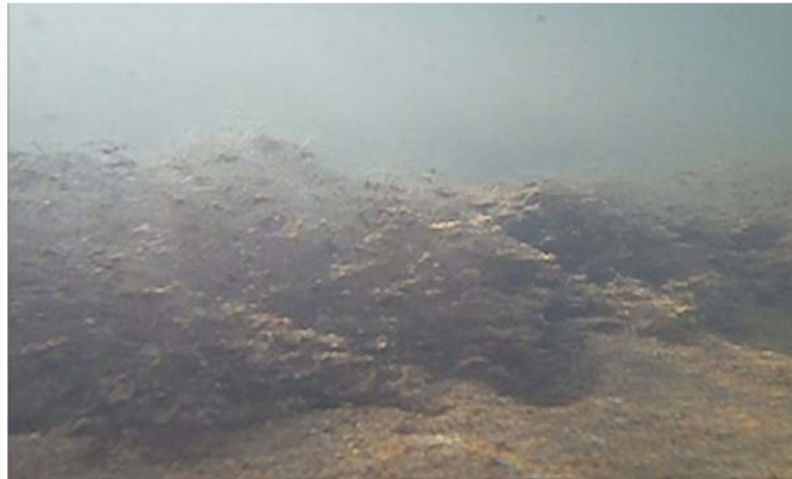


Figure 2.15 Anchor ice observed on a sand bed. Note that hydraulically transported sand is trapped in the ice, as well. (Photo courtesy of E. Kempema.)



Figure 2.16 Large anchor ice crystals from the Laramie River in Wyoming. (Photo courtesy of E. Kempema.)

Anchor ice can accumulate in large quantities and, particularly in small streams, this can result in the formation of anchor ice dams that significantly affect the river's hydraulics (Figures 2.17 and 2.18). Anchor ice can also fill river pools; this can take up valuable fish habitat (Figure 2.19) and can even cause flooding. In some cases, anchor ice can have a beneficial effect on fish habitat; by increasing water levels and reducing velocities upstream, they can encourage the formation of a protective ice cover.



Figure 2.17 Anchor ice dam observed on a small tributary of the Kananaskis River in Alberta. *(Photo courtesy of V. McFarlane.)*



Figure 2.18 Anchor ice dam observed on the Kananaskis River in Alberta. *(Photo courtesy of S. Emmer.)*



Figure 2.19 Anchor ice observed on the Ram River in Alberta.
(*Photo courtesy of R. Brown.*)

Some ice particles may only briefly adhere to the bed before accumulating in sufficient quantities to become buoyant enough to float to the surface, carrying particles of the bed material with it. Consequently, the frazil slush layer underlying the frazil pans may contain sediment particles. These will be apparent in any ice core samples extracted from the river ice cover (Figure 2.20). Vegetation can also be incorporated into the ice cover in this manner (Figure 2.21).



Figure 2.20 Example ice core sample showing fine sediment particles picked up by the frazil during the ice formation period. (*Photo source: F. Hicks.*)



Figure 2.21 Example of a layer of vegetation picked up by the frazil during the ice formation period, exposed later in a stranded ice floe at breakup.
(Mackenzie River photo source: F. Hicks.)

Anchor ice can also accumulate and/or grow in quantities sufficient to lift much larger sediments, including pebbles and cobbles (Figure 2.22), causing them to be carried downstream with the floating ice. The transport of sediment by this process is known as *sediment rafting* (e.g. see Kempema and Ettema 2011). The ice carrying these particles of sand and gravel usually form part of the river's eventual ice cover, and this is why particles of sand and gravel are often found embedded in river ice covers (Figure 2.23).

Anchor ice and anchor ice dams can also release from the bed in response to solar heating or river flow fluctuations. However at present, little quantitative data is available describing anchor ice release events, and so the mechanisms of release are not yet fully understood.

Malenchak and Clark (2013) provide an excellent review of anchor ice for those who would like to investigate this topic in more detail. Readers are also referred to the seminal papers by Kempema et al. (2001, 2002, 2004, 2008a, 2009, 2011) and by Stickler and Alfredsen (2005, 2009).



Figure 2.22 Sediment rafting by anchor ice.
(Photo courtesy of E. Kempema.)

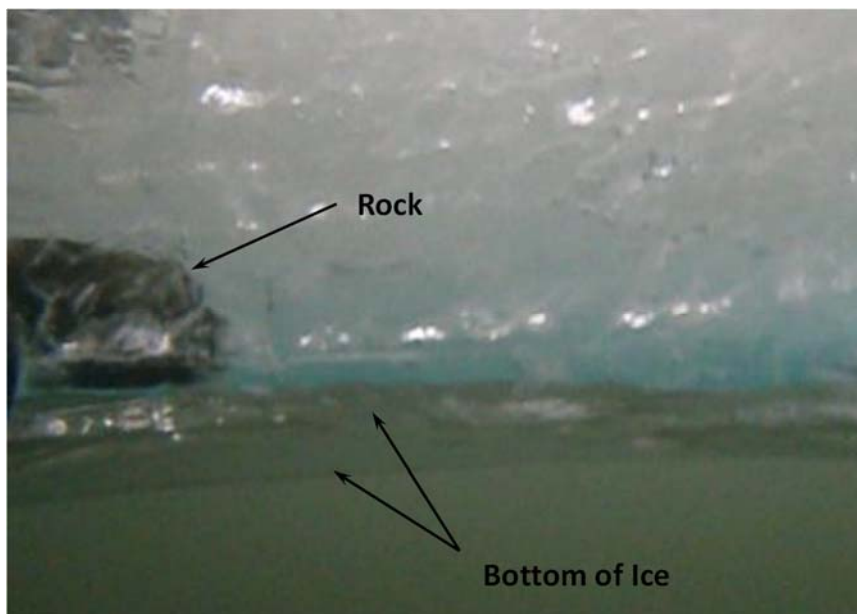


Figure 2.23 Example of a rock embedded in a river ice cover.
(North Saskatchewan River photo by F. Hicks.)

Bridging of Frazil Pans

As freeze-up progresses, more and more frazil pans and rafts form, and border ice encroachment on the channel also increases (Figure 2.24).



Figure 2.24 Freeze-up on the Bow River in Alberta.
(Photo courtesy of M. Loewen.)

As the surface concentrations of frazil pans increase beyond about 80 to 90%, *bridging* becomes likely. This involves a congestion of ice floes and a subsequent cessation of their movement at a site along the river. Typical bridging locations are at tight bends and at locations where the channel narrows, such as between bridge piers or at natural constrictions. Border ice growth can enhance or create constrictions that serve as bridging points as well (Figure 2.25).



Figure 2.25 Natural constrictions, and those enhanced by border ice encroachment, present likely spots for bridging to occur.
(Photo courtesy of T. Ghobrial and M. Loewen.)

Juxtaposed Ice Covers and Frontal Progression

Once bridging occurs, the incoming ice floes may lead to an upstream progression of the ice front by accumulating edge to edge on the water surface (Figure 2.26), creating a *juxtaposed ice cover*. However, when flow velocities are in excess of ~ 0.7 m/s and the flow Froude number is greater than ~ 0.1 , it is also quite possible that surface ice floes coming into the ice front may be swept under the ice front and then deposited on the underside of the cover². This process is known as *hydraulic thickening* (Figure 2.27). The increased thickness results in an increase in water level and a corresponding decrease in flow velocity. Once the flow velocity decreases sufficiently, ice floes are no longer swept under the ice cover and the ice front can continue its upstream progression. In extreme cases,

² Note: these threshold values are very approximate; actual values tend to be highly case and site specific. Dow et al. (2011a, b) provide a comprehensive review and analysis of hydraulic thickening physics and leading edge stability criteria.

velocities may be high enough that the entire ice cover formed at the bridging site may be swept downstream, after which bridging must re-occur before frontal progression of the ice cover can recommence.



Figure 2.26 Example of juxtaposed ice. (*Photo source: F. Hicks.*)

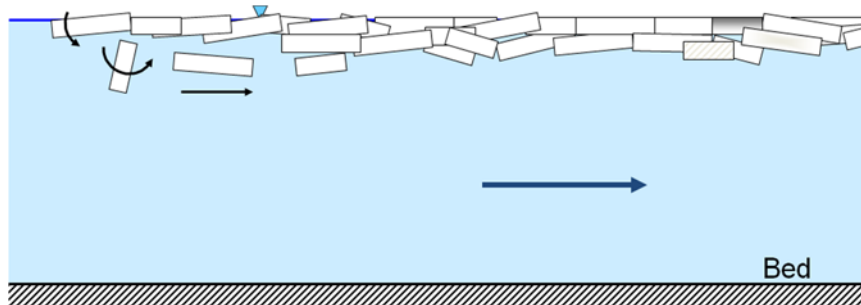


Figure 2.27 Schematic of hydraulic thickening
(*adapted from Healy and Hicks, 2001.*)

Hummocky Ice Covers and Freeze-up Ice Jams

As the ice front progresses upstream, either by juxtapositioning or by hydraulic thickening, the forces acting on the ice accumulation increase. These forces include the downslope component of ice weight within the ice accumulation, and the flow drag along the underside of the ice cover. These forces are resisted by the internal strength of the accumulation which, for freeze-up accumulations, is often enhanced by freezing between the individual ice floes, as well as by freezing of the pore water

Freeze-up and Winter Ice Processes

in the slush underlying the frazil pans. The forces acting on the ice cover increase as it lengthens, and when the magnitude of these forces approaches the internal strength of the ice accumulation, the ice cover is prone to collapse, or *shove*, and thicken substantially. The increased thickness and roughness of the ice cover resulting after such a collapse is usually reflected in a dramatic increase in water levels. The resulting accumulation, termed a *hummocky ice cover* (Figure 2.28), typically occurs when flow velocities are between about³ 0.7 and 1.5 m/s. Normally, once the accumulation has stabilized, the water between the ice floes freezes and gives strength to the accumulation, thereby inhibiting further consolidation. Hummocky ice covers are also referred to as freeze-up ice jams, although some specialists reserve this descriptor for extreme cases where the obstruction to flow results in overbank flooding.



Figure 2.28 Hummocky ice cover (freeze-up ice jam) formed at freeze-up on the Bow River in Alberta. (Photo courtesy of J. Blackburn and T. Hutchison.)

Ice Cover Growth and Snow Ice

As discussed earlier, the change in phase from water to ice releases the latent heat of fusion, which in turn warms the water, reducing the level of supercooling. This means that continued supercooling requires continued heat loss from the water surface. Thus supercooling cannot be maintained

³ Again, these are approximate numbers only; actual values tend to be highly case and site specific.

once a continuous ice cover forms on the water surface. Therefore, at this point local frazil production stops.

Subsequent thickening of the ice cover occurs both from above and below. For example, in the absence of an insulating snow cover, the ice cover grows down from its bottom as a result of thermal heat loss through the ice cover. At some point, the ice cover itself may approach a thickness which is self-insulating. The thickness at which this might occur depends on the severity of the prevailing meteorological conditions. Additional ice may also form on top of an existing ice cover when a snow cover is present. This occurs due to water seeping through cracks in the ice cover which then saturates the lower portion of the snow cover and then freezes (Figure 2.29). This can occur because ice buoyancy is relatively low; the presence of a snow cover of approximately half the thickness of the ice can be enough to submerge the ice surface below the phreatic surface⁴. Upon freezing, this new layer on top of the original ice surface is termed *snow ice* (Figure 2.30).

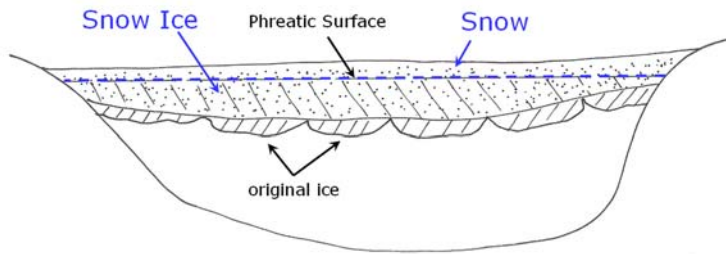


Figure 2.29 Schematic of snow ice formation (adapted from Michel 1971).

Figure 2.31 shows a typical ice core sample from a river experiencing all of these ice formation processes. In the center of the sample is the frazil ice which formed first. This can be distinguished by the fact that it contains particles of sediment, picked up from the bed before the frazil flocs were sufficiently large to float to the surface. To the left, which is the top of the ice core sample, is snow ice, which has a milky translucent appearance. To the right, which is the bottom of the ice, is the extremely transparent thermal ice (generally referred to as *columnar ice*).

⁴ The phreatic surface is the top of water in the river. Since ice floats with a large portion of its thickness submerged, the actual water level is above the bottom of the ice. This is discussed further in Chapter 4.



Figure 2.30 Snow ice layers exposed in broken sheet ice on the Peace River, Alberta. (Photo source: F. Hicks.)



Figure 2.31 Ice core sample from the Mackenzie River, illustrating the various ice components typically found within a river ice cover. (Photo source: F. Hicks.)

Thin slices of river ice, called thin sections, can be examined under polarized light to reveal individual grains corresponding to these various ice types (Figure 2.32). Snow ice and frazil ice are seen to have very small, roughly circular grains. In contrast, thermal ice grows in long thin grains, which is why it is termed *columnar ice*.

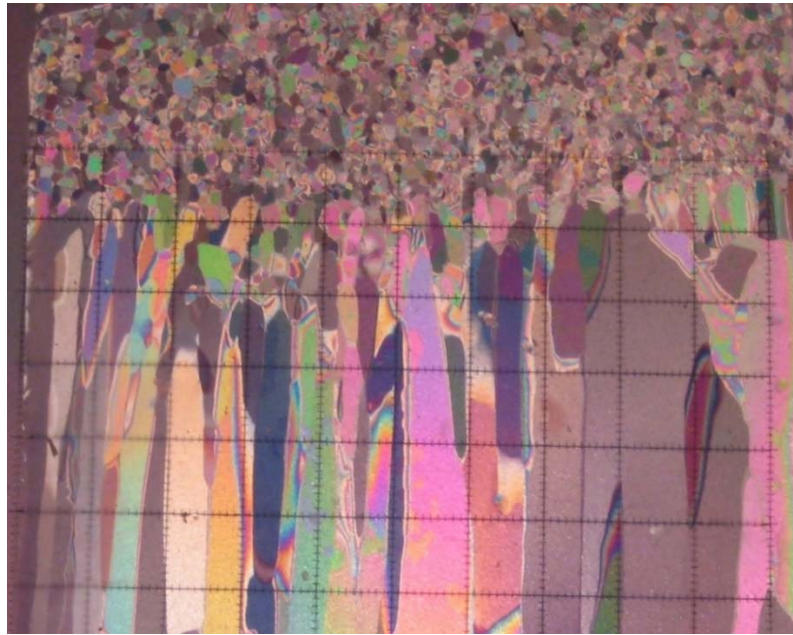


Figure 2.32 A vertical thin section from a sample of ice from the North Saskatchewan River, Alberta, viewed in profile under polarized light to expose the individual grains of ice. The grid squares are 1 cm x 1cm.

(Photo source: F. Hicks.)

Other Ice Formation Processes

Aufeis

In some rivers, winter flows are extremely low and the flow is sufficiently shallow for the river to freeze right to the bed. Subsequent flow can push through cracks in the ice up onto the surface (Figure 2.33), freezing in successive layers, each superimposed upon the previous. The resulting ice formation is termed *aufeis* which is German for ‘ice on top’ (Daly 2013b). This type of ice is also known by its Russian name, *naled*, and is sometimes referred to as an *icing*, as well (Daly 2013b).

If there is a snow cover, then water overflowing the ice surface will first saturate this snow and freeze to form snow ice (Figure 2.34). As a result, Kane (1981) describes snow ice creation as the first stage in river *aufeis* development. Over the course of the winter, the aerial extent and thickness of *aufeis* can be substantial, and can cause flooding (and *aufeis* formation) on the floodplain (Figure 2.35). Small tributaries and springs can also be a source of *aufeis* deposits on river ice covers (Figure 2.36).



Figure 2.33 Water flooding an ice surface and freezing to form aufeis.
(*Photo courtesy of S. Daly.*)



Figure 2.34 Snow ice forming as a result of overflow is considered by some to be the first stage of aufeis formation. (*Photo courtesy of S. Daly.*)



Figure 2.35 Water can spread into the overbank and freeze to form aufeis.
(Photo courtesy of S. Daly.)



Figure 2.36 Groundwater from springs can spread onto the ice cover to form aufeis. *(Photo by F. Hicks.)*

Freeze-up and Winter Ice Processes

Aufeis is a common source of flow obstruction in road culverts (sometimes called a *culvert icing*), since the small flows typically experienced on small streams in winter readily freeze to the steel pipe. Over the winter, the aufeis accumulations can fill the entire culvert creating a significant flow obstruction to spring runoff (Figure 2.37). This is a common cause of culvert failure in northern Canada.



Figure 2.37 Example of culvert icing. (Photo by F. Hicks.)

Culvert icings can be particularly severe when the channel has been widened to accommodate these conveyance structures, as the shallower wider flow freezes to the bed more easily. Stripping vegetation to facilitate construction also allows frost to penetrate deeper, increasing the risk of extensive aufeis formation.

Hanging Dams

In steep river reaches where flow velocities exceed about 1.5 m/s, an ice cover may not be able to form⁵. Such reaches may remain open throughout the winter, and persistent supercooling then leads to continuous frazil production. Vast quantities of frazil can be created and this ice typically comes to rest on the underside of the ice cover in slow velocity zones further downstream. As the schematic in Figure 2.38 illustrates, if this accumulation forms under the ice covering a deep pool in the river, a substantial accumulation of frazil can develop, forming a *hanging ice dam*.

⁵ Again, this is a very approximate number; actual values are very site and case specific.

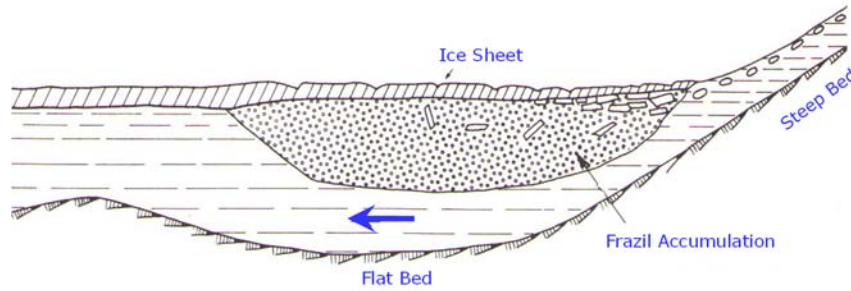


Figure 2.38 Schematic of hanging dam formation (*adapted from Michel 1971*).

Hanging ice dams can be quite massive. For example, Beltaos and Dean (1981) documented a hanging ice dam more than 10 m thick on the Smoky River, Alberta in 1975. Michel and Drouin (1981) documented a hanging ice dam on the LaGrande River, Quebec in 1973 that was more than 20 m thick in places and contained an estimated 56 million cubic meters of frazil slush. There is anecdotal evidence that even larger hanging dams have been observed in Newfoundland, Canada, although there is not yet any published information on this.

Granular Ice

Another interesting ice formation process can be attributed to these high velocity flow reaches, where open water tends to persist. Occasionally, solid ice pans and ice sheets formed upstream of these rapids break up into small pieces during passage through these high velocity zones. It has been suggested that these small pieces of solid ice are then transported downstream with the flow, moving along the underside of the ice cover in a manner similar to sediment transport movement on the bed of a river (Robichaud 2003). After dozens of kilometers of travel, these solid ice pieces become rounded through abrasion against other similar ice particles, just as gravel on a riverbed is rounded during transport by abrasion against other rocks. Figure 2.39 illustrates the resulting *granular ice* formed by this process. It has also been termed *marble ice*, because of its size and appearance.

Ice Discs

Another interesting freeze-up phenomenon is the occurrence of *ice discs* (Figures 2.40 and 2.41). These typically occur where the river currents have to curve around a river bend, especially in places where large surface eddies result. Curved or swirling flow paths create a curved drag force on

Freeze-up and Winter Ice Processes

the underside of the developing border ice. If the ice is really thin and frail, then the ice cover will simply break up and be washed away with the flow. If the ice cover is thick and strong, then it will withstand this rotational force and nothing will happen. However, if the ice is weak enough to be fractured but not weak enough to break up completely, then an ice disc may form (Figures 2.40 and 2.41). The rotating ice grinds against the remaining (shorefast) ice – rounding the edges and making the disc almost perfectly round.



Figure 2.39 Granular ice observed on the Athabasca River in Alberta.
(Photo courtesy of K. Unterschultz.)

Ice discs can also form when frazil pans and rafts get caught in a river eddy. As more and more pans are trapped, they freeze together and eventually form one very large spinning raft.



Figure 2.40 Rotating ice disc observed on the Exploits River in Newfoundland.
(Photo courtesy of R. Baird.)



Figure 2.41 Closer view of the Exploits River ice disc in Newfoundland. Note the blue barrel on the bank to get an idea of the scale.
(Photo courtesy of R. Baird.)

Effects of Streamflow Regulation of River Ice

Persistent Open Water Downstream of the Dam

On regulated rivers, where streamflow is impounded behind a dam within the reservoir, both water storage in the reservoir and flow release patterns have the potential to significantly affect winter water temperatures in the receiving river channel. This occurs because of the unique density characteristics of water. As with other fluids, water density varies with temperature; however, water density is maximum at 4°C, and decreases with both higher and lower temperatures. In deep reservoirs containing water at temperatures in excess of 4°C, the cooler, denser water is found at greater depths than the warmer, less dense water. This vertical stratification is stable because further heating of the surface layers of water only leads to reduced density in these upper layers. However, as water in a reservoir cools below 4°C, it develops an inverse temperature gradient. Initially, surface heat loss lowers the water temperature in the upper layers towards 4°C and this denser water then moves to the lower levels. As the water cools further, its density decreases and the colder (but less dense) water remains nearer the surface. The resulting profile is at 0°C near the surface and 4°C at the reservoir bed. Further heat loss through the winter season has the potential to cool the water through the entire depth. However, there will still be a temperature gradient until all of the water has been cooled to 0°C. This temperature gradient may persist throughout the winter in some reservoirs, as the formation of an ice cover on the surface insulates the water from cold air temperatures.⁶ Snow accumulations on the ice cover enhance this insulating effect.

It is important to note that the vertical temperature gradient does not persist once the water is released from the reservoir and enters the receiving channel, because of the turbulent nature of river flow. Instead, the region downstream of the dam will have a persistent open water reach, and frazil ice will form and evolve in this reach in the same manner as depicted in Figure 2.7. The extent of the open water zone downstream of the dam will vary with the prevailing weather conditions; it will be shorter in colder weather and longer in warmer weather. This open water reach provides a continuous frazil production zone for the entire winter and, as a result, massive quantities of frazil can be produced and transported under the ice cover downstream.

⁶ The water cooling processes described above for reservoirs, also occur on deep natural lakes.

Effects of Fluctuating Water Levels

On rivers regulated for hydro-power production, flow releases can be highly variable. In particular, if the dam is operated in response to changes in power demands, then a succession of waves will be released to the downstream channel in a process known as *hydro-peaking*. For example, water levels on the North Saskatchewan River at Edmonton routinely fluctuate by about 30 cm each day in response to hydro-peaking waves released from dams located far upstream (Figure 2.42).

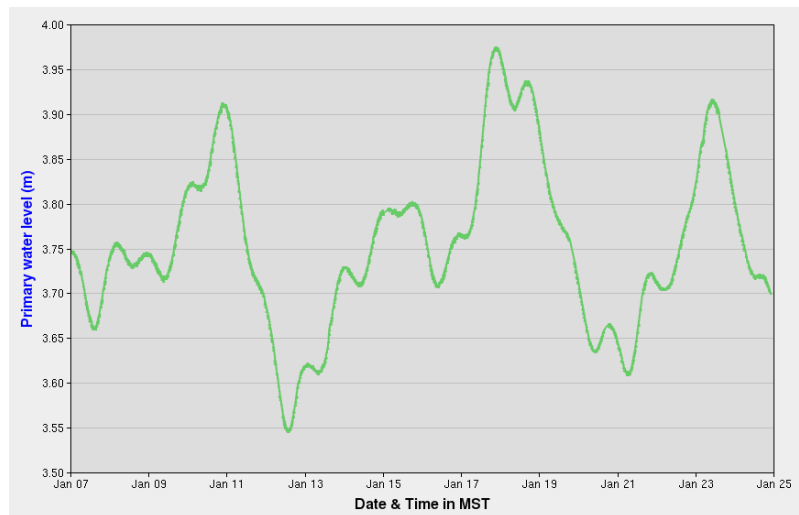


Figure 2.42 Example of typical winter water level fluctuations on the North Saskatchewan River at Edmonton, Alberta, in response to hydro-peaking. (Figure and data source: Water Survey of Canada.)

During the early ice formation period, when border ice first appears, these hydro-peaking waves can be sufficient to lift the border ice free from the banks. These sheets of ice are then transported downstream with the frazil pans and rafts (Figure 2.43), and can contribute to congestion and bridging.

Fluctuating water levels can also contribute to anchor ice development on regulated rivers. At night, when electrical power demand is lowest, the river flow is reduced and low water levels expose gravel and boulders to atmospheric temperatures. When power demand resumes in the morning, flow rates are increased and rising water levels submerge these extremely cold gravels and boulders, facilitating underwater nucleation on their surfaces (Figure 2.44).



Figure 2.43 Example of border ice released by hydro-peaking wave.
(Photo courtesy of T. Ghobrial.)



Figure 2.44 Example of anchor ice forming around a boulder.
(Photo courtesy of J. Nafziger.)

Summary

River freeze-up involves a multitude of unique and interesting ice processes. The variability of these ice processes are caused by variations in meteorological conditions, variability in streamflow and resulting hydraulics, and are highly dependent upon local river morphology.

Chapter 3

RIVER BREAKUP PROCESSES

The nature of breakup on a river can vary from one in which the ice gradually deteriorates and more-or-less melts in place (Figure 3.1), to one in which breakup occurs suddenly and violently, typically involving broken ice, ice runs, and ice jams (Figure 3.2).

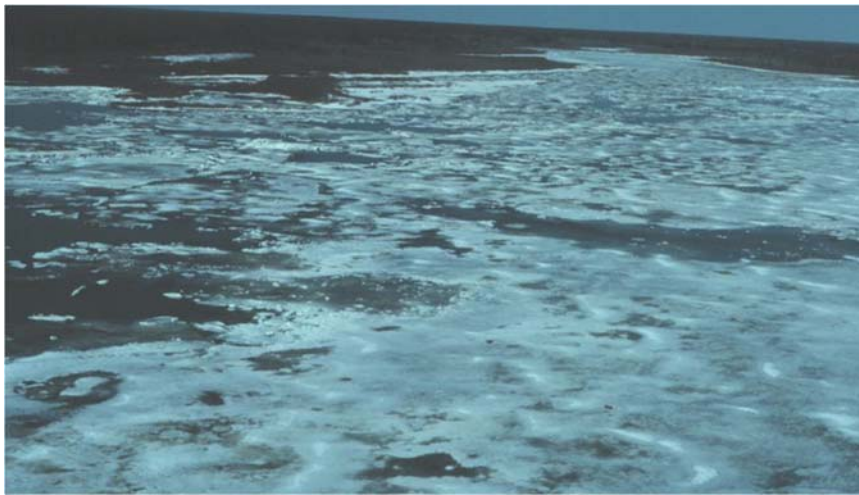


Figure 3.1 Example of thermal breakup on the Mackenzie River, NWT.
(Photo by F. Hicks.)

The manner of breakup depends on the relative importance of meteorological and hydrodynamic influences. Meteorological influences are always a factor in driving the river breakup, serving to melt snow on the ice cover and in the upstream basin, as well as to melt the ice itself. Hydrodynamic influences related to increasing river flows (and associated increases in flow velocities, shear stresses, and water levels), exert forces on the ice cover that can cause it to lift, rupture and move. Therefore, *thermal breakup* tends to occur in cases where there is no strong spring

runoff event. The ice deterioration occurs much as it would on a lake, in that there is relatively little ice movement. In contrast, dynamic breakups are typically associated with the rapid melt of a significant snowpack, with the resulting large snowmelt runoff wave instigating a violent breakup along the river as it passes downstream.



Figure 3.2 Example of dynamic breakup on the Hay River, NWT.
(Photo by F. Hicks.)

Thermal Breakup Processes

Stage 1 – Snowmelt on the Ice Cover

The first stage in a thermal breakup is usually the melting of the snow on the ice cover due primarily to incoming solar radiation and convective heat transfer from the warm overlying air. Initially, the heat energy from the sun has little influence on this snowmelt, since the albedo (or reflectance) of the snow cover tends to be quite high in late winter. However, the snow's albedo decreases as it melts (Figure 3.1) allowing more and more of the sun's energy to be absorbed. As a result, the rate of melt increases as thermal breakup progresses.

Stage 2 – Development of Open Leads

Flow turbulence can also contribute heat to an ice cover, and there are typically places along the thalweg (i.e. the deepest points) of a river where velocities are sufficiently fast that a thick ice cover never develops. Once warmer weather commences, the thinner ice in these areas tends to melt away first, creating open leads in the ice cover (Figure 3.3).



Figure 3.3 Open lead developing on the Mackenzie River, NWT.
(Photo by F. Hicks.)

These open leads are very important since the albedo of water is substantially lower than that of the ice or snow cover. Considerable heat energy can therefore be absorbed by the water, which then melts the ice from the underside, enlarging the opening. The enlarged opening can then absorb proportionally more heat. In this way, these openings in the ice cover can eventually enlarge at a near exponential rate (Figure 3.4).

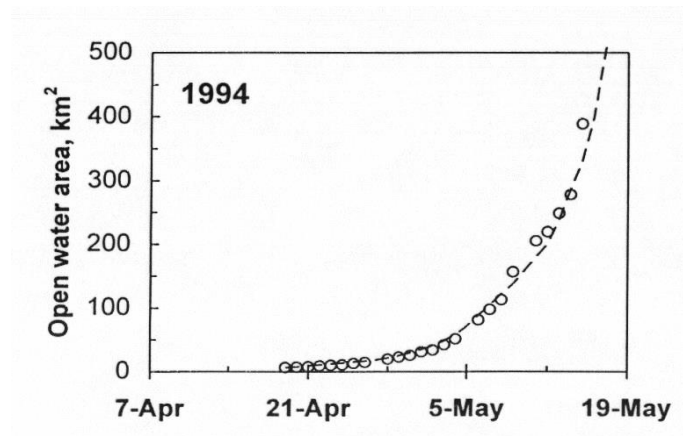


Figure 3.4 Open water development on the Mackenzie River, NWT
(adapted from Hicks et al. 1997a).

Stage 3 – Ice Melt

Ice decays first at its crystal boundaries; therefore, as columnar ice melts, it deteriorates into elongated pieces that look like candles. This *candled ice* (Figure 3.5) is a common feature of thermal breakup. At this stage the ice has very little inherent strength and crumbles into discrete pieces very easily. At this point, the candled ice may begin to move with the flow, causing a tinkling sound as the ice candles clink against each other. For many people who live in northern countries, this musical sound is a welcome harbinger of spring. Eventually all of the ice melts away and the river is once again open.



Figure 3.5 Candled ice observed on the Mackenzie River, NWT.
(Photo by F. Hicks.)

Dynamic Breakup Processes

Stages 1 and 2 – Snowmelt and Open Lead Development

The initial stages of dynamic breakup are often the same as that for a thermal breakup. Snow will melt on the ice cover and open leads will begin to develop along the channel thalweg. The difference in this case is that water levels are typically rising at a steady, often rapid, rate and the ice is subjected to strong forces as a result.

Stage 3 – Overflow from Open Leads

While the ice cover is still frozen to the banks, it will resist rising with the increasing water levels. If the rate of water level rise is particularly fast, water may push up through the open leads and spill onto the downstream ice cover (Figure 3.6).



Figure 3.6 Overflow from open leads on the Mackenzie River, NWT. This is a sign of rapidly rising water levels. (*Photo by F. Hicks.*)

Stage 4 – Formation of Hinge Cracks and Shorefast Ice Inundation

Usually the ice cover will not be able to resist the force of the rising water and it will eventually form *hinge cracks* along lines parallel to the banks.

River Breakup Processes

In wide rivers, these hinge cracks form in two lines, one along each bank (Figure 3.7). Once these cracks occur, the main ice sheet is free to float up with the rising water levels. The shorefast ice along the river banks is inundated by this rising water and melts away relatively quickly. On narrow rivers, a single hinge crack may form down the center of the channel (Figure 3.8).

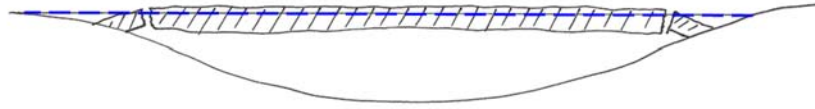


Figure 3.7 Schematic of hinge cracking (cross sectional view).



Figure 3.8 Single hinge crack formed in a narrow river.
(Photo courtesy of E. Kuusisto.)

Stage 5 – Formation of Transverse Cracks

As discharge and associated flow velocities increase, flow stress on the underside of the ice cover also increases. At this point, *transverse cracks* usually form. These are particularly likely to occur in river bends, where centrifugal forces create strong currents along the outer bank (Figures 3.9 and 3.10).

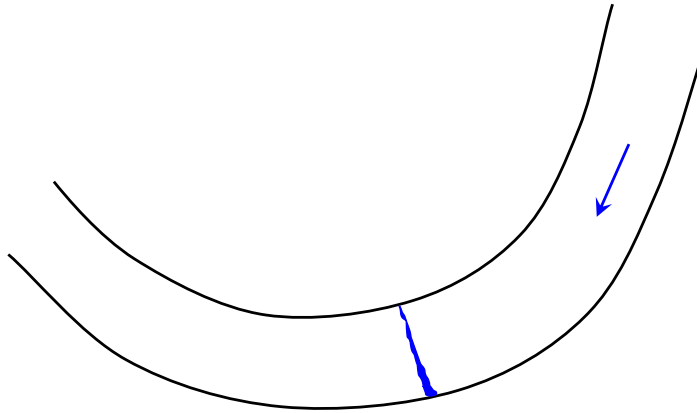


Figure 3.9 Schematic of transverse crack formation in a river bend.



Figure 3.10 Transverse crack observed on the Mackenzie River, NWT.
(Photo by F. Hicks.)

River Breakup Processes

At this point the ice is broken into discrete sheets; however, sheet ice movement is constrained by tight bends or islands in the channel (Figure 3.11). Consequently there is little ice movement. There will sometimes be some minor shifting of these ice sheets causing breaking and ridging (Figure 3.12).



Figure 3.11 Here the shorefast ice has melted away and the remaining ice has broken into discrete sheets; however the ice sheets cannot maneuver around the bends and so the ice is not yet moving.
(*Mackenzie River, NWT photo by F. Hicks.*)



Figure 3.12 Ice sheet ridging on the Athabasca River in Alberta. Flow is from left to right. (*Photo by F. Hicks.*)

Stage 6 – Sheet Ice Accumulations

The stopping and starting of ice sheets as they try to work their way downstream creates small, localized fluctuations in water levels which break the ice sheets into smaller pieces. These smaller sheets then start to shift and move, creating localized *sheet ice accumulations* (Figure 3.13).



Figure 3.13 Sheet ice accumulation on the Hay River, NWT. Flow is from left to right. (Photo by F. Hicks.)

Stage 7 – Ice Clearing

The sheet ice continues to shift and push in response to the flow drag and, as a result, they progressively break into smaller and smaller pieces. Eventually the ice pieces become small enough to overcome the river's geometric constraints and they begin to work their way around bends and islands, moving with the flow.

Stage 8 – Ice Jams

Variations in ice thickness, as well as in river alignment, slope, and velocity cause breakup to progress quicker in some areas along the river compared to others. This can lead to small accumulations of broken ice (~0.5 to 2 km long) upstream of short, intact segments of the ice cover (Figure 3.14). The creation and consolidation of these *mini-jams* result in small, localized fluctuations in water levels that in turn break away pieces of the intact ice sheets upstream. In this way, small ice jams increase in length as breakup progresses. Eventually this can lead to massive ice accumulations, tens of kilometers in length (Figure 3.15).



Figure 3.14 Mini-jam on the Hay River, NWT. Flow is from left to right. *(Photo by F. Hicks.)*



Figure 3.15 Ice accumulation (ice jam) on the Hay River, NWT. Flow is from top to bottom. *(Photo by F. Hicks.)*

Common locations where ice jams tend to occur include tight river bends, at obstructions (such as at islands or bridges), or at abrupt slope reductions

in the river bed. The ice may also jam up against intact ice further downstream. This is especially likely on north flowing rivers (which tend to break up in the headwaters first), where rivers enter a lake having intact ice (Figure 3.16), or at a confluence with another river that is yet to breakup.



Figure 3.16 Ice jammed against the intact ice on Great Slave Lake, NWT. Note the flooding along the left bank of the Hay River. Flow is from left to right.
(Photo by F Hicks.)

Ice jams are typically comprised of very thick and rough accumulations of ice and, consequently, they present a very substantial obstruction to the flow. As a result water levels will rise upstream and may eventually overtop the river banks, causing flooding (Figure 3.16). The water and ice impounded in an ice jam exert a tremendous driving force, and some ice jams will consolidate (shove and thicken) under the pressure, creating even higher water levels.

Stage 9 – Ice Jam Release and Ice Runs

In some cases, ice jams will melt out from the underside, due to heat transfer from incoming water warmed by the sun further upstream. However, this melting process takes time and often the ice jam is pushed out instead. The release of an ice jam sends a wave of ice and water rushing downstream at speeds to 3 to 5 m/s, or more (Figure 3.17). Beltaos (2009) refers to these *ice jam release waves* as *javes*. The moving ice is typically referred to as an *ice run*.



Figure 3.17 Ice run following ice jam release event on the Athabasca River in Alberta. Flow is from left to right – notice the ice jam reforming further downstream (top right corner of the photo). (Photo by F. Hicks.)

Ice jam release events sometimes progress downstream in domino fashion, with the ice runs from upstream ice jam release events instigating the release of the next downstream ice jam. In this case, the ice runs increase in size as they progress downstream. In addition, ice runs tend to stall at tight bends and islands. This temporarily re-jams the ice, causing water and ice pressures to build up and then release with renewed speed and magnitude.

When an ice jam releases, the ice out in the middle of the channel is carried away more quickly because of the faster currents there. In contrast, the ice closer to the river banks is usually grounded and cannot move as easily. This difference sets up a shearing interface between the moving ice and the grounded ice (Figure 3.18). Once the moving ice leaves, remnant ice is left behind in strips along the river banks (Figure 3.19). This remnant ice has a near vertical inner face, called a *shear wall* (Figure 3.20).



Figure 3.18 Shearing interface seen on the Hay River in the Northwest Territories. *(Photo by F. Hicks.)*



Figure 3.19 Remnant ice left behind after ice jam release on the Hay River in the Northwest Territories. *(Photo by F. Hicks.)*



Figure 3.20 The steep inner face on the remnant ice is called a shear wall.
(*Hay River, Northwest Territories - photo source: F. Hicks.*)

Summary

The nature of river breakup, whether thermal or dynamic, depends primarily on the river discharge. If the river experiences a very rapid and substantial increase in discharge due to snowmelt, then a dynamic breakup is much more likely. Conversely, if the discharge remains relatively low during the spring melt period, then a thermal breakup is much more likely.

Chapter 4

RIVER ICE PROPERTIES

In this chapter we will discuss some of the basic physical properties of frazil ice and polycrystalline ice covers. We will also discuss the most practically relevant thermal properties of river ice.

Physical Properties of Frazil Ice

The basic properties of frazil ice that are practically relevant include their shapes and sizes, suspended concentrations, and rise velocities. For frazil ice at the river surface, the primary characteristic of practical interest is the frazil pan thickness.

Frazil Particle Shape and Size

Very few studies of frazil ice have been conducted in the field, so most of what is currently known comes from laboratory investigations. Studies to date indicate that frazil particles generally occur in disc shapes (Figure 2.3) although needle shapes (spicules) have occasionally been observed, as well. Osterkamp (1978) suggested that spicules were more likely to occur at extreme supercooling temperatures; however, this has not been studied extensively. Laboratory frazil particles range from about 0.02 mm up to approximately 5 mm in diameter (Osterkamp 1978, Daly and Colbeck 1986, Clark and Doering 2004, 2006, McFarlane et al., 2012, 2015a), with mean values ranging from about 0.6 mm to 1.0 mm (Macfarlane et al. 2015a). Frazil particles beyond 5mm do not appear to be stable in laboratory or field settings (e.g. see Osterkamp 1978) as the larger particles tend to fracture into smaller pieces as a result of collisions. Researchers have consistently observed that the particle sizes for laboratory frazil tend to follow a lognormal distribution (e.g. see Figure 4.1). Preliminary field research (MacFarlane et al. 2015b) suggests that the same is true for frazil in natural rivers.

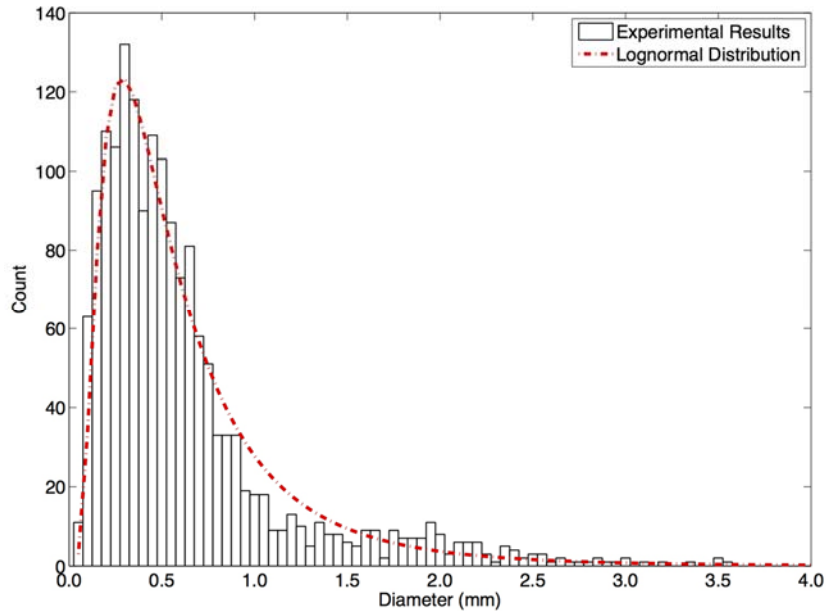


Figure 4.1 Example size distribution of laboratory frazil particles observed by McFarlane et al. (2013).

Frazil particle size appears to depend on the degree of flow turbulence though, to date, this has only been studied in laboratories. Clark and Doering (2008) found that mean particle size first increased, then decreased as turbulent kinetic energy increased. Ettema et al. (1984) and more recently, MacFarlane et al. (2015), observed that mean particle size consistently decreases with increasing turbulent kinetic energy. Field research is needed to fully understand this relationship for natural rivers.

Frazil discs are typically very thin; therefore, it is particularly difficult to measure their thicknesses precisely. Using a high resolution imaging system in a laboratory setting, McFarlane et al. (2014) documented frazil disc thicknesses ranging from 0.03 mm to 0.12 mm and aspect ratios (i.e. diameter/thickness) ranging from 11 to 71. Figure 4.2 shows some of the particles measured in that study.

Suspended Concentrations of Frazil Ice

To date, very few direct measurements of suspended concentrations of frazil ice have ever been conducted in the field (e.g. Gosink and Osterkamp, 1983, Tsang 1984, 1985, 1986). These have provided rough

estimates of the numbers of suspended frazil particles in the order of 10^4 to 10^7 particles/ m^3 . Suspended concentrations up to 0.25% were measured on the Beauharnois Canal, Quebec (Tsang 1984) and up to 0.03% on the St. Lawrence River, Quebec (Tsang 1986) using an instrument based on electrical conductivity. Unfortunately, this instrument, and subsequent techniques developed (e.g. Lever et al. 1992; Yankielun and Gagnon 1999; Doering and Morris 2003), were not particularly suited to the field application.

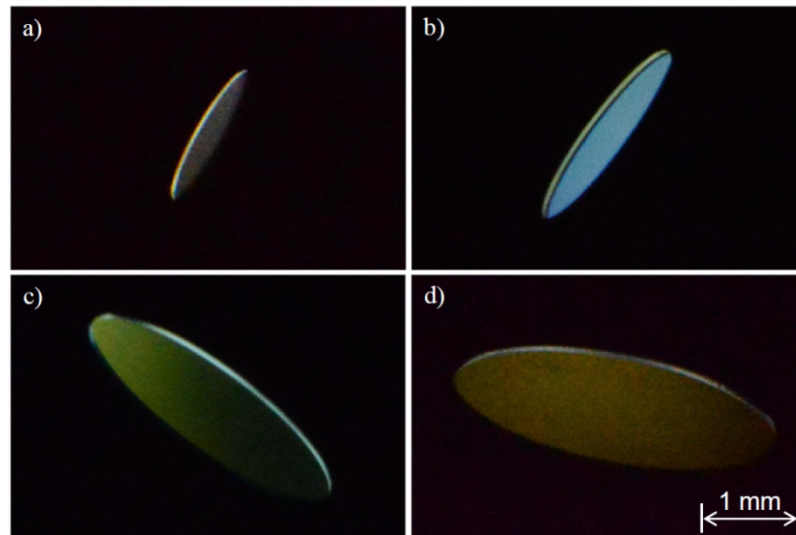


Figure 4.2 Example images in which frazil particle thicknesses were measurable. The particles had the following properties (where d = particle diameter and t = particle thickness): a) $d = 1.53$ mm, $t = 0.05$ mm, and $d/t = 30$; b) $d = 2.17$ mm, $t = 0.08$ mm, and $d/t = 27$; c) $d = 3.08$ mm, $t = 0.06$ mm, and $d/t = 49$; and d) $d = 3.43$ mm, $t = 0.05$ mm, and $d/t = 71$.
(McFarlane et al. 2014.)

More recently, researchers and practitioners have shown that sonar instruments can be used to effectively detect suspended frazil ice (e.g. Morse and Richard 2009; Richard et al. 2010; Marko and Jasek 2010a, b; Ghobrial 2013a, b). Figure 4.3 illustrates data from one such instrument in detecting suspended frazil. At present only the occurrence of suspended frazil particles can be observed; however, research is underway to expand their capabilities to quantitative measurements (e.g. see Ghobrial et al. 2012).

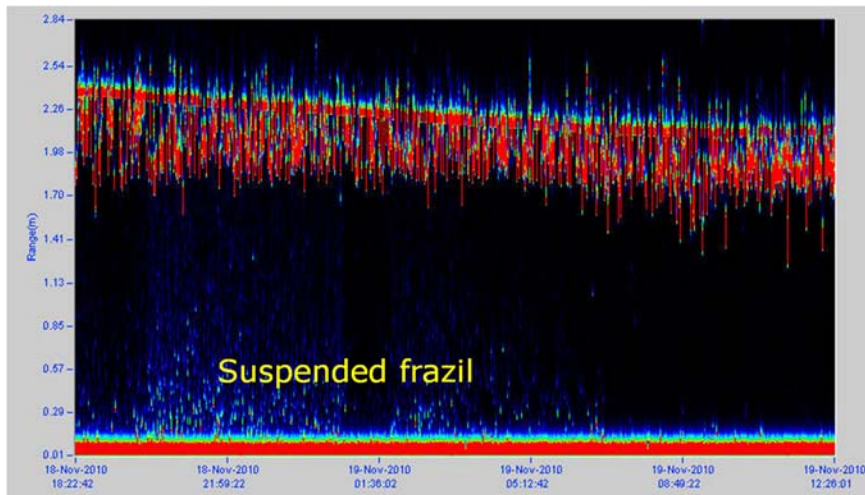


Figure 4.3 Example of suspended frazil ice detected on the North Saskatchewan River at Edmonton using a shallow water ice profiling sonar. The horizontal axis is time and the vertical axis is distance from the sensor, in m.
(Diagram courtesy of T. Ghobrial.)

Frazil Rise Velocity

Frazil rise velocity in natural rivers depends on many factors, including particles size and orientation, as well as the river velocity and degree of turbulence. In addition, frazil particles do not necessarily rise individually, most flocculate first and then rise together. Despite these complexities, knowledge of the rise velocity of individual particles is useful for determining where skim ice might form, as well as providing a logical first step in understanding frazil rise (in a manner analogous to studying sediment fall velocity as a first step in understanding sediment transport.)

Again, there have only been a few studies investigating this, most in the laboratory. Figure 4.4 illustrates the available data, which suggested that rise velocity is strongly dependent upon particle size and orientation. McFarlane et al. (2014) provide a complete literature review and details of viable theories.

Frazil Pan Thickness and Frazil Slush Porosity

Frazil pan thickness is comprised of two components, the frozen surface crust and the underlying porous frazil slush. Typically, the crust portion is initially only a few centimeters thick. The total thickness can be

measured with sonar instruments (e.g. see Morse et al. 2003, Jasek et al. 2005, and Ghobrial et al. 2013a). Figure 4.2 illustrates this; the red spikes indicate signal returns off of the bottom of frazil pans. For the example shown (North Saskatchewan River at Edmonton, AB, Canada) frazil pan thicknesses ranged from about 5 to 65 cm. Morse et al. (2003) documented pan thicknesses ranging from about 10 to 60 cm on the St. Lawrence River.

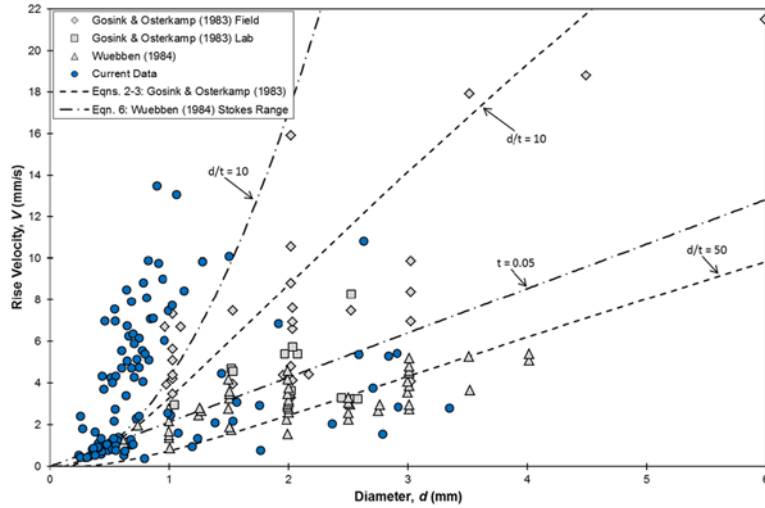


Figure 4.4 Rise velocities of frazil particles in quiescent water. (McFarlane et al. 2014.)

Frazil slush porosity is an important parameter for determining the total volume of frazil slush, and for determining how quickly the ice will freeze. However, there have been very few measurements of frazil slush porosity in the field. Table 4.1 summarizes some of the available values reported in the literature.

Table 4.1 Porosities of frazil slush reported in the literature.

Site	Porosities	Reference
unknown field site	0.65 to 0.85	Kivisild 1959
St. Lawrence River	0.50 to 0.60	Dean 1977
unknown field site, Alberta	0.50 to 0.65	Beltaos and Dean 1981
Smoky River, Alberta	0.43 to 0.65	Beltaos and Dean 1982
Peace River, Alberta	0.70	Andres and Spitzer 1989
lab experiments	0.85 to 0.90	Ghobrial, Loewen and Hicks 2010

Physical Properties of Polycrystalline Ice

Sizes of Ice Grains

The typical river ice cover is *polycrystalline*, being comprised of multiple ice types. For example, most river ice covers have surface layers of snow ice (and/or aufeis), frazil ice, and columnar ice (e.g. as was depicted in Figure 2.30). As discussed in Chapter 2, individual grains of ice can be detected in ice cover samples, using thin sections viewed under polarized light. Based on such measurements, Michel (1978) summarized the typical grain sizes shown in Table 4.2.

Table 4.2 Typical grain sizes observed in river ice (*adapted from Michel 1978*).

Ice Type	Typical Grain Sizes, mm		
	Small	Intermediate	Large
Snow Ice	1	2	4
Frazil Ice	1	2	4
Columnar Ice	5 (<i>top</i>)	10 (<i>middle</i>)	25 (<i>bottom</i>)

Air Bubbles and Impurities

River ice typically also contains impurities, including salts as well as both organic and inorganic matter (Figure 4.5). Most river ice also includes air bubbles of various sizes and configurations (Figure 4.6). For example, air is often entrained in frazil slush (Figure 4.7). Air bubbles can also form as air comes out of solution during the freezing process. Both circular and elongated bubbles, ranging in size from less than a millimeter to several centimeters, have been documented in river ice (e.g. see Gherboudj et al. 2007). Impurities and air bubbles are important in that they can have a significant effect on ice strength. In addition, both satellite (synthetic aperture) radar (SAR) and ground penetrating radar (GPR) are being used to classify ice type and to measure thickness, respectively, and the air bubbles and impurities scatter the radar signal making it challenging to interpret signal returns (e.g. see Unterschultz 2009).



Figure 4.5 Example of organic and inorganic impurities seen in horizontal slices through frazil ice from the Athabasca River in Alberta. Samples are 7 cm in diameter.
(Photo source: F. Hicks.)

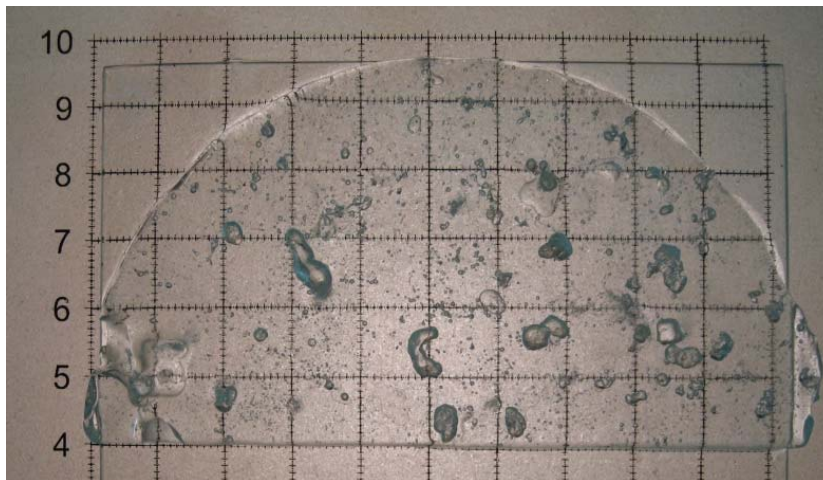


Figure 4.6 Example of air bubbles seen in a horizontal slice through frazil ice from the Athabasca River in Alberta. The grid squares are 1 cm x 1 cm.
(Photo source: F. Hicks.)



Figure 4.7 Example of air bubbles seen in a vertical slice of river ice from the Athabasca River in Alberta. Left: thin section, viewed under normal lighting conditions, showing where the bubbles were concentrated. Right: same thin section viewed under polarized light, exposing the layers: snow ice (top), frazil ice (middle), and columnar ice (bottom). In this case, the bubbles were primarily in the frazil layer, with the larger bubbles concentrated near the bottom, just above the columnar ice. (*Photos' source: F. Hicks.*)

Density of Ice

The density of ice, ρ_i , is less than the density of water, ρ , with the ratio of the two (ρ_i/ρ) being defined as the relative density of ice. Typical relative densities of polycrystalline river ice range from about 0.88 to 0.92 depending upon its composition, and the amounts and nature of the impurities and air bubbles it contains. Ice density also varies with temperature; however, the variation is negligible for practical engineering purposes (less than 0.5% variation between 0 °C and -30°C (Ashton 1986)). In the absence of actual measurements, it is generally considered reasonable to assume a constant value of 0.92 for the relative density of ice.

Because ice is lighter than water, it floats. However, as the difference is small (only 8% for a relative density of 0.92), most of the ice is still submerged. If the ice cover is free of snow, the ice will float with about 92% of its thickness submerged (assuming that the relative density of 0.92 applies). Therefore, when you drill a hole in a floating ice cover, the top of the water in the hole (i.e. the phreatic surface) will be slightly below the top of the ice. Snow on the ice cover weighs it down and, when it is substantial in depth, it can push the top of the ice below the phreatic surface. (As discussed in Chapter 2, this typically leads to snow ice formation.)

Thermal Properties of Ice

The primary thermal properties of practical interest are the latent heat of melting (freezing), the specific heat, the thermal conductivity and the thermal diffusivity. These ice characteristics are important when trying to model or predict ice formation and decay.

Latent Heat of Melting

The latent heat of melting is the heat energy required to change ice to water. The latent heat of ice melting, L_i , varies depending upon amounts and types of soluble impurities (e.g. salts), as these depress the melting point, T_m . However, the variation is not large and details of the impurity concentrations are seldom available in practical applications. Therefore, it is a relatively common practice to assume a constant value of 333.4 Joules/gram (J/g) for the latent heat of melting (Ashton 1986).

Specific Heat Capacity

The specific heat capacity of ice, c_i , is the amount of heat energy required to raise the temperature of a unit mass of ice by 1°C. This depends upon the ice temperature⁷, T_i , and its final melting point, T_m . Ashton (1986) provides the following empirical relationship (as determined by Dickenson and Osbourne 1915), which provides the specific heat in units of J/g°C:

$$c_i = 2.114 + 0.007789 T_i - 333.4 \frac{T_m}{T_i^2} \quad [4.1]$$

For example, the value of c_i at 0°C is 2.108 J/g°C. Equation [4.1] has less than 1% error for cases where the melting point is not less than -0.01 °C, which is valid for river ice in most cases.

Thermal Conductivity

The thermal conductivity of ice, k , is a measure of how easily heat energy can pass through the ice. It increases as ice density increases and as ice temperature decreases. The thermal conductivity of pure ice can be estimated using equation [4.2] (Ashton 1986):

⁷ The ice temperature varies throughout the ice thickness. It will be close to the air temperature on the ice surface (unless insulated by snow) and will be close to the water temperature on the ice bottom (i.e. ~0°C).

$$k = 2.21 - 0.011 T_i \quad [4.2]$$

Equation [4.2] provides only a crude approximation of the thermal conductivity of natural polycrystalline ice. This is because thermal conductivity is also affected by dissolved salts that depress the melting point of the ice. The thermal conductivity of ice is especially sensitive to temperature in cases where the melting point is significantly depressed (e.g. for T_m in the order of -0.01 °C), and particularly at ice temperatures approaching this melting point (Ashton 1986). Thermal conductivity is also strongly affected by the presence of air bubbles and impurities in the ice, not only due to their effects on ice density, but also due to the insulating effects of ice (Ashton 1986).

Typical values of the thermal conductivity of ice range from about 1.9 to 2.3 W/m°C (Ashton 1986); however, it is very difficult to quantify for natural polycrystalline ice because details of the amounts and nature of impurities and dissolved salts are seldom available in practical applications.

Thermal Diffusivity

The thermal diffusivity of ice, K , is the time rate of temperature change through a material (typical units are m^2/s). It can be obtained directly from measured values of the ambient air temperature and ice temperature as a function of time and depth (within the ice cover). Therefore, it is a useful derived parameter, given the difficulties in precisely quantifying some of the other physical and thermal characteristics of ice in most practical situations.

The thermal diffusivity is defined as (Ashton 1986):

$$K = \frac{k}{\rho_i c_i} \quad [4.3]$$

Values typically fall in the range of about 0.23 to 13.4×10^7 m^2/s (Ashton 1986).

Summary

Although frazil has been studied fairly extensively in the laboratory, we still know very little about the nature and variability of frazil ice properties in the field. In situ (stationary) ice covers have been studied much more extensively, as have the thermal properties of ice. However, the natural variability in all properties of polycrystalline ice makes it challenging to characterize many properties of a natural ice cover.

Chapter 5

HYDRAULICS OF ICE COVERED CHANNELS

The presence of an ice cover has a profound effect on river hydraulics. Most noticeably, it increases the wetted perimeter of the cross-section. In fact, for channels of high aspect ratio (i.e. a high width to depth ratio) the presence of an ice cover can effectively double the wetted perimeter. Also, because ice typically floats with about 92% of its thickness submerged, the ice cover obstructs part of the effective flow area. These two factors combine to reduce flow velocity and so, for the same discharge, the flow depth will be greater in an ice covered channel than it will be under open water conditions. This is the reason that a river “stages up” as the freeze-up front passes (Figure 5.1).

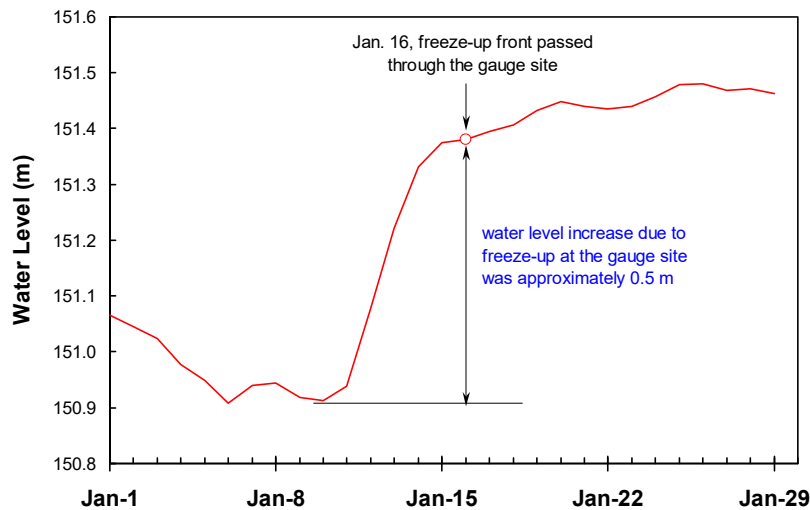


Figure 5.1 Example of the river stage increase that occurs as the freeze-up front passes a site. (*Mackenzie River, data source: Water Survey of Canada.*)

Not only does the ice affect the flow, the river currents affect the ice in return. As we saw in Chapter 2, if flow velocities are relatively low, then a juxtaposed ice cover may form. At higher velocities, ice pans may sink or under-turn as they approach the leading edge of the ice cover at the freeze-up front, forming a hydraulically thickened ice cover. At even higher velocities, the ice cover may collapse and form a thick and rough hummocky ice cover, or freeze-up ice jam. In some river reaches, where velocities are particularly high, an ice cover may not be able to form at all.

In order to calculate the water levels expected at a given discharge under various ice conditions, we must take these factors into account. In this chapter, we will look at how the hydraulics of ice covered channels are affected in the presence of a simple (continuous and intact) ice cover of known thickness. We will also look at some practical aspects of calculating the various relevant flow parameters for simple ice covered conditions.

Velocity Distribution Under a Simple Ice Cover

Figure 5.2 presents a schematic illustration of a typical velocity distribution under a simple, intact, stationary ice cover. Unlike the typical velocity distribution seen for open water conditions where the maximum velocity, V_{max} , is at or near the surface, here the velocity decreases to zero at the bottom of the ice cover (because of the no-slip condition). For ice covered conditions, the maximum velocity will be nearer to the center of the depth, closest to the smoother of these two boundaries.

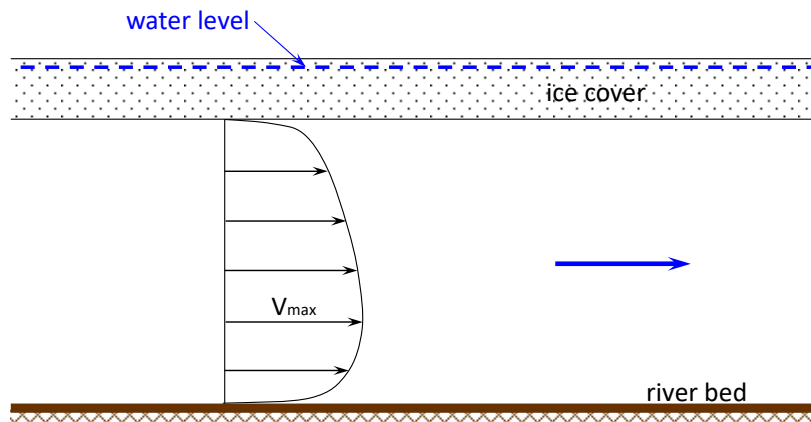


Figure 5.2 Schematic of the vertical velocity distribution under ice. The other important thing to note from Figure 5.2 is that the phreatic surface (i.e. the water level that we would observe if we drilled a hole in

the ice cover) is not at the bottom of the ice; it is actually near the top of the ice, an important feature to keep in mind whenever calculating the hydraulics of ice covered channels. This is because ice floats with about 92% of its thickness submerged, more if there is snow on top of the ice.

Hydraulic Analyses

Steady Gradually Varied Flow Hydraulics

In general practice, the hydraulic analysis of ice covered channels is typically achieved using a one-dimensional (1-D), steady, gradually varied flow approximation. Frictional resistance effects are often calculated using Manning's equation which, for SI units, can be written as:⁸

$$Q = \frac{1}{n} A R^{2/3} \sqrt{S_f} \quad [5.1]$$

in which Q is the discharge, n is the Manning's resistance coefficient, A is the flow area, R is the hydraulic radius of the flow (equal to A/P , where P is the wetted perimeter), and S_f is the friction slope (i.e. the slope of the energy grade line).

Because of the effects of ice on the flow, as discussed above, the application of this equation for the ice covered case requires a few special considerations. First, the width of the underside of the ice must be included when calculating the wetted perimeter. Second, the submerged portion of the ice must be excluded when calculating the flow area, as it obstructs the flow. The area to exclude, A_e , is equal to:

$$A_e = T 0.92(t_i) \quad [5.2]$$

where T is the top width of the channel (across the underside of the ice) and t_i is the thickness of the ice. Equation [5.2] assumes that the relative density of the ice is equal to 0.92; if it is not, the actual value should be substituted.

The second special consideration is that the Manning's n value used must represent the total roughness, n_t , of the ice covered section (including both bed and ice effects). Practically speaking, the best way to determine this total roughness is to calibrate values based on a known discharge, ice thickness, and measured water surface (or top of ice) profile. However,

⁸ For U.S. customary units, multiply the right hand side of equation [5.2] by 1.49.

most engineers prefer to consider ice and bed roughness separately, and most computer models (e.g. the U.S. Army Corps of Engineers' HEC-RAS program) require that the bed and ice roughnesses be input separately and then combines them into a composite (total) ice roughness for each cross-section.

Composite Roughness Equations

The basic premise of the composite roughness approach is to separate the cross-section in two zones, one affected only by the ice roughness, the other affected only by the bed roughness (Figure 5.3), where Y_i is the ice-affected depth of flow and Y_b is the bed-affected depth of flow. Common practice is to assume that the dividing line between these two zones follows the isoline of maximum velocity in the cross-section, as an approximation to a zero shear interface between the two zones. However, Hanjalic and Launder (1972) showed that the isoline of maximum velocity only represents a zero shear interface when the two surfaces have equal roughness (which is not the typical scenario for an ice covered river). In cases where the roughnesses are not equal, there is actually a momentum transfer across the maximum velocity isoline, rendering the whole concept of separate zones affected only by one or the other surface roughness essentially invalid.

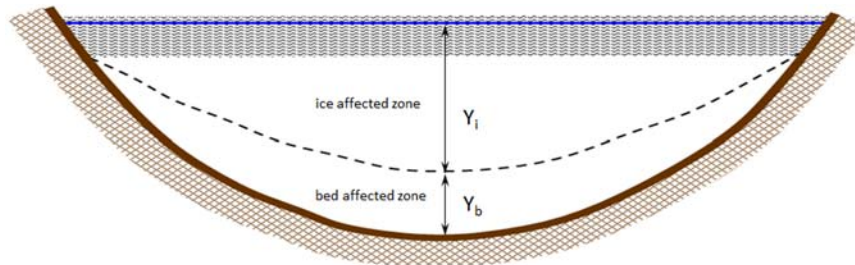


Figure 5.3 Schematic of the separation of a cross section in the bed and ice affected zones.

Even if the dividing line between the two zones could reasonably be approximated by the maximum velocity isoline, there is still an important practical limitation to this approach - it is rarely (if ever) feasible to conduct the velocity measurements necessary to locate it.

Uzunur (1975) presented a review of available equations for calculating the composite roughness of ice covered channels including the assumptions inherent in each. He recommended the use of the ones by

Hancu (1967) and Larsen (1969), as he found those two to be the most technically rigorous:

$$\frac{n_t}{n_2} = \frac{1}{\sqrt{2}} \left(\frac{R}{R_2} \right)^{1/6} \left[\left(\frac{V_2}{V} \right)^2 + \left(\frac{V_1}{V} \right)^2 \left(\frac{n_1}{n_2} \right)^2 \left(\frac{R_2}{R_1} \right)^{1/3} \right]^{1/2} \quad \text{Hancu (1967) [5.3]}$$

$$\frac{n_t}{n_2} = \frac{0.63 \left(\frac{Y_1}{Y_2} + 1 \right)^{5/3}}{\frac{n_2}{n_1} \left(\frac{Y_1}{Y_2} + 1 \right)^{5/3} + 1} \quad \text{Larsen (1969) [5.4]}$$

Here, the subscripts 1 and 2 represent the values for the bed and ice affected zones, with subscript 1 referring to the smoother of these two boundaries and subscript 2 the rougher. V is the cross-sectionally averaged velocity (with V_1 and V_2 referring to the sub-section average velocities); all other variables are as previously defined. Both methods require extensive data that, as noted above, is seldom available.

Uzuner (1975) also reported on a number of simpler composite roughness equations that do not require a priori knowledge of the values of Y_1 and Y_2 ; several assume that $V = V_1 = V_2$ (a somewhat arbitrary assumption). Beltaos (2001) noted that field measurements show that “*the point of maximum velocity, which approximately delineates the ice and bed-controlled layers, is near the mid-depth, regardless of how rough the ice cover might be relative to the conventional bed roughness.*” This is conceptually consistent with the findings of Hanjalic and Launder (1972), supporting the idea that there is momentum transfer between the layers beneath the ice cover that is not considered in the simple application of a two-layer model. However, it may also explain why some of these conceptually simpler composite roughness equations produce plausible results.

In choosing a composite roughness equation from among the many available, the additional assumptions inherent in each equation should also be considered; Uzuner (1975) discusses most of these. However additional, sometimes significant, assumptions are required for a number of them, beyond what is presented in Uzuner (1975).

Figure 5.4 illustrates some of these simpler composite roughness equations for the case of channels with a large aspect ratio (for which the wetted perimeter of the ice is approximately equal to the wetted perimeter of the bed). From a practical perspective, any method that produces a total (or composite) roughness, n_t , that is greater than both n_b and n_i when n_b is equal to n_i , does not make any physical sense. This excludes both Chow's and Belokon's methods. Of the remaining methods, it is the one by Sabaneev that has gained the most wide spread use to date. It is used in most hydraulic models that employ a composite roughness approach, including the U.S. Army Corps of Engineers' HEC-RAS model.

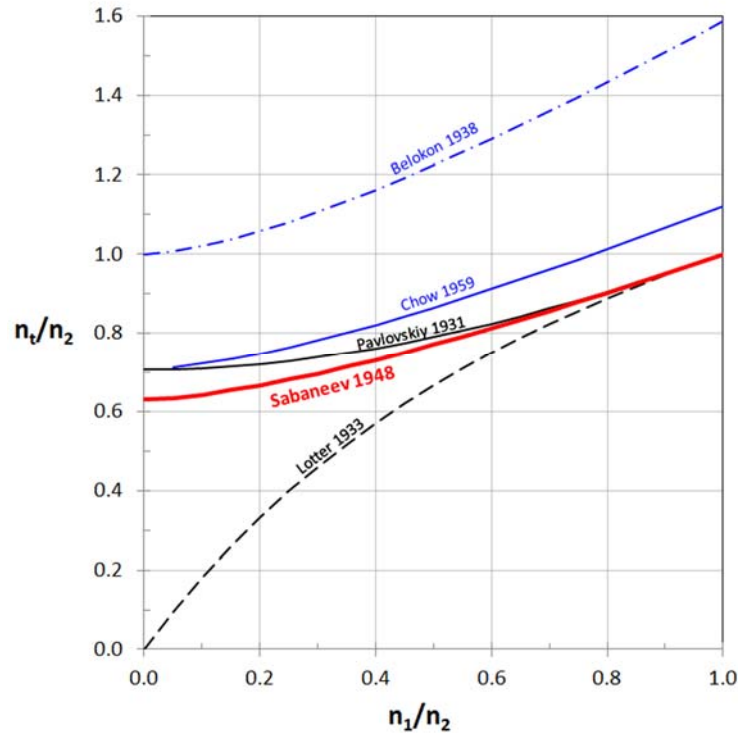


Figure 5.4 Variation of total (composite) roughness, n_t , as a function of the ratio of bed and ice roughness. In the figure, n_2 represents the rougher of the two boundaries.

Sabaneev's equation can be written as (Uzuner 1975):

$$\frac{n_1}{n_2} = \left[\frac{1 + \Phi \left(\frac{n_1}{n_2} \right)^{3/2}}{1 + \Phi} \right]^{2/3} \quad [5.5]$$

Where Φ is the ratio of the wetted perimeters of the ice and bed affected portions of the flow (i.e. $\Phi = P_2/P_1$). Ashton (1986) reported that reasonable accuracy could be obtained with Sabaneev's equation for $n_2 \leq 0.04$ and depths greater than 2 m. He also showed that Equation [5.4] (Larsen's method) reduces to Sabaneev's method when it is assumed that $V = V_1 = V_2$.

A very practical problem that arises when employing the composite roughness approach is the question of what bed roughness, n_b , to use. Bed roughness is known to vary with the discharge and depth, in part due to the consequent variations in relative roughness. It has been determined that this effect is exacerbated in the presence of an ice cover, with the bed roughness increasing as ice roughness increases (e.g. see Beltaos 2001). In many practical applications, the bed roughness used in the composite roughness equation is simply based on a calibration for open water conditions at either a similar discharge or depth; in either case this is a somewhat arbitrary approximation and it introduces additional uncertainty in the results.

It is important to keep in mind that any calibrated value of ice roughness will be limited by the approximations inherent in the composite roughness equation used, as well as by the relevance of the bed roughness assumed. Clearly there are numerous values of ice roughness that could be obtained for a given set of calibration data depending upon the choices made regarding composite roughness equation and bed roughness. However, the composite roughness will be consistent in all cases. Therefore, it is important to keep in mind that it is the calibrated composite roughness that is meaningful and defensible, and the value of ice roughness is best considered an approximate deduced parameter.

Ice Roughness from Velocity Profiles

It is possible to estimate the roughness height, k_i , of the underside of the ice from velocity profiles. Larsen (1969) presented the following relationship (Ashton 1986) based on the logarithmic Karmen-Prandtl velocity distribution:

$$k_i = 30Y_i e^{-a_i} \quad [5.6]$$

in which $a_i = V_{max}/(V_{max} - V_i)$. This approach also assumes that the maximum velocity isoline divides the bed and ice affected portions of the flow. However, it is only valid for limited roughness heights ($k_i/Y_i < 0.333$ (Ashton 1986)), as the applicability of the logarithmic velocity distribution is doubtful beyond this. This approach can also be used to determine bed roughness height.

Typical Values for Ice Underside Roughness

The roughness of the underside of the ice can change dramatically through the winter. Nezhikhovskiy (1964) determined the roughness of the developing ice cover using the composite roughness approach described above. As Table 5.1 and Figure 5.5 illustrate, he found that ice roughness increased with increasing thickness. It is important to note that these values were deduced based on the composite roughness approach using open water values for the bed roughness; therefore, they should be considered approximate.

Table 5.1 Manning’s roughness, n_i , for the underside of initial ice covers
(*adapted from Nezhikhovskiy 1964*).

Initial Thickness (m)	Manning's roughness, n_i		
	Cover formed from loose slush	Cover formed from frozen slush	Cover formed from sheet ice
0.1	-	-	0.015
0.3	0.01	0.013	0.04
0.5	0.01	0.02	0.05
0.7	0.02	0.03	0.06
1.0	0.03	0.04	0.07
1.5	0.04	0.06	0.08
2.0	0.04	0.07	0.09
3.0	0.05	0.08	0.10
5.0	0.06	0.09	-

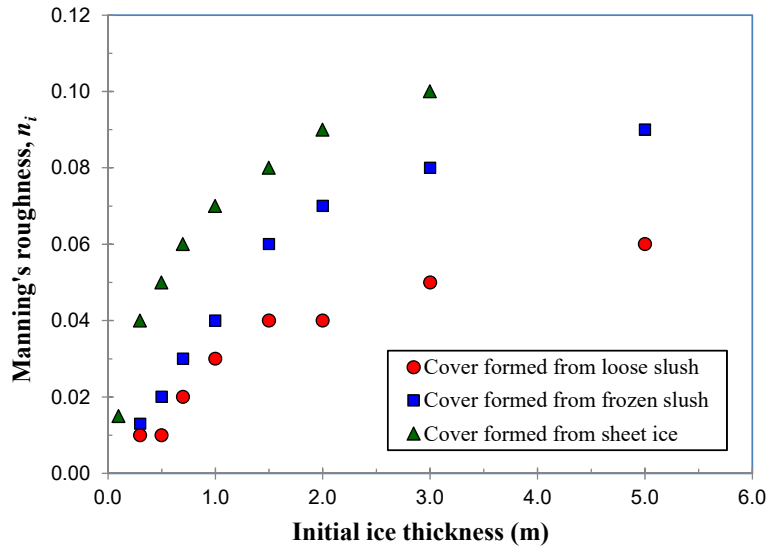


Figure 5.5 Manning's roughness, n_i , for the underside of initial ice covers (adapted from Nezhikhovskiy 1964).

Figure 5.6 shows a photo of the underside of an ice cover in mid-winter. Typically, at this time of year the ice cover is relatively smooth on the bottom, though it generally has gentle undulations and pockets. Typical values of the roughness of the underside of the ice, n_i , for this case range from about 0.010 to 0.015 (i.e. comparable to that for concrete).



Figure 5.6 Photo showing the underside of an ice cover in winter. (North Saskatchewan River photo by F. Hicks.)

Figure 5.7 shows an example of ripples formed on the underside of an ice cover. These typically form in response to turbulent heat transfer from the water, occurring when warm water (i.e. water at temperatures greater than 0°C) flows under the ice cover. The water might be warmed slightly by the sun in open leads upstream, as discussed in Chapter 3; other sources of warm water include municipal and industrial outfalls. Ripples are aligned transverse to the flow direction and their magnitudes and wavelengths depend upon the flow velocity. Ashton (1986) reported that ripple heights are typically about one tenth the wavelength and that typical values of wavelength times velocity are about 0.12 m²/s. Carey (1966) documented n_i values for rippled ice covers ranging from about 0.014 to 0.028.



Figure 5.7 Photo showing ripples formed on the underside of an ice cover during spring breakup. (Note the ice floe has been turned over.) These ripples were not typical of those described by the earlier researchers discussed above. These were relatively symmetrical with sharp peaks (amplitude: ~8 cm high) and the troughs were U-shaped with flat bottoms (wavelengths: ~18 to 22 cm).
(Mackenzie River photo by F. Hicks.)

Freeze-up and breakup ice jams present a more complex roughness feature, since the size of the individual roughness elements can approach the flow depth in these cases (especially for breakup ice jams). The underside of freeze-up accumulations tend to be smoother, since they are comprised of both frazil pans (solid ice) and the underlying frazil slush, and this slush is free to redistribute under the solid ice. For this reason, the surface texture of a freeze-up jam (or hummocky ice cover) is not likely to be a good indicator of what the underside looks like. In contrast, breakup jams are typically comprised of large, competent ice flows and

thus it has been speculated that the surface roughness might be a reasonable approximation of the underside texture.

To date, only Beltaos (2001) has successfully measured the topography of the underside of a breakup ice jam. His measurements do indicate that the variability in ice jam roughness is consistent with what is suggested by the surface appearance. Beltaos (2001) also showed that the underside roughness of ice jams was roughly proportional to the accumulation thickness, at least for ice jams up to 3 m thick. Values of n_i for ice jams were found to range from about 0.04 to 0.10; however, the validity of Manning's equation is somewhat doubtful at these extremes.

Special Considerations

A variety of practical conditions may complicate the hydraulic calculations for ice covered rivers. Primary among these is the fact that a uniform flow approximation is unlikely to be valid for any practical case. The variability of ice thickness and roughness, both spatially and temporally, generally results in a highly variable stage discharge relationship, one in which the discharge depends not only on the water level, but also on the slope of the water surface. As a result, it is generally impractical to develop rating curves for ice affected conditions, particularly during periods of highly variable thickness, roughness, and spatial extent.

During the initial development of the ice cover (e.g. border ice development), only portions of the cross-section may be ice covered (Figure 5.8). The flow hydraulics are generally more complex for this case than for a simple, continuous ice cover. Specifically, there will be a center portion of the flow for which open water hydraulics may be the most applicable, whereas near the river margins, ice covered flow hydraulics may be more applicable.

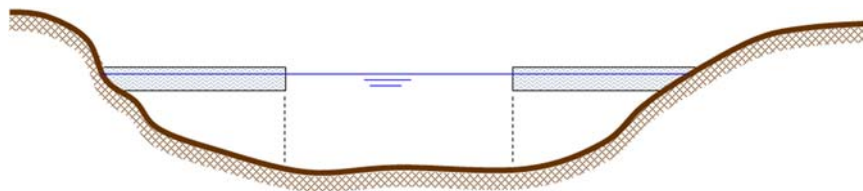


Figure 5.8 Cross-section schematic illustrating a partial ice cover.

Hydraulics of Ice Covered Channels

For channels of high aspect ratio, the effects of border ice development along the river margins may sometimes be neglected, if the proportions of the channel width affected are relatively small in comparison to the total width. In cases where ice covering part of the cross-section cannot be reasonably neglected, and details of the effects of the partial ice cover on flow hydraulics are important to determine, 2-D (depth averaged) flow modelling may be warranted.

The ice cover may also be discontinuous in the longitudinal direction, as in the example shown in Figure 5.9. In cases where the openings are few, and the length of the open water reach is comparable to the channel width (as shown in this example), the ice backwater effects dominate. A gradually varied flow analysis will typically show a negligible difference in results whether or not the open water is explicitly accounted for in the input data. In contrast, localized sections of intact ice in an otherwise open river may be important to consider, given the potential backwater effect caused by the ice.



Figure 5.9 Partial ice cover on the Mackenzie River. (*Photo by F. Hicks.*)

As was illustrated in Figure 2.18, anchor ice can occupy a large portion of the channel causing significant backwater effects. Anchor ice effectively changes the bed topography, and thus it has a very important effect on river hydraulics. Logistically, it is relatively challenging to measure

anchor ice topography, particularly on large rivers, such as shown in Figure 5.10. The temporal and spatial variability of anchor ice deposits further complicates the problem. In the absence of data describing the topography of anchor ice, the calculation of flow hydraulics for anchor ice infested waters should be considered very approximate.



Figure 5.10 Anchor ice observed on the Peace River, Alberta. Flow is from left to right and the river width is ~300m. (*Photo courtesy of M. Jasek.*)

Anchor ice can also have a significant effect on flow discharge when large masses of anchor ice release from the bed in a short period of time. Jasek et al. (2015) estimate that anchor ice release events on the Peace River in Alberta Canada can increase local river discharge by at least 10%, and up to 30%, or more, in some cases. Discharge increases associated with anchor ice release events are believed to play a key role in precipitating ice cover consolidation events during freeze-up.

Frazil ice moving under an intact or developing ice cover can also present a significant challenge for the accurate determination of flow hydraulics. At times, frazil deposits on the underside of the ice cover may be obstructing large portions of the waterway causing substantial backwater effects. However, mapping the spatial extent of frazil under the ice cover is laborious and usually impractical. Although little is known about the

Hydraulics of Ice Covered Channels

actual mechanisms of frazil transport, it is known that the spatial and temporal distribution of frazil under the ice cover can be quite variable. At present we have no practical way to deal with this problem and, as a result, the calculation of flow hydraulics for channels affected by frazil obstruction is necessarily quite approximate.

Summary

River ice can have a significant effect on river hydraulics and presents many challenges in the accurate determination of flow characteristics. The primary issues in reliably accounting for the effects of ice typically relate to practical difficulties encountered in quantifying spatial and temporal variations in ice characteristics. In addition, as it is seldom practical to obtain detailed velocity data under ice, only approximate determinations of underside ice roughness are currently possible.

Chapter 6

QUANTIFYING THERMAL ICE PROCESSES

There are typically three options available for quantifying thermal river ice processes: a full energy budget, a linear heat transfer approximation, or a simple temperature-index (degree day model). In this chapter, practical applications of each are discussed in order to provide a perspective on the practical usefulness and limitations of each. For a more in-depth treatment of the topic, see Hicks et al. (2009) and Ashton (2013).

Energy Budget Approach

The premise in applying the energy budget approach for quantifying ice formation, growth, and melt is that if all the other components of the energy budget can be quantified, the net heat gain (or loss) from a system can be attributed to ice formation (or melt). The practical challenges associated with applying an energy budget are twofold: first, the data requirements are significant and second, it is not always possible to quantify all heat components with the necessary degree of precision in order to reliably predict ice formation (or melt).

Let's begin with ice melt as an example. Ice melt commences once the ice cover becomes isothermal at 0°C throughout, in response to warming air temperatures and other heat inputs. If we express heat flux to and from an isothermal ice cover in terms of rates, we can write the energy budget for ice melt as:

$$\phi_i = \phi_s (1 - \alpha) - \phi_L + \phi_E + \phi_H + \phi_o \quad [6.1]$$

In which ϕ_i is the rate of heat flux available for ice melting, ϕ_s represents the heat flux due to incoming solar radiation, α is the albedo of the ice surface, ϕ_L is the net emitted longwave radiation flux, ϕ_E is the evaporative heat flux, ϕ_H is the net rate of convective heat transfer to the ice, and ϕ_o is the sum of the heat fluxes contributed from other sources (e.g. heat transfer from warm water, precipitation, river bed and banks, and/or groundwater). If we examine each of the heat flux components more closely, we can

begin to develop a picture of what data is needed to apply this method and what some of the practical limitations are.

Solar Radiation

We can easily quantify the amount of incoming solar radiation at any point on the earth given the latitude, declination, and time of day. However, not all of this solar radiation actually makes it to the ground. Figure 6.1 illustrates what typically happens to this incoming solar energy; some is scattered back to space, some is absorbed by the atmosphere, some comes directly to ground, and some either scatters to the ground or passes through clouds to the ground. However, whenever there is a cloud cover, substantial portions of the incoming solar radiation will be reflected back to space.

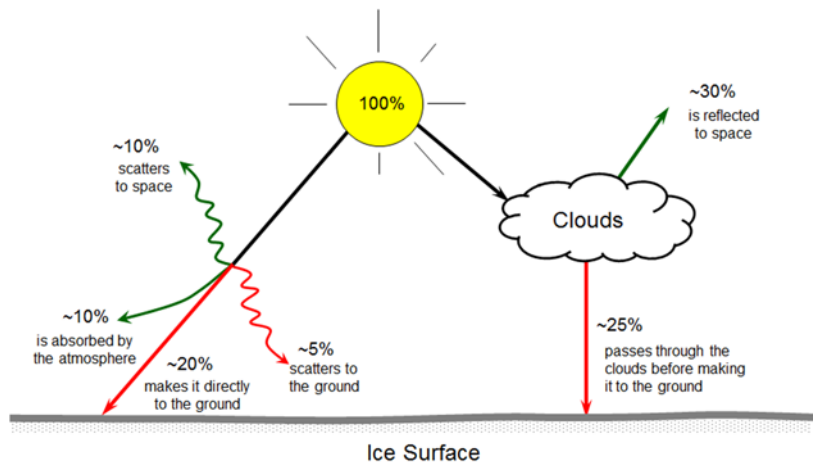


Figure 6.1 Typical disposition of solar radiation in the earth’s atmosphere (adapted from Gray 1970).

Although Figure 6.1 provides some typical (average) proportions for each of these possible outcomes, actual amounts are highly variable depending upon meteorological conditions (e.g. cloud cover and humidity). Local exposure conditions can also be an important factor (e.g. shading on narrow streams can dramatically decrease the amount of solar insolation actually received at the river surface.) Therefore, practically speaking, to quantify the amount of solar radiation that actually reaches the ground (or ice surface) at any particular location, we need to measure it.

A further complication is that not all of the solar radiation that makes it to the ground is actually absorbed. As discussed in Chapter 3, some is reflected, with the proportion reflected being referred to as the albedo. As Figure 6.2 illustrates, the albedo of an ice cover can be highly variable from location to location. Therefore, it is difficult to quantify reliably. Table 6.1 provides some typical values of albedo for various surfaces.



Figure 6.2 Variable ice albedo on the Mackenzie River ice cover.
(Photo by F. Hicks.)

Table 6.1 Typical albedos of various surfaces (adapted from Hicks et al. 2009).

Surface	Typcial Range in Albedo
New Snow	0.80 to 0.90
Old Snow	0.60 to 0.80
Melting Snow	0.40 to 0.60
Water	0.05 to 0.15
Snow Ice	0.30 to 0.55
Intact Columnar Ice	0.10
Candled Columnar Ice	0.40

Longwave Radiation

Any physical body which is at a temperature above 0°K (-273.2°C) will radiate heat. The rate, ϕ_{L-out} , follows the Stefan-Boltzmann law (Ashton 2013):

$$\phi_{L-out} = \varepsilon \sigma_{sb} T^4 \tag{6.2}$$

where, ε is the emittance (0.97 for ice, snow and water), σ_{sb} is the Stefan-Boltzmann constant (5.69 E -8 W/m² °K⁴), and T is the emitting body's temperature (°K). The longwave radiation heat energy emitted from the earth's surface far exceeds the incoming solar radiation. However, as radiation is emitted from the earth, a large proportion is absorbed and reflected back to the surface by the atmosphere. Clouds are particularly effective in absorbing and re-emitting long wave energy.

Brunt's (1934) formula, adapted by Bolz (1945) to account for cloud cover effects, provides a means of estimating the flux of longwave radiation reflected back to the earth:

$$\phi_{L-back} = (1 + k_L C^2) (a + b \sqrt{e_a}) \sigma_{sb} T^4 \tag{6.3}$$

Here, k_L is a constant (Wunderlich (1972) suggested using 0.0017), C is the cloud cover in tenths, e_a is the atmospheric vapor pressure (mb), and a and b are location specific constants. Anderson (1954) provided values of a and b from various researchers and locations (Table 6.2).

Table 6.2 Recommended coefficients in Brunt's formula (*Anderson 1954, adapted from Hicks et al. 1997a*).

Investigator	Location	a	b (mb ^{-1/2})	$a + b (e_a)^{1/2}$	r^2
Anderson	Oklahoma	0.68	0.036	0.77 [‡]	0.85
Angstrom	Algeria	0.48	0.058	0.62 [‡]	0.53
Askof	Sweden	0.43	0.082	0.63 [‡]	0.69
Dines	UK	0.53	0.065	0.69 [‡]	0.94
Eckel	Austria	0.47	0.063	0.62 [‡]	0.79

[‡]Note: example values are calculated for $e_a = 6$ mb

In snow investigations, the US Army Corps of Engineers (USACE 1959) found that $a+b(e_a)^{1/2} \approx 0.76$ for e_a values between 3 and 9 mb. For

comparison, Table 6.2 provides example values of $a+b(e_a)^{1/2}$ (for $e_a = 6$ mb) where it is seen that the various combinations of a and b produce comparable results. This information may be useful in preliminary studies where local values of a and b are not available. Ashton (1986) provides further discussion on this and alternate equations. Based on such formulae, the net longwave radiation heat flux, ϕ_L , in Equation [6.1] can be calculated as the difference between ϕ_{L-out} and ϕ_{L-back} .

Evaporation

The heat flux associated with evaporation (or condensation) occurs because the phase change consumes (or releases) heat energy. A variety of alternative approaches are available for quantifying the evaporative heat flux including the energy budget method, the water budget method, the mass transfer method, and combination methods. For this application, the energy budget method is not a viable alternative, since we are seeking the evaporative heat flux as an input to an energy budget for determining the heat available to melt (or form) ice. Since combination methods include an energy budget component, they are also not viable alternatives for this application. The water budget method is difficult to employ for this application since it is generally not easy to quantify all possible sources and sinks. This leaves only the mass transfer method. That does not mean that it is necessarily the most accurate approach, just the only viable one, practically speaking.

Mass transfer equations for estimating evaporative heat flux generally take the following form:

$$\phi_E = f(u) (e_s - e_a) \quad [6.4]$$

known as Dalton's Law (Ashton 1986), in which $f(u)$ represents some function of wind speed, u , and e_s is the saturation vapor pressure of the overlying air. The basic premise behind this approach is that the amount of evaporation is limited only by the available capacity of the overlying air to accept more water vapor, represented by the difference between the actual and saturation vapor pressures. The wind serves the purpose of carrying away moist air and replacing it with drier air (with more vapor capacity).

There are dozens of mass transfer equations that have been developed, but only a few for winter conditions. Ashton (1986) provides a few, including

the Russian winter equation for the evaporative flux (in W/m²) from water (Rimsha and Donchenko 1957):

$$\phi_E = \{6.04 + 0.263(T_w - T_a) + 2.95 u\} (e_s - e_a) \quad [6.5]$$

in which T_w and T_a are the water and air temperatures (°C), respectively, u is the wind velocity (m/s) at an elevation of 2 m, and e_s and e_a are the saturation and actual vapor pressures (mb), also at the 2 m elevation.⁹

The error in estimating the evaporative heat flux for typical ice process modeling applications can be high ($\pm 25\%$ or more). This might not be a serious deficiency, given that evaporation is often a small component of the overall energy budget for quantifying ice formation and decay; however, as we shall see next, this has important implications for quantifying the convective heat transfer rate.

Convective Heat Transfer

Convective heat transfer occurs when heat is moved from one place to another by a fluid; for example, when the wind transfers heat from warm overlying air to an ice cover. The rate of convective heat transfer, ϕ_H , is typically estimated from the evaporative heat flux, using Bowen's ratio, B (Ponce 1989):

$$\phi_H = B \phi_E \quad [6.7]$$

where:

$$B = c \left(\frac{P_a}{1000} \right) \left(\frac{T_w - T_a}{e_s - e_a} \right) \quad [6.8]$$

in which P_a is the atmospheric pressure (mb) and c is Bowen's constant (0.6°C^{-1}).

Convective heat transfer is an important component of the total energy budget when modeling ice processes. Therefore, the fact that it is has to be estimated based on the evaporative heat flux (which we know is likely to have a substantial error) can be a significant limitation.

⁹ See Hicks et al. (2009) for details on how to convert data that were measured at an elevation other than 2 m.

Heat Transfer from Other Sources

Other possible heat sources (or sinks), such as precipitation, groundwater, or turbulent heat transfer, are often neglected but can be quite significant at times. For example, 1 mm/h of snow falling on the water surface can represent a heat loss of $\sim 90 \text{ W/m}^2$. If the air temperature is quite cold, then this snow must first warm to 0°C before melting; for example, 1 mm/h of snow at -20°C can consume $\sim 105 \text{ W/m}^2$. Rain, of course, has the opposite effect. It can contribute heat to enhance the rate of snow (or ice) melt, and it can add heat to the water. Convection or conduction of heat from the bed and banks is typically small (0.1 to 0.2 W/m^2 (Ashton 1986)), but it can be important under ice. The heat conveyed by groundwater can be important (especially to fish); however, it is very difficult to measure and to quantify¹⁰.

The resulting total energy budget can be written in this form:

$$\phi_i = \phi_s (1 - \alpha) - \phi_L + \phi_E (1 + B) + \phi_o \quad [6.9]$$

An analogous energy budget could be developed to quantify heat loss for water cooling or ice formation, or to calculate the heat available to warm the ice cover to an isothermal state.

Linear Heat Transfer Approach

In this method, all of the temperature dependent terms are lumped and approximated as linear functions in quantifying the rate of heat transfer. Net incoming solar radiation is typically included explicitly, using the very same form as used in the full energy budget. For the case of heat transfer from the water to the air, this method can be expressed as follows (adapted from Lal and Shen 1989):

$$\phi_{wa} = \phi_s (1 - \alpha) + h_{wa} (T_w - T_a) + j_{wa} T_a + k_{wa} \quad [6.10]$$

in which h_{wa} and j_{wa} are linear heat transfer coefficients, k_{wa} is a linear heat transfer constant, and all other variables are as previously defined. The first term in the equation is the net incoming solar radiation and the second

¹⁰ When the heat from groundwater enters the river relatively uniformly over the entire bed area, its amount is directly proportional to the river width and thus could be specified as a function of river width.

term represents the heat flux components that depend upon the difference in temperature between the air and the water. The third term accounts for those heat flux components that may be temperature dependent but are not dependent upon the temperature difference. For example, if solar radiation data were not available and it could reasonably be assumed that the heat from the sun is correlated with air temperature, then this term could be used to approximate the solar heat flux.¹¹ The last term (the constant k_{wa}) accounts for non-temperature dependent terms such as valley shading effects.

Because the heat transfer coefficients and constant (h_{wa} , j_{wa} , and k_{wa}) must all be calibrated with site specific data, it is relatively common to further simplify equation [6.9] to the following form if solar radiation data are available:

$$\phi_{wa} = \phi_s (1 - \alpha) + h_{wa} (T_w - T_a) \quad [6.11]$$

or to this form otherwise:

$$\phi_{wa} = h_{wa} (T_w - T_a) \quad [6.12]$$

leaving just one parameter (h_{wa}) to calibrate.

In all cases, the heat transfer calculation must be applied to the appropriate area. For example, if we are calculating heat loss from the water surface on a river that has border ice present along the banks and/or frazil pans floating on the surface, then the corresponding heat flux applies only to the open (non ice-covered) portion of the river surface.

It is important to note that this heat transfer coefficient, h_{wa} , represents different heat transfer mechanisms and components depending upon the form of the equation used (e.g. equation [6.10], [6.11], or [6.12]). Consequently, the value of (and meaning of) the calibrated heat transfer coefficient will also vary depending upon the level of approximation used.

The linear heat transfer approach takes a similar form for the heat transfer between the water and the ice. For the simplest approximation, this becomes:

¹¹ Note that this is not always a valid premise. In many cases, particularly at freeze-up and breakup, warmer temperatures are associated with cloudy weather and colder temperatures with clear weather due to the reduction in net long-wave radiation emission under cloud cover.

$$\phi_{wi} = h_{wi} (T_w - T_i) \quad [6.13]$$

and for the heat transfer between the air and the ice, it would be:

$$\phi_{ia} = h_{ia} (T_i - T_a) \quad [6.14]$$

One challenge in applying this method is determining the appropriate ice temperature, T_i . Generally, the temperature of the river ice cover varies from a value near 0°C at the bottom (at the interface with the water) to something approaching the air temperature near the surface (if the ice cover is snow free). However, if we are calculating the melting of an isothermal ice cover, then it would be reasonable to assume that T_i is the melting temperature of the ice.¹²

Typical values of these linear heat transfer coefficients (h_{wa} , h_{ia} and h_{wi}) range from about 8 to 20 W/m²/°C (Andres 1988).

Cumulative Degree-Day Approach

This method assumes that the temperature dependent heat transfer terms dominate and that heat fluxes can be represented empirically by the accumulated degree-days. Both freezing and thawing degree-days can be calculated simply by summing the mean daily temperatures. For example, during freeze-up, if the mean daily temperatures on three consecutive days were -5°C, -10°C and -15°C, then the accumulated degree days of freezing would be 5, 15 and 30 °C-days, respectively.

In the case of freezing degree-days, it is a common convention to begin summing mean daily air temperatures starting with the first five¹³ consecutive days of sub-zero mean daily temperatures. The reasoning behind this approach is that, if there is a brief cold spell followed by warm weather, then it is unlikely that freezing actually had a chance to get underway and would not have persisted. There are different conventions in terms of handling the occasional above 0°C mean daily temperatures when calculating freezing degree-days. Some engineers ignore any days

¹² An energy budget or linear heat transfer approach can also be used to calculate the warming of the ice cover to isothermal conditions; Ashton (1986) provides an explanation of how to do this including consideration of snow cover on the ice.

¹³ Any reasonable number of days might be used, depending upon site specific considerations. The important thing is to be consistent in the number of days chosen for a particular site. Five days is given as an example here, as it has proven useful for sites in western and northwestern Canada.

with mean daily temperatures above freezing, others deduct that value from the accumulated degree-days of freezing. Either approach is defensible, especially give the empirical nature of the method; it is just important to be consistent.

Degree-days of thaw are also calculated simply by summing up the mean daily air temperatures, similarly starting with the first five¹⁰ consecutive days of above 0°C mean daily temperatures. However, because the sun's heat is typically much stronger at breakup, and very important to the melt process, it is sometimes better to use -5°C as the base for calculating degree-days of thaw instead of 0°C. For example, if the mean daily temperature was +3°C, then 8 degree-days of thaw would be counted for that day. In such cases, it would also be appropriate to start accumulating degree-days of thaw beginning with the first five¹⁰ consecutive days of above -5°C mean daily temperatures. Occasional days for which the mean daily temperature was below the base temperature might be neglected, or might be deducted; either approach is reasonable as long as a consistent method is employed.

The degree-day methods are highly empirical and are therefore being used less and less as more deterministic models become prevalent. One of the most common applications of the degree-day method is for estimating ice growth, using the Stefan equation approach (Ashton 1986):

$$t_i = a_1 \sqrt{ADDF} \quad [6.15]$$

where t_i is the ice thickness (m), ADDF is the accumulated degree-days of freezing (°C-days) and a_1 is a site and situation specific coefficient that has to be calibrated based on measured data. This coefficient varies depending upon the wind conditions and snow cover (due to the snow's effect in insulating the ice cover and inhibiting ice growth). Table 6.3 presents some typical values suggested for this coefficient.

In applying this method, it is important to keep in mind that it is most relevant to the growth of thermal (i.e. columnar) ice, as the Stefan equation is based on a solution of the heat transfer equation (with simplified boundary conditions). Other ice formation processes affecting the ice thickness (such as snow ice or aufeis formation on the surface, and/or frazil deposition on the ice underside) may not be well represented by this approach and, consequently, it may be difficult to determine reliable and consistent values of the coefficient for those cases.

Table 6.3 Typical values of the coefficient a_1 in the Stefan equation (*adapted from Michel 1971*).

Snow and Wind Conditions	Coefficient a_1 ($m/^\circ C^{1/2} day^{1/2}$)
Windy lakes, no snow	0.027
Average lake, with snow	0.017 to 0.024
Average river, with snow	0.014 to 0.017
Sheltered small stream with rapid flow	0.007 to 0.014

Comparison of Methods

Although the full energy budget is the most rigorous approach, it is significantly limited by intensive data requirements and by the fact that the convective heat transfer rate must be estimated based on somewhat less than optimal estimates of the evaporative heat flux. Many parameters need to be calibrated for the various relationships, which introduces a lot of empiricisms into this method. In contrast, the linear heat transfer method has much more modest data needs (air temperature and, if possible, solar radiation) and, practically speaking, fewer parameters, to ultimately calibrate.

Hicks et al. (1997a) compared the two methods for forecasting open water development on the Mackenzie River at the outlet of Great Slave Lake, and found it difficult to get good results with a consistent set of calibrated parameters using the energy budget method (Figure 6.3). In contrast, the model developed based upon the less data intensive linear heat transfer method produced very good results for a single set of calibration parameters (Figure 6.4). In addition, an extra year of calibration data was available due to the less intensive data needs of the linear heat transfer model.

Given the advancements in deterministic thermal ice process modelling in recent years, the use of the degree-day approach has become less and less prevalent, even for simple ice thickness prediction. However, it is still sometimes useful for providing an indication of comparative winter severity and for estimating the approximate timing of certain key events. For example, in a study of freeze-up on the Athabasca River, AB, Andrishak et al. (2008) found that the first ice and complete ice cover occurred at ~ 10 and ~ 50 $^\circ C$ -days of freezing, respectively, and was therefore useful for planning field team deployment.

Quantifying Thermal Ice Processes

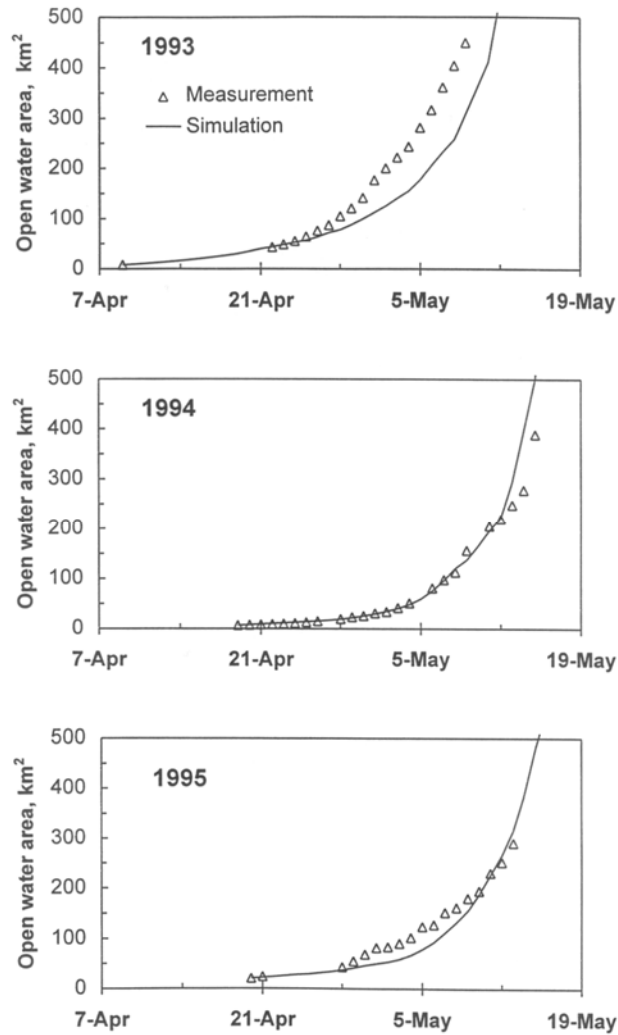


Figure 6.3 Comparison of modelled versus observed open water areas for the Mackenzie River at the outlet of Great Slave Lake based on a full energy budget model (adapted from Hicks *et al.* 1997a). Calibrated ice surface albedos were 0.45 for the early melt period and 0.35 for the late melt period. The water surface albedo was assumed equal to 0.08, Anderson's values were used in Brunt's formula, and Bowen's constant was set to 0.6.

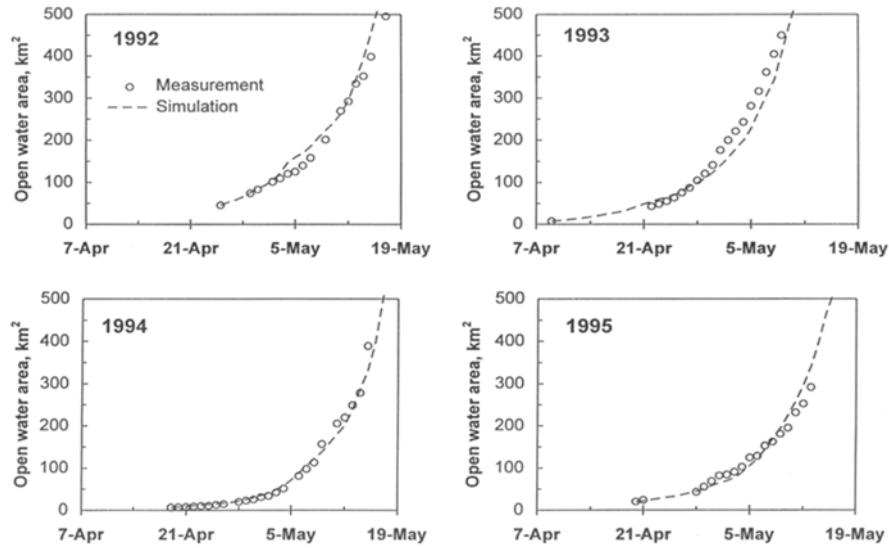


Figure 6.4 Comparison of modelled versus observed open water areas for the Mackenzie River at the outlet of Great Slave Lake based on a linear heat transfer model (adapted from Hicks *et al.* 1997a). Calibrated ice surface albedos were 0.9 for the early melt period and 0.8 for the late melt period. Calibrated heat transfer coefficients were: $h_{ia} = 8 \text{ W/m}^2/\text{°C}$ and $h_{wa} = 20 \text{ W/m}^2/\text{°C}$.

Summary

There are three basic approaches to quantifying thermal ice processes: the energy budget, the linear heat transfer approach and degree-day methods. The energy budget method is the most sophisticated and, although it is not difficult to apply, it is data intensive. Furthermore, several of the terms, such as longwave radiation, evaporation, and convective heat flux, must be quantified empirically, given the practical limitations on the amount and type of data that are generally available. For most practical applications, the linear heat transfer method provides the most feasible balance between data requirements and level of technical sophistication needed for consistent and reliable results.

Chapter 7

ICE JAM FORMATION AND RELEASE

Ice jams are significant because they can cause severe flooding at relatively low discharges, compared to those needed to cause flooding under open water conditions. Ice jam floods also tend to happen much more quickly than open water floods; water levels can rise several meters in just a few minutes. Ice jam release events are particularly dangerous, producing waves of ice and water that travel downstream at much higher velocities than the normal river flow. Although the analysis of ice jam formation and release events is beyond the scope of the typical civil engineer's duties, for any engineer designing river engineering works in northern climates, it is important to have a basic understanding of these processes.

Ice Jam Formation

Ice Jam Classification

Ice jams can be classified in a number of ways. For example, they may be classified by their mode of formation which can occur either by hydraulic thickening or by consolidation, as discussed in Chapter 2. They may also be classified by season of occurrence (i.e. freeze-up ice jams versus breakup ice jams) as illustrated in Figure 7.1. As described in Chapter 2, freeze-up ice jams occur during the ice formation period, typically when the river becomes engorged with frazil ice and pans. This may occur when there are vast quantities of frazil ice generated during a sudden cold spell when there is rapid advancement of the freeze-up front. As the length of the ice cover increases, so does the downslope component of ice weight. This weight can collapse the fragile developing ice cover before it has an opportunity to gain sufficient strength by additional freezing. The risk of such a collapse is particularly high if a period of rapid ice front

advancement during extreme cold weather is followed by sudden warming. Freeze-up jams are generally floating ice jams. Even those that do not cause flooding directly during freeze-up may cause problems at breakup, as they can present a significant obstruction to incoming ice runs.



Figure 7.1 Ice jam classification by season of occurrence. *Top: freeze-up ice jam. (Bow River, AB, photo courtesy of J. Blackburn and T. Hutchison.) Bottom: breakup ice jam. (Athabasca River, AB, photo courtesy of R. Andrishak.)*

Ice Jam Formation and Release

Breakup ice jams form in spring when the entire river experiences a complete and sustained thaw. They typically occur when strong, competent ice is exposed to a large and rapid increase in discharge, typically caused by runoff from a significant snowpack or in response to a rain-on-snow event. Because the ice accumulation forms from thick, strong ice and, typically, does not gain any added internal strength from freezing, these are usually the thickest and roughest ice jams.

Breakup ice jams can also occur during the winter months, if a mid-winter thaw causes localized segments of a river to break up. Because such thaws are typically short in duration, flow increases are not usually extreme or sustained and so, typically, these ice jams are smaller than those seen during spring breakup. However, the resulting ice jams can still cause flooding and, once cold weather resumes, these accumulations freeze in place, potentially creating a significant obstruction at breakup. It is possible that the frequency and severity of mid-winter breakup ice jams might increase as a result of climate change, should mid-winter thaws occur more frequently, and for longer durations.

Ice jams can also be classified in terms of whether they are floating or grounded (Figures 7.2 and 7.3). Grounded ice jams extend right to the river bed, leaving only the voids between the ice floes as a path for water to pass. This is much less hydraulically efficient than flow underneath the ice accumulation, causing water to back up more severely upstream.

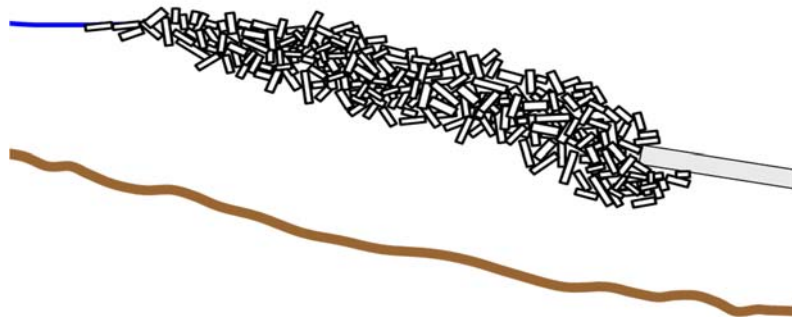


Figure 7.2 Schematic of a floating ice jam.

Grounding can occur by a variety of mechanisms. For example, it may occur due to the sudden halt of an ice run (Figure 7.4), the collapse of a

floating ice jam once the water wave passes downstream, when entrained floes get caught up under the ice cover blocking the passage of other ice floes, or when progressive shoving and thickening occurs in large or steep rivers. The portion of the accumulation that is actually grounded may not extend across the entire width of the channel or along the entire length of the accumulation. This extent of grounding depends upon a variety of factors, such as local channel bathymetry, channel planform pattern and mechanism by which the grounding occurs.



Figure 7.3 Schematic of a grounded ice jam.



Figure 7.4 Gravel bars created on the Athabasca River, AB as a result of the grounding of an ice jam toe. This occurred due to the sudden halt of an ice run. (Photo source: F. Hicks.)

Calculating Ice Jam Profiles

It's important to be able to calculate the water levels expected when ice jams form in order to be able to determine flood risk zones and to design the height of flood protection works such as dikes and floodwalls (Chapter 8). At present, we only have the ability to do such calculations for certain parts of an ice jam (Figure 7.5). Based on field and laboratory observations, the head of the ice jam (i.e. the upstream extent of the jam) is believed to behave as a hydraulically thickened accumulation, extending for approximately 1 to 1.5 times the river width downstream from the head of the accumulation. Very little is actually known about the ice jam toe region at present, as it is both dangerous and logistically challenging to measure ice jams.¹⁴ Therefore, we do not yet have equations to describe its configuration.

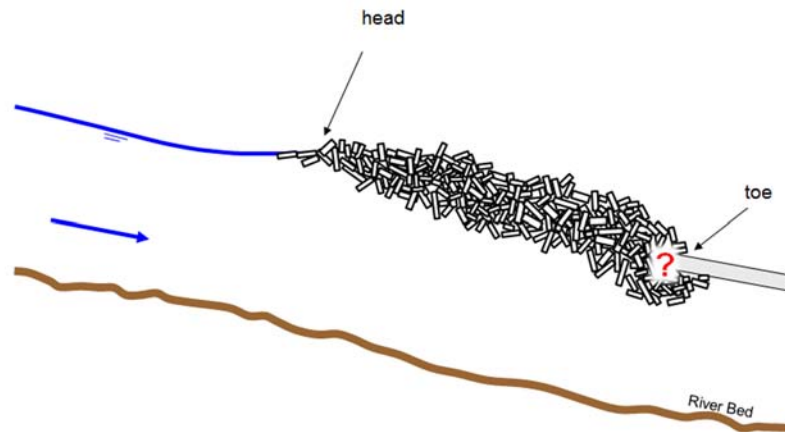


Figure 7.5 Schematic of regions within an ice jam.

Most current models of the portion of the ice jam between the head and the toe regions are based upon approximating the physics of the ice jam accumulation as a floating granular mass, using Mohr-Coulomb theory

¹⁴As discussed earlier, ice jams often release, sending waves of ice and water downstream, and so it is extremely unsafe to venture out onto an ice jam to conduct measurements. The toe region is typically the first area to open up and start moving during an ice jam release event; consequently, it is the most unsafe part of the ice jam.

(Pariset et al. 1966, Uzuner and Kennedy 1976). The resulting *jam stability equation* is then solved in conjunction with a steady gradually varied flow analysis to determine the ice jam profile. More recently, other researchers (e.g. Shen et al. 1993, 2000, She et al. 2009a) have explored more sophisticated techniques for modeling ice jams based upon viscous-plastic constitutive models and including consideration of unsteady flow. However, further research has confirmed that quite reasonable approximations of observed ice jam profiles can be achieved using the simpler approach, involving the jam stability equation and a steady gradually varied flow approximation (Healy and Hicks 1999a, She et al. 2008). Therefore, the simpler approach still remains the most prevalent method employed in current engineering practice.

Ashton (1986) provides the following form of the jam stability equation:

$$t_i \frac{dt_i}{dx} = a_2 + b_2 t_i + c_2 t_i^2 \quad [7.1]$$

where:

$$a_2 = \frac{\tau}{2 K_x \gamma_e} \quad [7.2]$$

$$b_2 = \frac{g \rho_i S - \left(\frac{2 C_f}{B} \right)}{2 K_x \gamma_e} \quad [7.3]$$

$$c_2 = \frac{-C_o}{K_x B} \quad [7.4]$$

$$\gamma_e = \frac{g \rho_i}{2} (1 - e) \left(1 - \frac{\rho_i}{\rho} \right) \quad [7.5]$$

Here, t_i is the thickness of the accumulation, B is the width of the accumulation, S is the slope of the river bed, K_x is a passive pressure coefficient normally taken as $\tan^2(45+\phi/2)$, and C_o and C_f are coefficients in the Mohr-Coulomb relation. C_o is normally taken as $(\tan \phi)$, where ϕ is the angle of internal friction of the accumulation and C_f represents the

cohesion. τ is the shear stress caused by the flow on the underside of the accumulation, ρ_i is the density of ice, ρ is the density of water, e is the porosity of the accumulation, and x is the longitudinal dimension, measured along the river bed. B , t_i , S , and τ are all local functions of x .

Various researchers have developed computer software for solving the ice jam stability equation together with the steady gradually varied flow equation. Flato and Gerard (1986) created the ICEJAM program which solved the two equations in an iterative sequence, stepping downstream with the jam stability equation from a known upstream ice thickness, and then the gradually varied flow (energy) equation stepping upstream from a known depth. The unknown toe condition was handled simply by a user specified allowable maximum velocity under the toe, V_m . Beltaos and Wong (1986) developed the RIVJAM model in which they neglected the velocity head term in the energy equation, then combined the result with the jam stability equation. They solved the combined equation stepping in either direction. RIVJAM also included consideration of seepage flow through the ice accumulation, but did not have any approximation included for the jam toe.

The U.S. Army Corps of Engineers HEC-RAS software uses an approach very similar to Flato and Gerard's (1986) ICEJAM model, but a slightly different form of the ice jam stability equation (USACE 2010):

$$\frac{dt_i}{dx} = \frac{1}{2k_x \gamma_e} \left(\rho_i g S_w + \frac{\tau}{t_i} \right) - \frac{C_o k_t t_i}{B} \quad [7.6]$$

in which S_w is the slope of the water surface and k_t is a coefficient of lateral thrust, defined as:

$$k_t = \overline{\sigma}_y / \overline{\sigma}_x \quad [7.7]$$

where, $\overline{\sigma}_y$ and $\overline{\sigma}_x$ are the vertical and longitudinal stresses, respectively.

The following form of Sabaneev's equation is used to calculate a composite roughness for the hydraulic calculations:

$$n_t = \left(\frac{n_b^{3/2} + n_i^{3/2}}{2} \right)^{2/3} \quad [7.8]$$

HEC-RAS requires the following user input to model an ice jam:

1. channel and floodplain geometry (i.e. river cross-sections);
2. carrier discharge;
3. location and length of the ice jam;
4. static ice cover thickness and water level downstream of the ice jam toe (or ice thickness and slope if a uniform flow approximation will be used for this downstream boundary condition);
5. thickness of the ice at the head of the ice jam;
6. angle of internal friction of the accumulation, ϕ (default value 45°);
7. porosity of the ice accumulation, e (default value 0.4);
8. coefficient of lateral thrust, k_t (default value 1/3);
9. Manning's n of the bed, n_b ;
10. Manning's n of the underside of the ice jam, n_i ; and
11. maximum velocity on the underside of the ice jam for toe thickness calculation, V_m (default value 1.524 m/s, i.e. 5 ft/s).

Healy and Hicks (1999b) investigated the sensitivity of the input parameters on calculated ice jam profiles, and provide advice on selecting the parameter values. The first four input parameters are generally determined based on measurements and observations; however, it is logistically difficult to measure river discharge under ice jam conditions, so this value is often an approximate estimate. Parameter 5, the thickness at the head of the ice jam, is generally estimated based on the typical thickness of ice floes contributing to the ice jam. Engineers often use the default values for parameters 6, 7 and 8, since these parameters are not readily measurable. Parameter 9, the roughness of the bed, is often taken as the calibrated open water bed roughness for the same discharge; however, as discussed in Chapter 5, this may not be particularly representative.

Parameters 9 and 10, the Manning roughness values for the bed and the underside of the ice accumulation, respectively, are typically determined based on calibration. The bed roughness is often assigned based on a calibration for an open water flow of a similar stage or discharge; however, as discussed in Chapter 5, this is definitely an approximation. The roughness of the underside of the ice jam is typically calibrated based on measured ice jam profiles at the same site. This is achieved by adjusting

the input value(s) of this parameter within physically realistic bounds, until a reasonable match between observed and computed ice jam profiles is achieved. However, the validity of the results will depend upon the values chosen for the other parameters and the reliability of the input discharge estimate. Values of the ice jam underside roughness as high as 0.09, or more, have been documented (e.g. see Carson et al. 2003). This is well beyond the upper range of validity of Sabaneev's equation¹⁵, therefore reduced accuracy should be expected. In addition, if the bed roughness selected is based on an open water calibration, this will potentially further reduce the validity of the calibrated under ice roughness.¹⁶

Some engineers vary the ice accumulation's roughness along the length of the ice jam during calibration, to improve the agreement between observed and calculated water levels. However, given the approximate nature of the analysis including: the limitations associated with using high roughness values in Sabaneev's equation, the numerous unknown and essentially unquantifiable parameters, the fact that ice jam thickness is almost never actually known, and the often considerable uncertainty in the discharge estimate, varying ice jam roughness along the length of the jam just to improve the match between observed and computed profiles is usually difficult to justify.

Parameter 11, the maximum allowable velocity on the underside of the ice jam (V_m), is used to facilitate the calculation of a continuous profile along the channel, by enabling the calculation to proceed through the toe region (for which we currently have no analytical model). Specifically, wherever the velocity calculated by the ice jam stability equation exceeds V_m , this maximum allowable velocity is used to calculate the flow depth under the ice. This approach does not have a particularly rigorous physical basis; consequently, it can sometimes produce unrealistic looking results for the toe thickness. This is not normally a critical limitation in practical applications, considering the overall approximate nature of the solution method and the typical uncertainties associated with choosing the other input parameters. However, it can make it particularly challenging to model grounded ice jams, as HEC-RAS does not account for bed scouring

¹⁵ Ashton (1986) reported that reasonable accuracy could be obtained with Sabaneev's equation for $n_2 \leq 0.04$ and depths greater than 2 m.

¹⁶ As in the case of profile calibration for simple ice covers, the most consistent and reliable approach is to simply report and compare composite roughness values, as this will at least eliminate the inconsistencies in under ice roughness values deduced using Sabaneev's equation and a bed roughness of questionable validity.

under the toe or seepage flow between the ice floes comprising the ice accumulation¹⁷ in these calculations. In some cases, large and unrealistic values of V_m may be needed to achieve a reasonable match to observed water (or top of ice) levels. However, this typically affects a very small portion of the overall ice jam length (e.g. see Figure 7.6), so as long as we keep in mind that this portion of the profile is quite approximate, we can still use the results for the rest of the profile.

Beltaos and Tang (2013) suggest simply inputting a very high value for this parameter (e.g. 10 m/s) to limit the length over which this approximation is being used. However, Healy and Hicks (1997) found that, in some cases, inputting high values for this parameter could produce erratic results. Therefore, an iterative approach might be more expedient, starting with the default value and increasing V_m gradually until a physically representative profile is achieved.

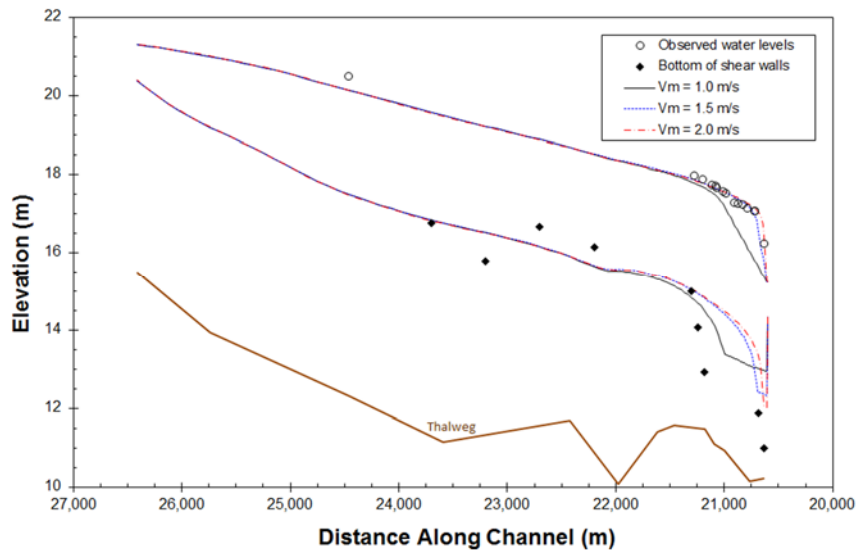


Figure 7.6 Example illustrating the effect of increasing V_m on computed ice jam profiles. In this case, the bottom of the shear walls were documented, providing an estimate of the location of the bottom of the ice accumulation. (Figure adapted from Healy and Hicks (1997); ice jam data source S. Beltaos.)

¹⁷ Beltaos and Wong (1986) did include consideration of seepage through the ice accumulation in their RIVJAM model.

As with any profile calculations, it is essential to have a sufficient number of cross-sections. There must be enough both to ensure an adequate representation of the channel geometry and to make sure that there are enough computational points along the profile to capture the water surface profile shape adequately. HEC-RAS can interpolate cross-sections to deal with the latter issue, and you should employ these interpolated cross-sections whenever the shape of the computed profile is not smooth. However, interpolated cross-sections should not be considered an appropriate way of dealing with inadequate survey data, as it is important to adequately capture the variability of the channel geometry.

To predict ice jam profiles, it is best to have first modeled (and calibrated) a few ice jams at the site. That way, hopefully, it will be possible to determine some typical values for the ice underside roughness and to assess the validity of the values selected for the other input parameters.

It is always important to make sure that the ice jam profiles that you calculate are physically realistic for your site. One way to do this is to compare the volume of ice in the computed ice jam to the available volume of ice coming in from the contributing area upstream. HEC-RAS provides the volume of ice in the computed ice jam as a model output to facilitate this check. To estimate the ice available from upstream, you need to multiply the thickness of the ice cover by the surface area of the river in this contributing reach. Of course, this means that you need to know how big the contributing reach actually is; this is one of the reasons why it is important to have some knowledge of ice processes along the river you are modelling. You should also keep in mind that not all of the ice from upstream is likely to make it down to your site. Some will melt and some will get left behind (in shear walls if there were other ice jams upstream that moved down to your site, or stranded along the banks upstream by falling water levels). It is not uncommon for the computed volume of ice to be as little as 50 percent of the total volume of ice estimated for the contributing reach. Therefore, if the computed volume of ice in your case is greater than the volume of all of available ice from upstream, then you can be pretty confident that your modelled ice jam is not realistic.

Equilibrium Ice Jams

Generally, as more ice is contributed to an ice jam, the resulting accumulation gets both thicker and longer, and the resulting top of ice and water level profiles also get higher. However, if the channel shape is not

too variable, then a developing ice jam may ultimately reach a point where the incoming ice serves to further lengthen the accumulation, but does not increase its maximum thickness or the maximum water depth along its length. In this case, there will be an equilibrium section within the ice jam in which the accumulation thickness is relatively consistent and for which the slope of the water surface is approximately parallel to the bed. This ‘equilibrium section’ of the ice jam (Figure 7.7) will also be associated with the maximum flow depth the ice jam causes. For this reason, it is sometimes useful to calculate the maximum depth associated with an equilibrium section of an ice jam to determine a “worst-case” scenario.

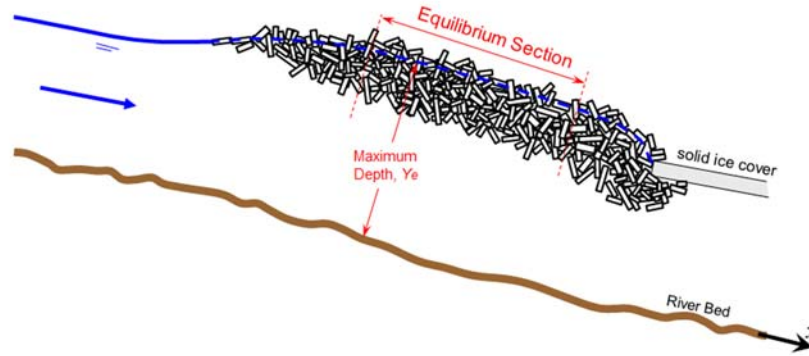


Figure 7.7 Schematic depicting the ‘equilibrium section’ of an ice jam. Note that within the equilibrium section the accumulation thickness is relatively uniform, the slope of the top of the ice accumulation is parallel to the bed (as is the slope of the water surface), and the flow depth is a maximum.

Beltaos (1983) presented a relationship for calculating the maximum flow depth associated with an equilibrium ice jam, Y_e :

$$\eta = \frac{Y_e}{SB} = 0.63 f_o^{1/3} \xi = (5.75 / \mu) \left[1 + \sqrt{1 + 0.11 \mu f_o^{1/3} (f_i / f_o) \xi} \right] \quad [7.10]$$

where, S is the bed slope (equal to the water surface slope in the equilibrium section), f_i is the friction factor of the underside of the ice jam, f_o is the composite friction factor for the flow under the ice jam ($f_o = 0.5 f_i / f_b$, where, f_b is the friction factor of the river bed under the ice jam), and μ is an internal friction coefficient which is generally believed to range

from about 0.9 to 1.2 (Ashton 1986).¹⁸ ξ is the non-dimensional discharge, defined as:

$$\xi = \frac{\left(\frac{q^2}{gS} \right)^{1/3}}{S B} \quad [7.11]$$

Where q is the specific discharge (i.e. discharge per unit width of the river) and g is the acceleration due to gravity.

This equation is a bit inconvenient, in that river engineers normally quantify the bed, ice, and composite roughnesses using Manning's n rather than with the friction factor, f . Henderson (1966) illustrates the derivation of a relationship between the friction factor and Manning's n for uniform flow, which gives:

$$f = \frac{8g n^2}{R^{1/3}} \quad [7.12]$$

Here again, as noted earlier (in Chapter 4), R is the hydraulic radius.

The equilibrium ice jam condition is analogous to uniform flow under open water conditions, in that the slope of the water surface is parallel to the bed (i.e. there are no backwater or drawdown effects in the equilibrium section). However, as with the open water case, this idealized scenario is only applicable when the channel characteristics are not changing in the longitudinal direction. As most natural channels are highly variable in shape, slope, and roughness, it may be challenging (and possibly even irrelevant) to try to apply this equation to determine worst-case scenarios for expected ice jam flood levels. Fortunately, it is often possible to assess this using ice jam profile calculations (e.g. using HEC-RAS) to conduct an equilibrium ice jam analysis. This simply involves specifying increasing ice jam lengths (for a given discharge) until a worst-case scenario is reached. Initially at least, the computed ice jam profile will get thicker and thicker and the water levels at each site of interest will get higher and higher. However, if the channel characteristics are not excessively variable, you may reach a point where lengthening the ice jam

¹⁸ Healy and Hicks (1999) conducted an extensive sensitivity analysis on this (and other parameters associated with ice jam profile calculation) and found that a value of μ of 1.0 is reasonable for most practical applications.

no longer increases water levels in the reach of interest, thus providing a worst-case scenario for the site.

There is one important caveat to using this approach for design and that is that you must be sure that there is actually going to be sufficient ice coming in from upstream to create such a big ice jam. Otherwise, your worst-case scenario might be completely unrealistic.

Ice Jam Release

An ice jam presents a formidable obstruction to the flow; this is why water levels increase and flooding often results. As more water and ice approaches, the downstream forces on the accumulation increase. Sometimes this will result in a further consolidation of the ice cover. However, depending upon the restraining forces holding the ice jam in place, it may not be able to withstand this pressure and the ice jam can release, sending a wave of ice and water to the downstream channel (Figure 7.8). Ice jam release events can also be initiated by incoming waves of ice and water from upstream; for example, those originating from the release of an upstream ice jam.



Figure 7.8 Ice jam release event on the Athabasca River, Alberta. Flow is from left to right. (*Photo by Faye Hicks.*)

The speed and severity of ice jam release events can be quite dramatic. For example, water level increases of more than 4 m have been

documented rising at rates of up to 0.8 m/min (Hutchison and Hicks 2007). In addition, wave speeds of 5 to 6 m/s are not uncommon (Beltaos and Burrell 2005a, Hutchison and Hicks 2007) and discharges can increase by a factor of 5 or more (Figure 7.9). Consequently, ice jam release events present some of the most terrifying and dangerous flood risk situations encountered. Only a small number of researchers have studied these events intensively (e.g. Jasek 1996, 1998, 1999, 2003, Beltaos and Burrell 2005a and b, Kowalczyk and Hicks 2003, Hutchison and Hicks 2007, She et al. 2009b, Watson et al. 2009); therefore, our ability to predict the occurrence of such events is still relatively limited.

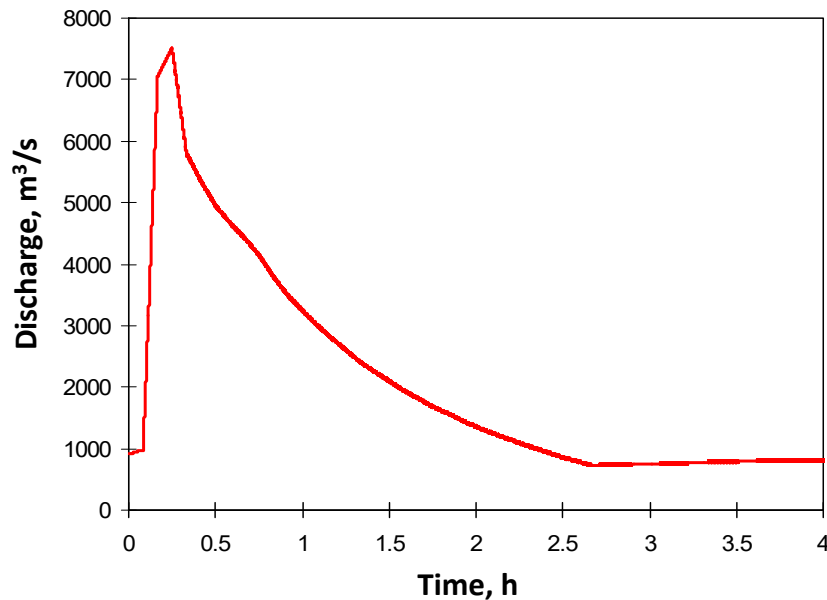


Figure 7.9 Estimated discharge hydrograph at the toe of the ice jam release event documented by Kowalczyk and Hicks (2003) on the Athabasca River, Alberta in 2002.

Ice Jam Release Mechanisms

Ice jam release events are generally classified as impeded or unimpeded (Jasek 2003). An unimpeded ice jam release event occurs when there is minimal intact ice downstream of the ice jam to interfere with the release of ice and water. In contrast, impeded ice jam release events occur when there is substantial intact ice downstream of the releasing ice jam,

inhibiting the downstream progression of released ice and water. Impeded ice jam release events are further classified as *sheet breaking fronts* or *rubble breaking fronts*. A sheet breaking front occurs when the releasing ice jam pushes the intact ice sheet ahead of it, causing fracturing and ridging (Figure 7.10). In contrast, a rubble breaking front ‘eats’ its way through the downstream ice cover, directly incorporating the broken ice into the propagating rubble mass (Figure 7.11). Jasek (2003) provides an excellent discussion of these various modes of ice jam release.

It is currently very difficult to predict precisely when an ice jam will release; however, it has been observed that open leads often develop downstream of the ice jam toe just prior to release (Figure 7.12). It has also been observed that the flow accelerates in these open leads just moments before the release.



Figure 7.10 Photo of a ‘sheet breaking front’ ice jam release event on the Athabasca River, Alberta. Flow is from left to right; the releasing ice jam (lower left) is pushing the sheet ice ahead of it, causing fracturing and ridging. The channel width shown here is approximately 300 m. (Photo by F. Hicks.)



Figure 7.11 Photo of a ‘rubble breaking front’ ice jam release event on the Liard River, NWT. The releasing ice jam breaks its way through the downstream ice cover, directly absorbing the pieces of ice it creates into the rubble mass. *(Photo courtesy of T. Prowse.)*



Figure 7.12 Photo of an open lead developing at the toe of an ice jam on the Athabasca River, Alberta (flow is from left to right). A noticeable increase in the flow velocity was observed in this open lead just prior to the ice jam release. *(Photo courtesy of Y. She.)*

Hydraulics of Ice Jam Release Events

Henderson and Gerard (1981) were the first to suggest that ice jam release events could be modeled using the classic open channel flow dam break solution (neglecting friction effects) and subsequently such events were referred to as *ice jam release surges*. Later researchers (e.g. Beltaos and Krishnappan 1982, Hicks et al. 1997b, Blackburn and Hicks 2003) found that reasonable approximations for the speed of the released water wave could be achieved by modeling the release event using the full 1-D open channel unsteady flow (St. Venant) equations (i.e. by including friction effects); however, ice effects were either neglected or handled through additional frictional resistance in these models. As a result, wave peak magnitudes and associated water levels were not well approximated. Newer versions of these models now include ice effects more explicitly (e.g. Liu and Shen 2004, She and Hicks 2005, 2006) and this has improved their ability to predict the expected peak water levels and discharges at sites downstream of the ice jam release point (Figure 7.13). Also, as our understanding of the hydraulics of ice jam release events has improved, and more scientific data have become available, it has become apparent that these are not actually steep fronted waves (i.e. they are not actual surges). Consequently, they are now referred to as *ice jam release waves*, which Jasek and Beltaos (2009) abbreviate as *javes*.

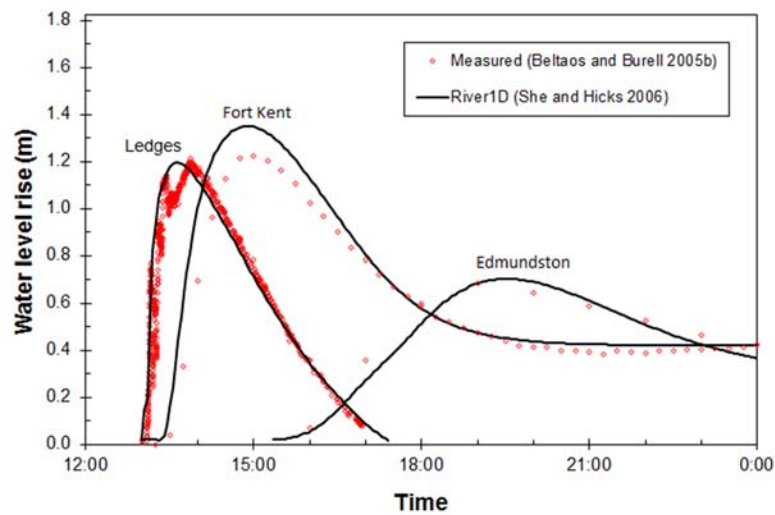


Figure 7.13 Comparison of measured water level rise at different downstream stations for 2002 Saint John River, New Brunswick ice jam release event documented by Beltaos and Burrell (2005b) to River1D model results. (Figure adapted from She and Hicks 2006.)

Ice Jam Formation and Release

Javes are initially highly dynamic waves but frictional resistance effects quickly dominate the wave propagation. As a result, the wave peaks are attenuated as they travel downstream, with peak flows and water levels decreasing in the downstream direction. This is illustrated in Figure 7.14 for an ice jam release event documented on the Athabasca River, Alberta in 2002 (Kowalczyk and Hicks 2003). At the jam toe, the water level rose 4.1 m in less than 15 minutes; by the time the jave reached station G135 (approximately 9 km downstream), the wave peak height was less than half this value. The speed of the jave also tends to decrease as it goes downstream, as illustrated by this same example in Figure 7.15. The initial wave speed was very close to the dynamic wave speed.

Jave peaks do not always appear to attenuate; some have appeared to maintain peak water levels or even increase in height as they propagate downstream. This can be explained by the fact that the ice run moving with the water wave tends to be decelerated by geomorphic features, such as islands, tight bends and constrictions. In the most extreme cases the ice stops completely, reforming a new ice jam, such as occurred in the event shown in Figure 7.14. (Note that a portion of the water wave continued propagating downstream, underneath the intact ice, while the remaining ice and water formed the new ice jam.) Even if the ice run does not actually stop, its deceleration through such geomorphological obstructions can cause the water wave to rebuild such that its peak and speed approach that of a newly released ice jam (Hutchison and Hicks 2007). In this way, peak wave heights, large discharges, and high wave speeds can be sustained over long reaches. If observational sites are sparsely located it can appear from the data that the wave peak is not attenuating, or even that it is increasing in height; however, this is because the wave attenuation between rebuilding sites is simply not being documented.

The deceleration of ice runs by geomorphological features also affects the comparative speeds of the ice and water. As a consequence, if the jave propagates over a substantial distance, the front of the water wave will eventually move out ahead of the front of the ice run (e.g. see Jasek 2003, She et al. 2009b, Watson et al. 2009). Although the speeds of both javes and ice runs have been documented separately on numerous occasions, there is still very little available simultaneous data of both types for events propagating over long distances. As a consequence, most models cannot yet reliably account for the effects of geomorphological features on ice run speeds.

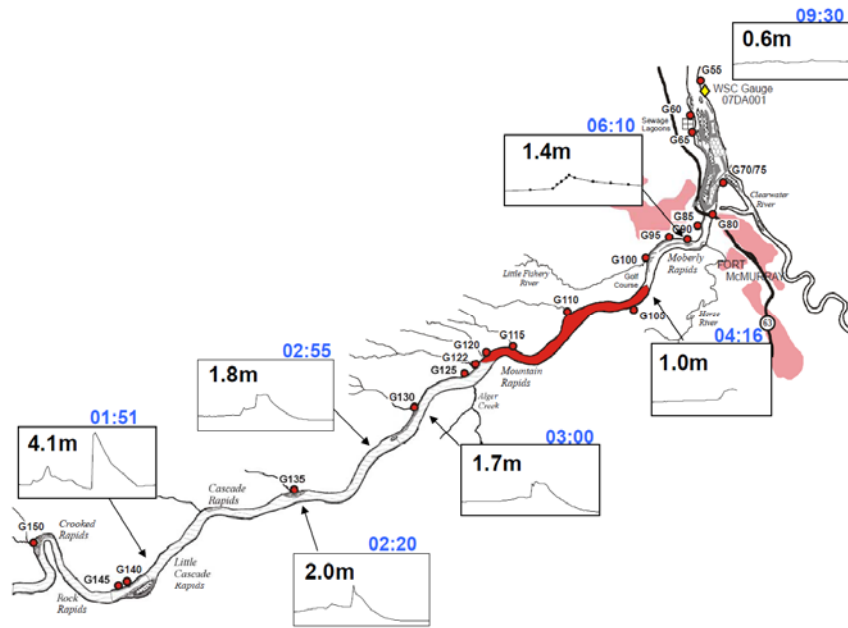


Figure 7.14 Details of ice jam release event documented on the Athabasca River, Alberta in 2002. The toe of the original (released) ice jam was at G140; the location of the reformed jam is shown in red. The inset graphs show the water level hydrographs recorded at each site along the river, with the peak height shown in metres for each. The time of the peak water level at each site is also shown above each graph (*adapted from Kowalczyk and Hicks 2003*).

Summary

Ice jam formation and release events are highly dynamic, unsteady flow processes. Despite this, quite reasonable approximations of ice jam profiles can be determined using steady flow approximations based on the maximum discharge occurring during the event. In contrast, predicting the wave peak magnitudes and speeds associated with ice jam release events requires consideration of the full dynamic equations of unsteady flow and explicit consideration of the ice effects. More data is needed to expand our knowledge and capacities in predicting these events.

Ice Jam Formation and Release

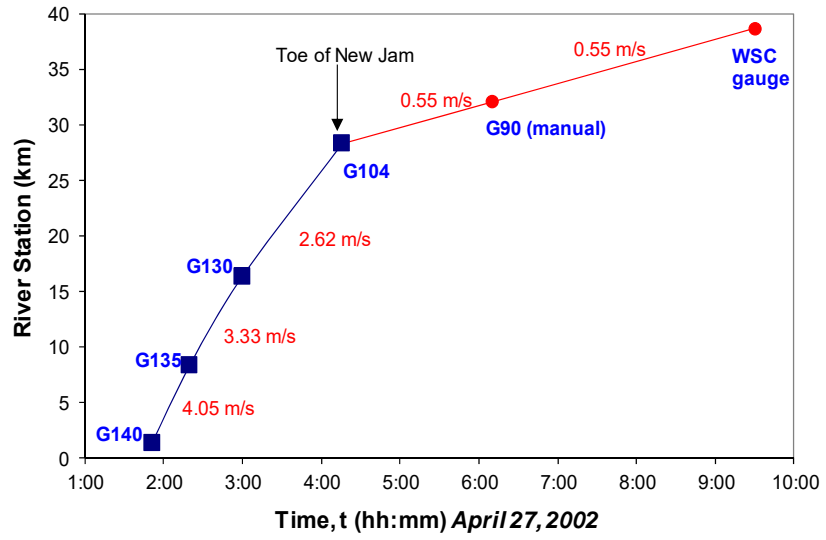


Figure 7.15 Jave peak speeds for the ice jam release event documented on the Athabasca River, Alberta in 2002 (*adapted from Kowalczyk and Hicks 2003*).

Chapter 8

ICE JAM FLOOD MITIGATION

In this chapter we will discuss the various mitigation measures available to reduce the damages caused by ice jam floods. These can be preventative measures (undertaken before a flood occurs) or reactive measures (undertaken once a flood is underway). In general, preventative measures are more effective; however, they tend to be more expensive, as well. Preventative measures can be divided into two categories: structural and non-structural. Structural methods are typically more reliable but also more expensive; non-structural methods are generally more economical but are often less effective.

Non-Structural Flood Mitigation Techniques

Non-structural measures include proactive measures, such as floodplain management, flood proofing, and flood forecasting. Other proactive measures include ice cutting, breaking, blasting, and surface treatments. Reactive measures also include blasting as well as mechanical removal.

Floodplain Management and Flood Proofing

Floodplain management typically involves conducting hydraulic analyses in order to determine the expected water levels associated with large floods. These flood levels are then delineated on a contour map to determine the extent of the flood hazard zone, and development is then restricted or prohibited in this flood hazard zone. In communities known to experience ice jams, both open water and ice jam floods should be considered, in order to determine which is expected to produce the more severe flood scenario.

For open water floods, flood hazard zones are typically assessed based on a delineation of the water levels associated with a flood discharge of a particular return frequency (e.g. for the 1:100, or 1:200, year flood). However, this approach is not suitable for the delineation of ice jam floods, because flood levels depend on ice conditions as well as the river discharge. Consequently, very severe ice jam floods can occur at discharges that would be completely harmless in the absence of ice. Given

the typical scarcity of data describing historical ice jam flood events, it can be challenging to get meaningful results using statistical analysis of historical events. However, should adequate data be available, it is important to conduct the analysis using flood levels, not discharges, since the latter does not take any ice effects into account. Gerard and Karpuk (1979) provide guidance on how to approach this problem statistically, including advice on how to incorporate historical information on extreme events. In cases where this is not practical due to data limitations, it is sometimes relevant to model the largest ice jam flood event on record and use this profile to delineate the flood hazard zone. Alternatively, it may be more appropriate to conduct ice jam profile modelling to determine the largest ice jam water levels that might feasibly occur, by conducting an equilibrium ice jam analysis using HEC-RAS (as was discussed in Chapter 7).

Because many communities were developed before the technology existed to determine flood hazard zones, and because municipalities often succumb to pressure to allow development within flood risk zones, these zones are often developed. Flood proofing measures can be very helpful in mitigating damages to buildings situated in the flood risk zone. These can include very simple measures to block openings in buildings, such as the use of plywood and/or sandbags, to cover window and door opening below the expected flood level (Figure 8.1). More rigorous measures include bracing foundation walls, installing additional structural measures to anchor buildings to foundations, and raising buildings on fill or frames to ensure all occupied levels will be above the anticipated flood level. It is important to have electrical and other infrastructure above the flood level and to ensure that doors do not trap people in the basement.

Flood Forecasting

Flood forecasting is an essential part of the flood mitigation efforts that must be undertaken for any communities that are at risk of ice jam floods. Figure 8.2 illustrates one possible breakup ice jam flood forecasting strategy. It begins several weeks ahead of the breakup season with a “preparedness” forecast. This is a qualitative forecast of the expected severity of breakup, based on site specific conceptual-empirical models. The idea is to provide residents with an idea of the potential flood severity several weeks in advance of breakup so that, if needed, they can start moving belongings from the lower levels of their homes and businesses. It also gives community officials an idea of the resources that need to be on hand to deal with an emergency (e.g. sand-bags, heavy equipment, etc.)

Once breakup is underway, a moderate lead-time (i.e. 12 to 24 hours) “event” forecast can be issued, based on ice jam release event modeling (as discussed in Chapter 7); these provide the time of arrival and magnitude of the flood wave expected in the community should an ice jam release event occur upstream. The third component is the actual evacuation forecast which provides a short lead-time warning (~3 to 6 hours) of the expected flood levels associated with the ice jam expected to form. This would involve 1-D or 2-D ice jam modeling (Chapter 7) using the discharge from the event forecast, or local experience.



Figure 8.1 Example of simple flood proofing measures: blocking low openings with plywood and sandbags. (Photo by F. Hicks.)

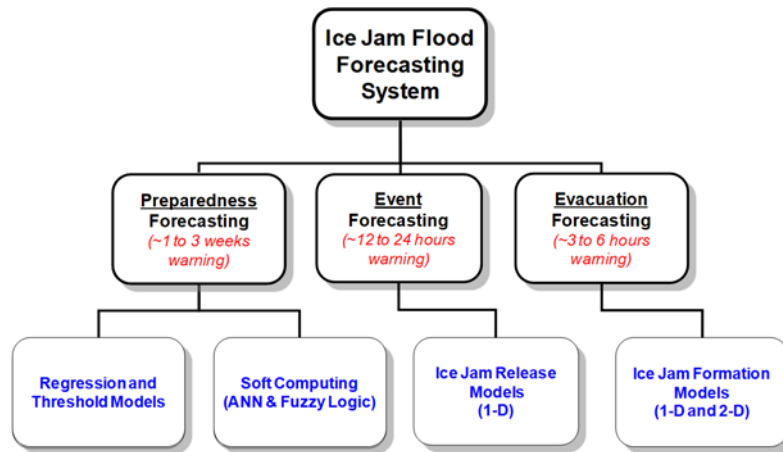


Figure 8.2 Proposed flood forecasting strategy.

Preparedness forecasts are the most challenging to develop; this is partly because so many of the factors affecting the severity of breakup are not known until breakup is already underway. Most are weather related; therefore, until we can reliably forecast the weather more than a few days in advance, preparedness forecasts for breakup severity will necessarily be quite approximate. However, Beltaos (1995) provides an excellent conceptual framework for preparedness forecasting that can be expressed in the simplest terms as follows:

Premise 1 – The ice must lift above the freeze-up level to start an ice run; otherwise, it will simply sit and melt in place (thermal breakup expected).

Premise 2 – Once an ice run occurs, an ice jam event is likely, since there are so many places for the ice to get caught up (dynamic breakup likely).

To apply this conceptual model, we must consider two things: the freeze-up level (since it must be exceeded for the ice to be free to move) and the expected spring runoff, since it is the snowmelt runoff wave that will be responsible for lifting the ice above this freeze-up level, should it happen.

Figure 8.3 illustrates the potential scenarios that might be expected. Under Scenario 1 (case of a LOW freeze-up level), the ice will likely start moving at a very low discharge, since the water level will not have to rise too much to get above the freeze-up level. Therefore, a dynamic breakup is expected for both low and high snowmelt runoff events. However, because things will get underway at a low discharge, the ice jams will occur at a relatively low flow. Therefore, only low to moderate severity ice jam events might be expected. In contrast, under Scenario 2 (case of a HIGH freeze-up level), it is going to take a substantial discharge to get the ice moving. If the snowmelt runoff event is low, then the ice is unlikely to move; instead it will sit and melt in place (i.e. there will be an innocuous thermal breakup). However, if a high snowmelt runoff event occurs, then a very severe dynamic breakup should be expected, since ice jams will occur at the very highest of flows.

This conceptual model is very useful, particularly if there is very little snow in the basin, as this means that we can be fairly confident that the snowmelt runoff will be low. The difficulties arise when the snowpack in the basin is moderate or high, since in this case, we could expect either a low or high snowmelt runoff event, depending upon the weather. If the

snow melts quickly then all of the water will come at once, and the snowmelt runoff peak will be high. If the snow melts slowly, then the peak will be lower. Of course breakup severity actually depends on many other factors as well and there are often complex relationships between all of these variables. For example, rainfall events during breakup can accelerate the rate of snowmelt and turn a moderate snowpack into an extreme snowmelt peak. For detailed information on more sophisticated ice jam flood forecasting models see White (2003), Mahabir et al. (2006, 2007), Beltaos (2009) and Zhao (2009), and their cited references.

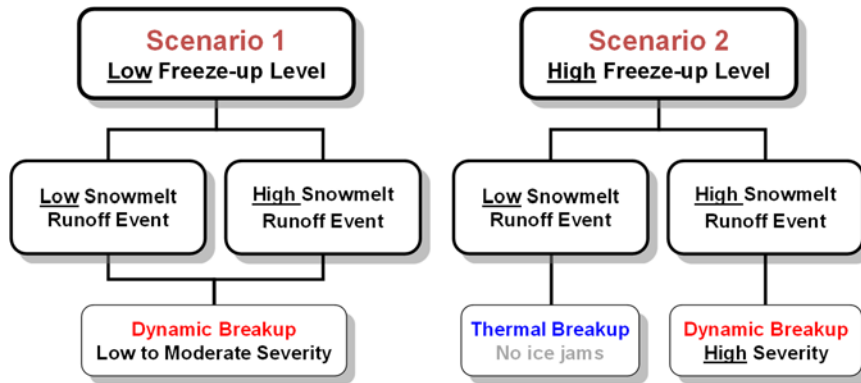


Figure 8.3 Expected scenarios in the simplified conceptual preparedness model (adapted from Beltaos 1995).

Ice Cutting, Breaking, and Blasting

Ice jams often occur where waves of ice and water encounter strong competent ice; therefore, the risk of severe ice jam flooding can often be mitigated by reducing the ice cover's strength prior to breakup. This can be achieved by cutting and/or breaking the strong, intact ice cover into discrete pieces (Figures 8.4 to 8.7). At some sites (e.g. on the Rideau River in Ottawa, Canada), blasting has been used in the past for this same purpose. On large rivers actual ice breakers have sometimes been used. In addition to reducing the ice cover's strength, mechanically reducing the intact ice cover to discrete pieces helps to accelerate clearing of ice during breakup, such that incoming ice runs can more readily pass by the community. Ice cutting and breaking also create open water areas that absorb heat quite effectively, and the warmed water further accelerates the

Ice Jam Flood Mitigation

ice cover deterioration by melting it from the underside (Figures 8.8 and 8.9).

Surface ice treatments (e.g. sand, dyes, chemicals and/or water) have sometimes been used in the past to accelerate the thermal deterioration of the ice cover. The idea is to reduce the surface albedo of the ice so that it is more effective at absorbing short wave radiation from the sun. Although this can often be as effective as mechanical cutting/breaking in reducing the ice strength in advance of breakup, it is not always an environmentally acceptable option. In addition, it is highly weather and time dependent. Therefore, mechanical cutting and breaking is more prevalent, in Canada at least.

In actual fact, it is nearly impossible to prove that any of these approaches actually work to reduce ice jam damages. However, it is important to do something when lives and property are at risk, even if the utility of what is being done is difficult to prove.



Figure 8.4 Ice cutting machine used to ‘score’ the ice cover on the Red River, Manitoba. (*Photo courtesy of S. Clark.*)



Figure 8.5 Ice surface appearance after completing of ice cutting on the Red River, Manitoba. Note the triangle-like shapes visible on the ice surface where the cutting occurred. *(Photo courtesy of S. Clark.)*



Figure 8.6 Mechanical equipment used to break up the ice cover on the Sainte-Anne River in Québec. The machine, known as an Amphibex, uses its bucket to pull itself onto unbroken ice and its self-weight will cause the ice to break. *(Photo courtesy of T. Simard-Robitaille.)*



Figure 8.7 Lines of broken ice left along the Red River, Manitoba, after completion of the ice breaking process by an Amphibex. (Photo courtesy of S. Clark.)



Figure 8.8 Ice saw being used to cut up an ice bridge on the Athabasca River, Alberta. (Photo courtesy of Alberta Environment and Sustainable Resource Development.)



Figure 8.9 Aerial view of the Athabasca River, Alberta site shown in Figure 8.8. The low albedo of the open water areas created help to accelerate the ice deterioration as the water absorbs short wave radiation and then melts the ice from the underside. (*Photo courtesy of Alberta Environment and Sustainable Resource Development.*)

Structural Flood Mitigation Techniques

Structural flood mitigation methods include engineering works such as dikes, floodwalls, channel modifications, diversions and flood control dams.

Dikes and Floodwalls

Dikes and floodwalls work by providing an embankment or wall between the river and the flood risk zone. These structures must be high enough to contain the ice and the floodwaters; the required height is typically determined by conducting 1-D or 2-D ice jam profile modeling (Chapter 7). An additional height allowance, or freeboard, must be included in the design so as to account for any uncertainties in the determination of these expected flood levels as well as to account for waves and ice ride-up.¹⁹

¹⁹ A common mistake in some jurisdictions is to plant trees on dikes. Over time, this compromises the structural integrity of the dikes and so it should be avoided.

Channel Modifications

Ice jams tend to form wherever the ice discharge capacity is locally reduced (e.g. at natural or man-made constrictions, islands, tight bends, etc.). Therefore, channel modifications aimed at eliminating these features should have the potential to reduce the likelihood of ice jams occurring. Examples of these channel modifications include: channel straightening (to remove tight bends); channel enlargement (to eliminate constrictions); and, island removal (to take out obstructions). In all cases, channel modifications affect the natural morphology of the river and adverse environmental impacts usually result. The resulting problems generally involve a loss of channel stability and can include severe bank erosion (which endangers infrastructure in and near the river) and sedimentation (which is extremely harmful to fish). Therefore, such measures should be avoided if at all possible, and permits for such works may require extensive habitat compensation elsewhere.

Ice Control Structures (ICS)

Freeze-up ice jams and hanging ice dams occur when copious amounts of frazil are generated, and they are particularly prevalent downstream of river reaches that remain open for all or most of the winter (e.g. rapids) where persistent frazil production occurs. In some cases, ice booms (Figure 8.10) can alleviate this problem by capturing frazil pans in the early freeze-up period and initiating an ice cover (Figure 8.11). Ice booms also help to create slower surface velocities, which also enhances the likelihood of early ice formation. Once the ice cover forms, frazil production stops. As a result, the total amount of frazil created is dramatically reduced.

There are ice control structures that are effective for mitigating breakup ice jam floods as well; however these work in a somewhat different way. The idea is not to prevent ice jams from occurring, but instead to move the ice jam somewhere upstream of the threatened community. This is achieved by using closely placed piers, or similar structures, to obstruct the passage of ice (Figure 8.11). These structures may also incorporate a low weir to reduce upstream velocities and to form an intact ice cover upstream, that can decelerate the ice run before it hits the piers. Ideally, the structure is located in an area where one or both overbank areas are relatively low and unobstructed so that water can easily enter the floodplain and divert around the trapped ice. This not only reduces pressure on the ice control structure, it ultimately leaves much of the

captured ice above the resulting water level and, as a result, it melts away more quickly.



Figure 8.10 Example of an ice boom in place prior to freeze-up.
(Photo courtesy of R. Abdelnour).



Figure 8.11 Example of ice cover forming upstream of an ice boom.
(Photo courtesy of R. Abdelnour).



Figure 8.12 Ice control structure on the Sainte-Anne River in Québec (*photo courtesy of the Ville de Saint-Raymond, Québec and the Centre d'expertise hydrique du Québec*).

Weirs (and even dams) can also work as ice control structures, both by reducing upstream flow velocities (encouraging ice cover development) and by obstructing the passage of ice. Weirs are considerably more expensive than the more basic pier-type ice control structures; therefore, ice control is typically a secondary benefit of a weir. For more detailed information on different types of ice control structures and other structural ice control methods, see Tuthill (1995, 2005, 2006).

Reactive Flood Mitigation Techniques

Often it is necessary to attempt reactive mitigation measures for ice jam floods. For example, this might be necessary at sites when ice jam floods occur only rarely and preventative measures are not cost effective. However, reactive measures may also be needed in communities at frequent risk of ice jam flooding simply because the resources are not available to construct flood mitigation structures.

In reactive cases, the most common measure undertaken is the mechanical removal of ice. On small streams, this can often be achieved simply by clearing ice from the channel using a backhoe working from the banks. On larger rivers, amphibious backhoes are often used (e.g. as shown in Figure 8.6); these work right in the river channel. Other possible measures include blasting; however, this is far more effective as a preventative

measure, since the explosives must be positioned on the underside of the ice to be effective and this is much more difficult to achieve once an ice jam is already present. Also, considerably more explosives are needed for the large quantities of ice and extreme thicknesses associated with ice jams. Care is also required to ensure that the sudden release of an ice jam at one location does not create a new problem for communities downstream.

Summary

Ice jam floods can cause water levels to rise several meters in just minutes and that, combined with the threat to structures caused by rapidly moving ice floes and ice sheets, make ice jam floods particularly dangerous. Consequently, the most effective means by which to prevent or mitigate ice jam flood damages and threat to life, is through effective and strict floodplain management practices. Where that is impractical, dikes, flood walls, and/or ice control structures may be used. Reactive measures, such as the mechanical removal of ice can also be employed. However, preventative measures are almost always more effective.

Chapter 9

DESIGNING AND IMPLEMENTING A SAFE FIELD PROGRAM

If you have ever worked on a river, then you know that no two are the same. You also know that it is essentially impossible to design any river engineering works without first obtaining site specific data for the river site in question. Whether you are looking to determine the expected water levels for a bridge design or seeking a suitable location for a river water intake, you first have to know details of the channel shape, slope, flows and bed material. This is also the case when river ice is involved. Although there are now sophisticated computer models for predicting river ice processes and ice cover formation and clearing, none of these have any hope of providing even remotely reasonable predictions if you have no information on the nature of ice processes that occur at your site. As a result, the first step in any river ice engineering project is to conduct field measurements and observations of river ice processes.

In the following discussion, it is assumed that you already know how to conduct basic measurements of rivers including cross-section surveys, water surface profile measurements, and streamflow measurements. It is also assumed that you have a basic understanding of the equipment typically used to conduct these measurements. Similarly, it is assumed that you have a basic understanding of hydrology and the instruments used to conduct basic hydrologic and meteorological measurements.

In this chapter you will learn about the various types of data needed for ice studies and how to collect each type. In all cases, it is especially critical to conduct these measurements safely. Andrishak and Hicks (2015) provide general advice on how to work on river ice covers safely. However, it is essential for all workers to get certified ice safety training before venturing onto a river ice cover.

Basic Data Needs

The relevant data types fall into four categories: geomorphological data, meteorological data, hydrometric data, and ice process data. Each of these will be discussed below.

Geomorphological Data

Most civil engineers recognize the importance of documenting a basic physical description of the river, in terms of measuring channel shape (i.e. bathymetry or cross-sections), channel slope, and roughness features, as these are all essential for conducting hydraulic modelling. Assuring that you can adequately model the study reach for open water conditions is usually an essential first step in assessing these data needs. However, the geomorphological features of a river also have a profound effect on river ice processes. Therefore, the first thing you need to do in any river study (whether or not ice is involved) is to place the river in its geomorphological context. Specifically, what are the bed and banks of the river comprised of (i.e. boulders, cobbles, gravel, sand, cohesive soils, or a combination of two, or more, of these)? What are the major geomorphological features that can affect the river hydraulics and ice processes (e.g. rapids, pools and riffles, meanders, islands, constrictions, bifurcations, slope changes and discontinuities)? A geomorphological assessment will not only aid you in designing your channel surveys, it will assist you in determining what river ice processes are expected, and in what sequence these processes are happening and where. An excellent and essential reference for this is the global river ice classification model presented by Turcotte and Morse (2013).

Meteorological Data

Since weather conditions drive all river ice formation and melt processes, meteorological data is fundamentally vital to most river ice studies. The types of data needed will depend upon the nature of the study undertaken and the approach used to quantify these thermal processes. Therefore, as a first step in planning these measurements, you should be familiar with the various methods available for quantifying thermal ice processes (as described in detail in Chapter 6).

Once you have decided on a method, you can make a list of the various data types needed. The most common of these will be air temperature and solar radiation. In Canada, air temperature data are continuously collected

Designing and Implementing a Safe Field Program

at Environment Canada's meteorological stations across the country²⁰ and strong correlations are generally obtained when comparing data between stations in a region. As a result, you can usually obtain reliable temperature data for most sites in or near to populated regions. Although air temperature conditions will be affected by local exposure conditions at river level, these published data are generally sufficiently applicable for most practical studies.

Data on incoming solar radiation is considerably more difficult to obtain, as this parameter is not generally measured at government stations, at least not in Canada. At some stations, data on daily hours of bright sunshine may be available for the period prior to 1996; based on manual observations conducted using sunshine balls (Figure 9.1). However, since automation, incoming solar radiation data have not been collected, as the available devices (e.g. Figure 9.2) do not meet Environment Canada's quality standards. In addition, these data usually do not correlate well between stations, even if they are in relatively close proximity, because of the highly localized and variable nature of cloud cover conditions. As a result, if you need this type of data, you must generally collect it yourself right on site.

Given the importance of snow in reflecting solar energy and in insulating the ice cover, knowledge of this parameter is also essential for most river ice studies. In addition, quantifying the snow water equivalent (SWE) of the snowpack in the basin is essential information needed for estimating spring runoff during river breakup. Although data are available from automated government weather stations and snow courses, snow depth can vary greatly depending upon exposure conditions and so tends to be relatively site specific. Therefore, it is always a good idea to obtain local measurements, as well. Because snow density varies both spatially and temporally, the most accurate way to determine the SWE of the snowpack is to weigh a core sample taken of the entire snow depth. This can be done using a snow sampler. However, supplemental estimates can be obtained using depth measurements alone; these are particularly useful for documenting spatial variability.

Other types of meteorological data that may be useful include wind speed, relative humidity and atmospheric pressure. These can usually be obtained from government weather stations. Satellite and regional/global

²⁰ Canadian data can be accessed at this link <https://weather.gc.ca>; in the U.S.A., weather data is available at <http://www.nws.noaa.gov/>.

model data is also available and can be downloaded for your site and/or basin.



Figure 9.1 Prior to 1996, sunshine balls were used to obtain manual measurements of hours of bright sunshine at Canadian meteorological stations. A glass ball (top photo) would focus the sunlight which, when sufficiently strong, would burn a hole in the replaceable card (bottom photo) providing an indication of the number of hours of bright sunshine. This could then be converted to an estimate of incoming solar radiation based on location and date.
(Photos by F. Hicks.)



Figure 9.2 A pyranometer can be used to obtain automated measurements of incoming solar radiation. (*Photos by F. Hicks.*)

Hydrometric Data

Hydrometric data includes water levels, water velocity, and river discharge measurements. As discussed earlier, you will need sufficient data to adequately calibrate an open-water hydraulic model of your river reach before conducting any analyses considering ice. During the ice affected seasons, you will also need details of water levels, velocity, and discharge. Obtaining such data under ice-affected conditions can be quite challenging, especially during periods of variable ice conditions, such as during freeze-up, mid-winter thaws and spring breakup. Wherever possible, it is desirable to automate the measurements, both for safety and to minimize costs (as manual measurements tend to be quite labour intensive).

Water level data are relatively easy to obtain using automated equipment, especially if you do not need the data on a real-time basis (i.e. as it occurs). Various self-contained devices are available that record water pressure that can readily be converted to a depth, since it is generally reasonable to assume a hydrostatic pressure distribution in typical river scenarios. However, these devices measure total pressure, and therefore vary in response to atmospheric pressure variations as well as to water depth changes. Therefore, it is essential to correct the data taking atmospheric pressure changes into account. You can use your own barometric pressure

sensor to document the atmospheric pressure variations, or you can obtain data from a nearby government weather station.

The primary challenge in measuring water levels during ice affected conditions is the threat of damage to the sensor, or even loss of the sensor, due to moving ice. Dr. S. Beltaos, and his colleagues at Environment Canada, devised a means of minimizing this risk by enclosing the sensors in heavy metal cases and then embedding them in the river bed at low flow. Figure 9.3 shows an adaptation of this approach employed by the University of Alberta river ice research group.

Once the sensor is in place, it is important to record its exact position and elevation, typically using a Real Time Kinematic Global Positioning System (or RTK GPS). It is also essential to document the referenced elevation of the water level at the site at the time of installation, at removal, and as often as practical during the intervening period. This facilitates conversion of the data into actual water levels, and provides a means of checking against instrument drift.



Figure 9.3 *Left photo:* metal case for protecting the water level recorder (self-contained pressure sensor and datalogger shown in the foreground). Note that the ends of the case are covered only with a wire mesh, so that the sensor, placed inside, can detect the water pressure changes. *Right photo:* the case is placed (flat side up) in the river bed during low flow. If the bed material is coarse, then manual excavation and backfilling may be required. If the bed material is fine, then it may be possible to just push the casing into the bed. (A silt sock should be placed around the sensor if it will be exposed to fine sediments.) (Photos' source F. Hicks.)

In some cases, such as flood forecasting applications, it is essential to access the data on a real-time basis. Where practical, this can be achieved using acoustical sensors; these measure the water level by determining the time taken for an emitted sound pulse to reflect off of the water or ice

Designing and Implementing a Safe Field Program

surface and return to the sensor. If a suitable high bank is available, these can be mounted on a boom and suspended over the river (as shown in Figure 9.4). Alternatively, they can be suspended from some other structure, such as a bridge. This device can be wired to a datalogger on high ground and the data downloaded manually as needed, or it can be connected to a communications system (e.g. wireless phone data or satellite link) for remote data acquisition. Here again it is essential to document the water level at the site at the time of installation, at removal, and as often as practical during the intervening period.

Knowledge of river discharge is essential to most hydraulic analyses and should be measured whenever safe and practical. Generally, the principles of streamflow measurement are the same in winter as in summer, though the logistics can be considerably more challenging. When there is an intact ice cover that can be safely traversed, then it is possible to measure flow velocity by drilling holes in the river ice cover to allow access of the current meter to the flow underneath. Currently the most prevalent instruments for measuring flow velocity are Acoustic Doppler Velocity (ADV) meters and Acoustic Doppler Current Profilers (ADCPs) (Figure 9.5).



Figure 9.4 Acoustic water level sensor mounted on a boom and suspended over a river. (Photo courtesy of J. Nafziger.)

The usual practice is to measure the depth-averaged velocity at 20 to 25 vertical transects across the river, just as is done in the direct measurement of discharge under open water conditions. Each depth-averaged local velocity is assumed to be representative of the average velocity of the sub-area extending halfway to each adjacent measurement transect. Multiplying this depth-averaged velocity by the corresponding sub-area (i.e. the local flow depth times the width of the sub-area measured halfway to each adjacent transect) provides the sub-area discharges that can then be summed to get the total river discharge. Transects are spaced such that each sub-area contains no more than 5% of the total discharge.

Current meters provide point velocity measurements and the proper approach is to measure the velocity at 0.2 and 0.8 of the flow depth under the ice. The depth-averaged velocity is then calculated as the average of these two point measurements. Hicks and Steffler (1996) provide an explanation of why these particular points are appropriate for two-point measurements, as well as details of the correct measurement points for three-point measurements. Where the flow depth is less than 1 m (~3 feet) a single point measurement, taken at 0.6 of the flow depth below the bottom of the ice, is representative of the depth-averaged velocity.



Figure 9.5 *Left:* Acoustic Doppler Velocity (ADV) current meter used for measuring flow velocity at a discrete point. *Right:* Acoustic Doppler Current

Designing and Implementing a Safe Field Program

Profiler (ADCP) used for measuring the average velocity over the full depth.
(Photos' source F. Hicks.)

In extreme cold weather, it can be challenging to conduct a complete discharge measurement. Drilling 20 to 25 holes in very cold ice is highly time consuming, and instrument batteries do not tend to hold up well under severe cold conditions. Therefore, in some cases, it may be necessary to resort to fewer measurements, obtaining an approximate estimate of the discharge instead of a precise measurement. Hicks et al. (1995) found that the discharge estimate obtained using only 5 holes was less than 10% different from the value obtained using the usual 20 to 25 holes. When faced with the prospect of having no discharge data, the alternative of an approximate measurement with only 5 holes is highly preferable. However, to achieve reasonable results, it is important to space the measurement locations across the channel such that each captures no more than 20% of the total flow.

The question often arises as to how to automate discharge measurement for ice affected conditions, such as is done for the open water case. In particular, the usual practice is to measure both the stage (i.e. the water level) and the discharge over a wide range of flows and to plot the data on a graph. If the flow is well approximated as uniform, then there will be a unique relationship between the stage and the discharge; this is called a *rating curve*. This rating curve enables the discharge to be determined on a continuous basis merely by measuring water level. Unfortunately, as noted earlier, the highly variable nature of river ice covers (in terms of thickness, roughness and extent) means that the flow is never well approximated as uniform and thus unique (single-valued) rating curves cannot be obtained. Figure 9.6 presents an example of this using data from the Liard River in northern Canada. The dots and symbols in the figure represent direct discharge measurements under the winter ice cover, plotted against the corresponding measured water level. As the data show, the ice creates significant and highly variable backwater conditions, producing considerable scatter.

Rating curves cannot be developed for ice affected conditions because the flow is gradually varied, and thus not well approximated by a uniform flow assumption. Specifically, the discharge is dependent upon the water level and the water surface slope, rather than just upon the water level. Hicks and Healy (2003) compared a variety of methods for automating winter discharge measurement including hydraulic modelling and stage-fall analyses.

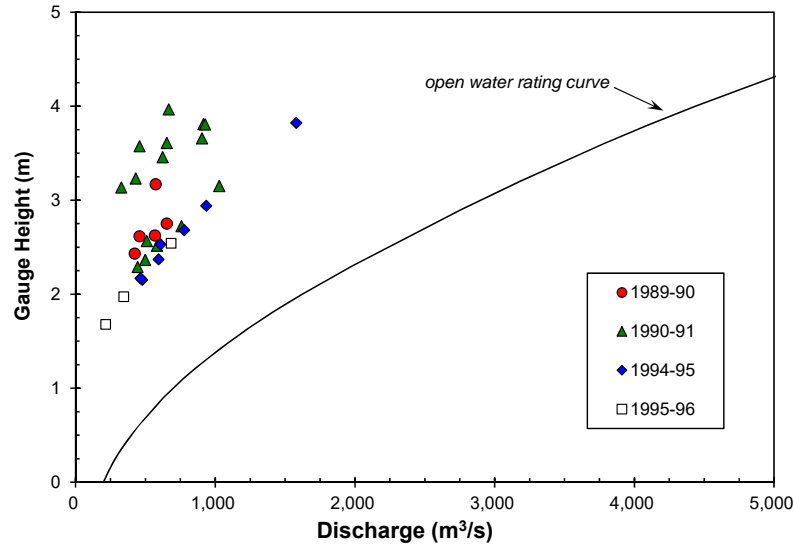


Figure 9.6 Comparison of an open water rating curve (solid black line) and the stage-discharge data pairs for ice affected conditions. (*Liard River data source: Water Survey of Canada.*)

Recently progress has been made in developing index-velocity methods for winter discharge automation (e.g. see Healy and Hicks 2004 and Morse et al. 2005); these involve continuous measurement of a point or depth-averaged velocity at a key location in the cross-section which has been shown (empirically or theoretically) to provide a good representation of the average flow velocity for the entire cross-section. In addition the water level is monitored continuously (as is done for the open-water case) to enable calculation of the flow area based on known channel geometry at the site. The discharge is then calculated as the product of the velocity and the flow area. Continuous measurement of the index velocity can be achieved using an ADCP positioned on the river bed at the appropriate location. However, this is usually only practical when the ice is stationary, as there is always a risk of damage to or loss of equipment that is exposed to ice jams or ice runs.

During periods of major ice movement, such as occurs during freeze-up and breakup, it is not really safe or practical to conduct direct discharge measurements. Therefore, this is the most difficult time to obtain discharge measurements, despite the fact that this is generally the most critical time such data are needed. The index-velocity method can be adapted usefully in some cases, as long as the ice floes are drifting freely

Designing and Implementing a Safe Field Program

and not inhibited by the bed and banks or by interactions with other ice floes. This is because the surface velocity is an index-velocity of a sort itself; specifically, the surface velocity in straight sections of relatively wide, shallow rivers is typically about 1.15 times the average flow velocity for the cross-section. If the ice is freely flowing, then ice floes near the middle of the channel will be moving at this surface velocity and measurements of their speed will enable a reasonable estimate of the mean flow velocity that can be multiplied by the flow area (determined based on known cross-section geometry and a measured water level) to obtain a reasonably good discharge estimate. These ice flow velocity measurements can be conducted by physically tracking the time that the ice floes take to travel a known distance (e.g. based on map measurements) or by more sophisticated instruments such as specially adapted radar guns, similar to those use by police to catch speeders (Figure 9.7).

Ice Process Data

Documenting the characteristics of the river ice, primarily ice thickness and top of ice elevation, are critical to both hydraulic and ice process modelling that may be required for your project. Measurement of water temperature is typically grouped under ice process data as well, as it too is fundamental to ice process modelling. It is also important to document ice cover formation and breakup processes.



Figure 9.7 Specially adapted radar guns can be used to measure the velocity of floating ice pans and moving ice floes. (*Photo source: F. Hicks.*)

A variety of sensors are available for automated measurement of water temperature and the type you choose will depend on how accurately and precisely you need to measure the water temperature. For most practical ice process modelling applications we only need to know when the ice temperature reaches 0°C as this is when we can expect ice formation to begin. Sensors capable of tracking the temperature to within $\pm 0.2^{\circ}\text{C}$, or better, are relatively economical ($\sim \$100$ each). However, for more rigorous scientific studies, or practical freeze-up studies where supercooling must be documented, more expensive sensors will be warranted (usually costing $\$1000$ or more each). Nafziger et al. (2013) provide a comprehensive review of the capabilities of a variety of commercially available water temperature sensors.

Ideally, the water temperature should be documented at multiple sites along the study reach (e.g. Figure 9.8). This is especially important on regulated rivers where warm water is being released from a reservoir, as it is important to document the water cooling along the river.

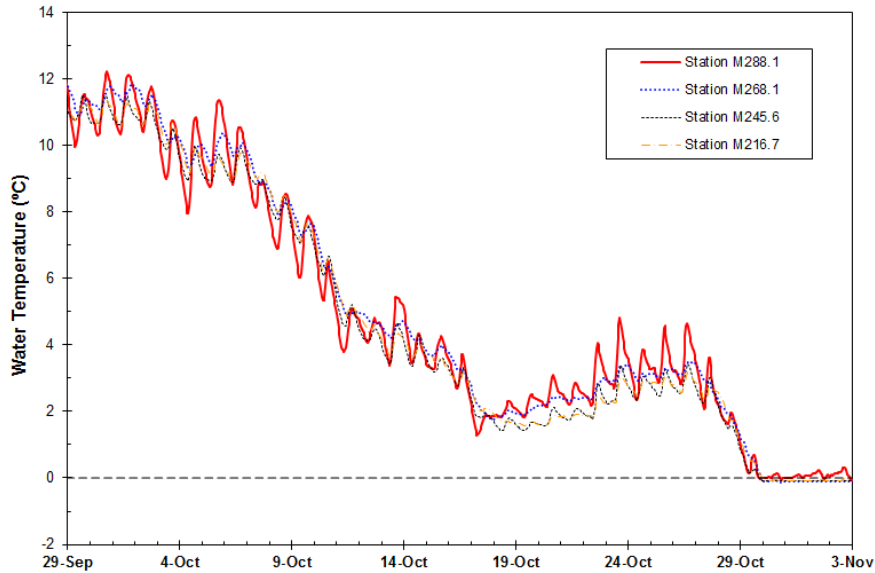


Figure 9.8 Water cooling measured during 2006 freeze-up on the Athabasca River in Alberta. (Data source: *Andrishak et al. 2008.*)

As with any sensor measurements conducted on ice affected rivers, the major concern is loss of equipment (and data) as a result of ice movement or impact. On small streams, this may be prevented by tethering the instrument to a tree on the bank using a coated steel cable (e.g. a length of clothesline cable) as shown in Figure 9.9. However, care should be taken not to leave the cable exposed, especially above water, as it may present a tangling hazard to some animals. Concealing the mooring cable can also help to reduce the risk of theft. Stronger cables may be employed on larger rivers, although it may be difficult to find coated steel. Exposed metal can be expected to accumulate anchor ice that may lift and break the cable.²¹ It is generally desirable to have a mix of self-contained sensors (with on-board data logger) and sensors connected to data loggers placed well above expected ice levels. The latter provide data, whether or not the sensor itself is lost but are generally much more expensive per station.

Once ice starts forming, it is often useful to document the increasing surface concentrations of frazil pans and the lateral growth of border ice. This can be done using photographs taken from an aircraft but, as the

²¹ Coatings (e.g. plastic) may reduce or delay anchor ice accumulation on these cables.

flights are generally expensive and often impeded by bad weather, it is generally worthwhile to supplement these data using ground based time-lapse cameras positioned at key sites along the river. Figure 9.10 shows a typical camera setup, which includes a half section of plastic pipe positioned above the camera to act as a snow shield. Figure 9.11 presents an example of the ice concentration data that can be obtained.



Figure 9.9 Water temperature sensor installed on a small creek. Here, the sensor has been attached to a concrete block, for ballast, and tethered to the bank with a coated steel cable. (*Photo courtesy of J. Nafziger.*)

Game cameras offer a relatively inexpensive option for this application, particularly if many observational sites are needed. However, most do not provide useful images at night and this can be particularly problematic at higher latitudes where the daylight hours are quite limited, especially considering that night is when heat loss is generally highest and ice formation most prevalent. However, for most applications, sufficient data is obtained for practical purposes.

For more in-depth studies, where continuous surface ice concentration data are needed, an ice profiling sonar can be employed. Figure 9.12 shows an example equipment platform ready for deployment onto the river bed. It includes two acoustic ice profiling sensors (on the left) and an ADCP (on the right). Notice that all metal surfaces on the equipment platform have been covered with plastic (affixed using contact cement) to minimize or delay the adherence of frazil ice (which could accumulate and float the platform).



Figure 9.10 Game camera installed on tree for ice process documentation.
(Photo courtesy of J. Nafziger.)

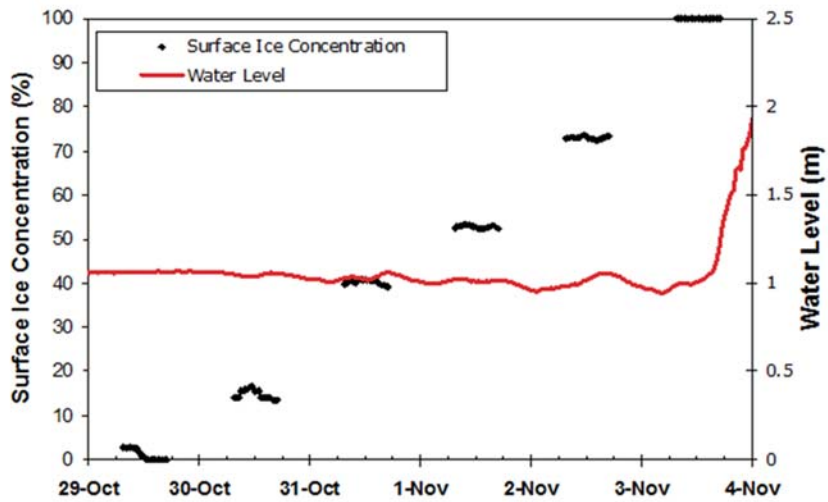


Figure 9.11 Surface ice concentrations on the Athabasca River, Alberta, derived from time-lapse camera data. (Figure courtesy of N. Abarca.)



Figure 9.12 Example setup for deployment of shallow water ice profiling sonars for surface ice measurement. (Photo courtesy of T. Ghobrial.)

Figure 4.2 showed an example of the type of data that can be obtained using an ice profiling sonar aimed upward from the river bed. This data includes details of the frazil pan thicknesses and concentrations. The bottom of the frazil pans are detected acoustically and, in this particular diagram, their thicknesses appear as vertical red lines. Surface ice concentrations can be determined continuously as the proportion of time that frazil pans are detected compared to the total observation period. In addition to surface ice concentrations and frazil pan thicknesses, the ice profiling sonar can also provide data on pan and raft lengths, if surface velocity is measured simultaneously. This is the reason for deploying the ADCP with the ice profiling sonar, as seen in Figure 9.12. Jasek and Marko (2007) and Ghobrial et al. (2013a) provide details of deployments of, and data obtained, using ice profiling sonars on large prairie rivers.

In addition to point observations of developing ice conditions, it is always useful to develop maps of the ice coverage during variable ice conditions (such as at freeze-up and breakup). Most commonly this information is obtained by flying along the river and photographing the surface ice conditions along the entire study reach. This information can then be transferred to maps, preferably using Geographic Information Systems (GIS) as shown in Figure 9.13. Considerable success has also been achieved using satellite radar for documenting and classifying surface ice conditions, particularly at breakup (for examples, see: Leconte and Klassen 1991, Weber et al. 2001, Gauthier et al. 2001, Tracy and Daly

Designing and Implementing a Safe Field Program

2001, Pelletier et al. 2001, Jasek et al. 2003, Unterschultz et al. 2009, and van der Sanden and Drouin, 2011).

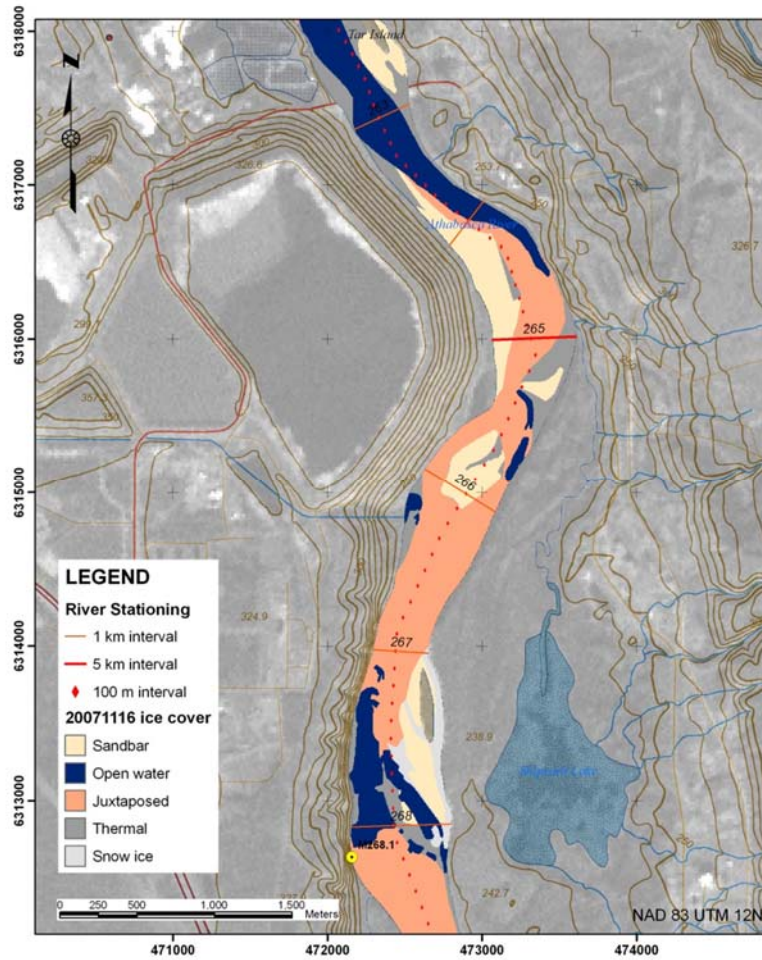


Figure 9.13 Example of GIS map documenting freeze-up ice conditions on the Athabasca River. (Adapted from Andrishak et al. 2008.)

Where local regulations permit, small drone aircraft can provide a very inexpensive means of monitoring ice conditions from above. Figure 9.14 illustrates an example of this type of small aircraft and Figure 9.15 shows an example photo taken during freeze-up on the Peace River, Alberta.



Figure 9.14 Example of a small drone aircraft used for photographing surface ice conditions. *(Photo courtesy of A. Wall and S Clark.)*

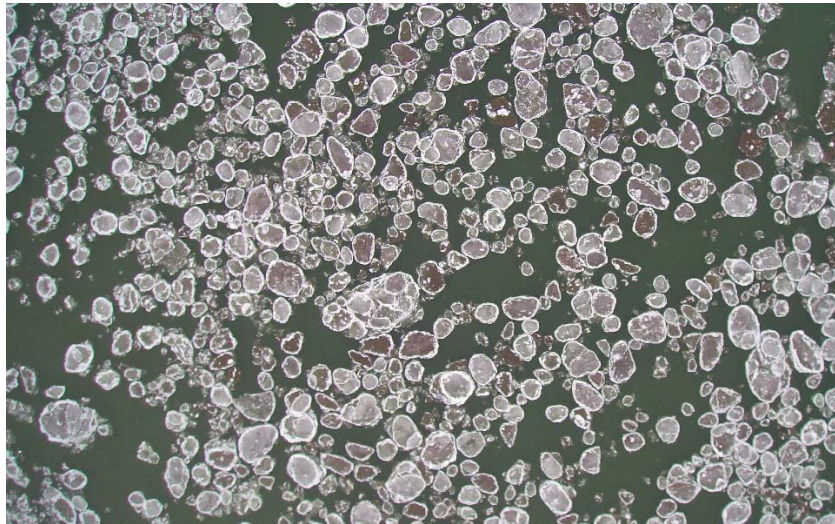


Figure 9.15 Example photo taken with a small drone aircraft. This type of image is very useful for measuring the surface concentration of ice pans. *(Photo courtesy of H. Kalke, V. MacFarlane, and M. Loewen.)*

Winter observations of ice processes typically involve documenting the ice thickness. Although it can be useful to document ice growth over the winter period, this is often not economically feasible for practical

Designing and Implementing a Safe Field Program

applications. Also, ice thickness can be highly variable spatially, and can be dangerous to measure due to the unpredictable nature of river ice covers. For many studies, knowledge of the ice thickness in mid to late winter is sufficient for practical purposes.

Ice thickness is most often measured directly, by drilling a hole in the ice cover, and using a tape measure or rod. The challenge is to locate the bottom of the ice cover; this can be achieved by affixing a weighted rod to the end of the tape measure as shown in Figure 9.15. The end of the rod is connected to a wire, to facilitate slipping it into the hole (*see photo on the left*). Then the wire is released and the tape measure (attached to the center of the rod) is pulled taut against the bottom of the hole (*see photo on the right*).



Figure 9.15 Simple ice thickness measurement apparatus. (Photos by F. Hicks)

Manual ice thickness measurements, though accurate, are time consuming and labor intensive to obtain. Where large areas are to be documented, direct measurements can often be supplemented with data from a ground penetrating radar (GPR). This is a relatively portable device that can be pulled behind a snowmobile (Figure 9.16) or under a helicopter. However, it is best used as an interpolation device (i.e. for documenting ice thickness variations between manual measurements as shown in Figure 9.17), as it requires calibration to local conditions at each new site as results are highly dependent upon the type of ice and amount of impurities and air bubbles within the ice. In many jurisdictions, the use of a GPR to map ice

thickness requires supervision and interpretation by a professional geophysicist.



Figure 9.16 Example application of a GPR device being towed behind a snowmobile. (Photo source: F. Hicks)

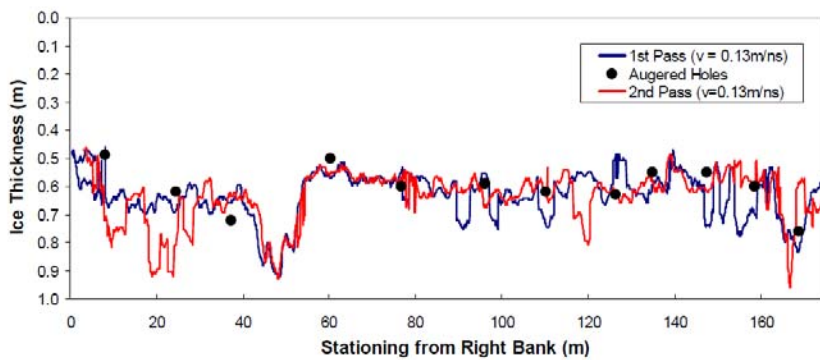


Figure 9.17 Comparison of calibrated GPR data and manual measurements of river ice thickness. (Source: F. Hicks)

As noted earlier, it is always important to document water level profiles for hydraulic model calibration. Once the winter ice cover has formed, it is often useful to measure a top of ice profile; this, together with measured ice thicknesses can facilitate the calibration of the hydraulic model for simple ice covered conditions. At breakup (and sometimes during freeze-up, depending upon the purpose of your investigations), it is also important to measure top of ice jam profiles for hydraulic model

Designing and Implementing a Safe Field Program

calibration. As the ice surface can be quite irregular (Figure 9.18), it is generally desirable to measure the elevation of the top of ice at several points at each site along the study reach. The average of these measurements can then be taken as representative of the top of ice for that particular site. The top of ice can be measured using a conventional rod and level; however, this can be time consuming as each measured level must be tied into a temporary benchmark (TBM) of known elevation. Ice jam profiling can be much more efficiently handled with an instrument such as a RTK GPS. Dow Ambtman and Hicks (2012) provide a detailed explanation of how to measure ice jam profiles and how to use these data to obtain field estimates of discharge during ice jam events.

Ice jams can be highly unstable, being subject to consolidation and/or release. Therefore, it is very important to have appropriate personal protective equipment (e.g. flotation device, helmet, and throw rope) and to ensure that there are observers, both with the person measuring and at points upstream, to watch for any sign of potential ice movements.



Figure 9.18 Measuring the top-of-ice profile along a river ice jam.
(Photo source: F. Hicks.)

In cases where the river banks will be inaccessible during ice jam events, staff gauges can be employed (Figure 9.19). These can be simply

constructed from 2x6" lumber, painted red and white in 0.5 m increments. These are positioned along the bank at overlapping elevations, and must be surveyed in at the time of installation so that the elevation of each mark is known. Once ice jams occur, these staff gauges can be photographed from a helicopter to document the ice elevation at each site.



Figure 9.19 Staff gauges may be used for measuring top-of-ice levels in areas that are inaccessible during ice jam events. (*Photo by F. Hicks.*)

Summary

As for any effective field program it is vitally important to prepare a detailed plan and equipment list well in advance of your field trip. It is also important to test equipment and to rehearse measurements and emergency procedures (outside in the cold) before leaving for the field. This will give you the best indication of how feasible your plans and schedules are. Typically, you can expect it to take at least 3 to 4 times as long to conduct field measurements under winter conditions compared to the time required for similar measurements in summer. It is critical to employ redundancy in all things, as equipment tends to fail or break down much more easily in severe cold. Finally, don't get stressed when things go wrong, as things will definitely go wrong. The key is to recognize that certainty and to plan for it.

List of Variables

a	location specific constant used in Brunt's formula
a_1	site and situation specific coefficient used in calculating ice growth by the Stefan equation approach
a_2	coefficient in the ice jam stability equation
a_i	parameter used in calculation of ice roughness height from velocity profiles ($= V_{max}/(V_{max} - V_i)$)
A	cross-sectional flow area
$ADDF$	accumulated degree-days of freezing
b	location specific constant used in Brunt's formula
b_2	coefficient in the ice jam stability equation
B	width of ice accumulation
c	Bowen's constant (0.6°C^{-1})
c_2	coefficient in the ice jam stability equation
c_i	specific heat of ice
C	cloud cover in tenths
C_f	coefficient in the Mohr-Coulomb relation, representing the cohesion of the ice accumulation
C_o	coefficient in the Mohr-Coulomb relation, normally taken as $(\tan \phi)$
d	frazil particle diameter
e	porosity of an ice jam accumulation
e_a	atmospheric vapor pressure
e_s	saturation vapor pressure
f	friction factor
f_i	friction factor of the underside of an ice jam

f_b	friction factor of the bed
f_o	composite friction factor for the flow under an ice jam
g	acceleration due to gravity
h_{wa}	linear heat transfer coefficient
j_{wa}	linear heat transfer coefficient
k	thermal conductivity of ice
k_i	roughness height of the underside of the ice, or ice accumulation
k_L	constant used in Brunt's formula
k_t	coefficient of lateral thrust
k_{wa}	linear heat transfer constant
k_x	coefficient in the ice jam stability equation
K	thermal diffusivity of ice
K_x	passive pressure coefficient in the ice jam stability equation
n	Manning's resistance coefficient
n_b	Manning's resistance coefficient of the river bed
n_i	Manning's resistance coefficient for the underside of the ice or ice accumulation
n_t	composite (total) Manning's resistance coefficient for an ice covered section
P	channel wetted perimeter
P_a	atmospheric pressure
Q	river discharge
r^2	coefficient of determination in regression analysis
R	hydraulic radius of the channel flow ($= A/P$)
S	river bed slope
S_f	friction slope (slope of the energy grade line)
S_w	water surface slope
t	frazil particle thickness
t_i	ice cover or ice accumulation thickness

List of Variables

T	emitting body's temperature (°K), for longwave radiation emission calculation
T_i	ice temperature
T_a	air temperature
T_m	ice melting point temperature
T_w	water temperature
u	wind velocity measured 2m above the ground surface
V	cross-sectionally averaged flow velocity
V_i	average flow velocity in the ice affected portion of the flow
V_{max}	maximum velocity in a vertical velocity profile
V_m	allowable maximum velocity under an ice jam toe
Y	flow depth
Y_e	maximum flow depth associated with an equilibrium ice jam
Y_i	flow depth for the ice affected portion of the cross-section
x	longitudinal distance coordinate, measured along the river bed
α	albedo of the ice, snow, or water surface
ε	emittance (0.97 for ice, snow and water)
ε_i	roughness height of the underside of the ice or ice accumulation
ϕ	angle of internal friction of an ice jam accumulation
ϕ_E	evaporative heat flux
ϕ_H	net rate of convective heat transfer to the ice (or water)
ϕ_i	rate of heat flux available for ice melting
ϕ_{ia}	heat flux between the ice and the air
ϕ_L	net emitted longwave radiation flux
ϕ_{L-back}	reflected longwave radiation flux
ϕ_{L-out}	emitted longwave radiation flux

ϕ_o	sum of the heat fluxes contributed from other sources (e.g. heat transfer from warm water, precipitation, river bed and banks, and/or groundwater)
ϕ_s	heat flux due to incoming solar radiation
ϕ_{wa}	heat flux between the water and the air
ϕ_{wi}	heat flux between the water and the ice
Φ	ratio of the wetted perimeters of the ice and bed affected portions of the flow
σ_{sb}	Stefan-Boltzmann constant ($5.69 \text{ E } -8 \text{ W/m}^2 \text{ } ^\circ\text{K}^4$)
$\overline{\sigma}_x$	longitudinal stresses in an ice jam accumulation
$\overline{\sigma}_y$	vertical stresses in an ice jam accumulation
τ	shear stress caused by the flow acting on the underside of an ice accumulation
ρ	density of water
ρ_i	density of ice

Cited References²²

- Anderson, E.R. (1954) “Energy budget studies”, Geological Survey Professional Paper 269, United States Government Printing Office, Washington.
- Andres, D.D. (1988) “Observation and prediction of the 1986 breakup on the Athabasca River upstream of Fort McMurray, Alberta”, Alberta Research Council Report No. SWE-88/03.
- Andrishak, R., J. N. Abarca, A. Wojtociwz and F. Hicks (2008) “Freeze-up study on the lower Athabasca River (Alberta, Canada)”, Proc. 19th IAHR Ice Symposium, 1:77-88.
- Andrishak, R. and F. Hicks (2015) “Working safely on river ice”, Proc. 18th CGU-HS CRIPE Workshop on River Ice, 10 pp.
- Ashton, G.D. (1986) River and Lake Ice Engineering, Water Resources Publications, Littleton, CO, 485 pp.
- Ashton, G. (2013) “Chapter 2 – Thermal Processes”, in River Ice Formation, (S. Beltaos, ed.), CGU-HS CRIPE, 19–76.
- Beltaos, S. (1983) “River ice jams: theory, case studies, and applications”, ASCE Journal of Hydraulic Engineering, 109(10):1338-1359.
- Beltaos, S. (editor) (1995) River Ice Jams, Water Resources Publications, Highlands Ranch, Colorado, USA, 372 pp.
- Beltaos, S. (2001) “Hydraulic roughness of breakup ice jams”, ASCE Journal of Hydraulic Engineering, 127(8): 650-656.
- Beltaos (editor) (2009) River Ice Breakup, Water Resources Publications, LLC, 480 pp.

²² In these cited references, the following acronyms are used: CGU-HS CRIPE refers to the Canadian Geophysical Union – Hydrology Section’s Committee on River Ice Processes and the Environment (proceedings available at www.cripe.ca), IAHR refers to the International Association for Hydro-Environment Engineering and Research, and ACSE refers to the American Society of Civil Engineers.

- Beltaos, S. and B. C. Burrell (2005a) “Field measurements of ice-jam-release surges”, *Canadian Journal of Civil Engineering*, 32: 699-711.
- Beltaos, S. and B.C. Burrell (2005b) “Determining ice-jam surge characteristics from measured wave forms”, *Canadian Journal of Civil Engineering*, 32: 687-698.
- Beltaos, S. and A.M. Dean (1981) “Field investigations of a hanging ice dam”, *Proc. 5th IAHR Ice Symposium, II*: 475-488.
- Beltaos, S. and B. G. Krishnappan (1982) “Surges from ice jam release: a case study”, *Canadian Journal of Civil Engineering*, 9: 276-284.
- Beltaos, S. and P. Tang (2013) “Applying HEC-RAS to simulate river ice jams: snags and practical hints”, *Proc. 17th CGU-HS CRIPE Workshop on River Ice*, 10 pp.
- Beltaos, S. and J. Wong (1986) “Downstream transition of river ice jams”, *ASCE Journal of Hydraulic Engineering*, 112(2):91-110.
- Blackburn, J. and F.E. Hicks (2003) “Suitability of dynamic modelling for flood forecasting during ice jam release surge events”, *ASCE Journal of Cold Regions Engineering*, 17(1): 18-36.
- Bolz, S.H. (1949) “The dependence of the infrared counter-radiation on cloud mass” (in German), *Zeitschrift fuer Meteorologie*, 3:201-203.
- Brunt, D. (1934) Physical and Dynamical Meteorology, Cambridge University Press, UK.
- Carey, K.L. (1966) “Observed configuration and computed roughness of the underside of river ice, St. Croix River, Wisconsin”, *Geological Survey Research, U.S. Geological Survey Prof. Paper 550-B*, B192-B198.
- Carson, R., D. Healy, S. Beltaos, and J. Groeneveld (2003) “Tests of river ice jam models – phase 2”, *Proc. 12th CGU-HS CRIPE Workshop on River Ice*, 15 pp.
- Clark, S. (2013) “Chapter 3 - Border and Skim Ice”, in River Ice Formation, (S. Beltaos, ed.), CGU-HS CRIPE, Edmonton, Alberta, 77–106.
- Clark, S. and J.C. Doering (2004) “A laboratory study of frazil ice size distributions”, in: *Proc. 17th IAHR Ice Symposium*, 291–297.

- Clark, S. and J. Doering (2006) “Laboratory experiments on frazil-size characteristics in a counterrotating flume”, *ASCE Journal of Hydraulic Engineering*, 132(1): 94–101.
- Daly, S. F. and S.C. Colbeck (1986) “Frazil ice measurements in CRREL’s flume facility”, *Proc. 8th IAHR Ice Symposium*, 427–438.
- Daly, S., J. Zufelt, P. Fitzgerald, A. Gelvin, and S. Newman (2010) “Aufeis formation in Jarvis Creek and flood mitigation”, Letter report to the USARAK, Fairbanks, AK. ERDC/CRREL Report.
- Daly, S. (2013a) “Chapter 4 - Frazil Ice”, in River Ice Formation, (S. Beltaos, ed.), CGU-HS CRIPE, Edmonton, Alberta, 107–134.
- Daly, S. (2013b) “Chapter 6 - Aufeis”, in River Ice Formation, Beltaos, (S. Beltaos, ed.), CGU-HS CRIPE, Edmonton, Alberta, 159–180.
- Dickenson, M.C. and N.S. Osbourne (1915) *Bulletin of the Bureau of Standards*, 12: 49-81.
- Doering, J.C. and M.P. Morris (2003) “A digital image processing system to characterize frazil ice”, *Canadian Journal of Civil Engineering*, 30: 1–10.
- Dow Ambtman, K., F. Hicks and P. Steffler (2011a) “Experimental investigation of the pressure distribution beneath a floating ice block”, *ASCE Journal of Hydraulic Engineering*, 137(4): 399-411.
- Dow Ambtman, K., P. Steffler and F. Hicks (2011b) “Analysis of the stability of floating ice blocks”, *ASCE Journal of Hydraulic Engineering*, 137(4): 412-422.
- Dow Ambtman, K. and F. Hicks (2012) “Field estimates of discharge associated with ice jam formation and release events”, *Journal of the Canadian Water Resources Association, North American Stream Hydrographers' Special Issue*, 37(1) 37-46.
- Dunne, T. and Leopold, L.B. (1978) Water in Environmental Planning, WH Freeman, San Francisco.
- Ettema, R., M.F. Karim and J.F. Kennedy (1984) “Laboratory experiments on frazil ice growth in supercooled water”, *Cold Regions Science and Technology*, 10(1): 43-58.
- Flato, G.M. and R. Gerard (1986) “Calculation of ice jam profiles”, *Proc. 4th CGU-HS CRIPE Workshop River Ice*, Paper C-3.

- Gauthier, Y., T.B., M.J. Ouarda, M. Bernier and A. El Battay (2001) “Monitoring ice cover evolution of a medium size river from RADARSAT-1: preliminary results”, Proc. 11th CGU-HS CRIPE Workshop River Ice, 11 pp.
- Gerard, R. and E.W. Karpuk (1979) “Probability analysis of historical flood data”, ASCE Journal of Hydraulic Engineering, 105(9): 1153-1165.
- Gherboudj, I.A., M. Bernier, F. Hicks, and R. Leconte (2007) “Physical characterization of air inclusions in river ice”, Cold Regions Science and Technology, 49(3): 179-194.
- Ghobrial, T. R., M.R. Loewen and F.E. Hicks (2012) “Laboratory calibration of upward looking sonars for measuring suspended frazil ice concentration”, Cold Regions Science and Technology, (70): 19-31.
- Ghobrial, T. R., M.R. Loewen and F.E. Hicks (2013a) “Continuous monitoring of river surface ice during freeze-up using upward looking sonar”, Cold Regions Science and Technology, 86: 69–85.
- Ghobrial, T. R., M.R. Loewen, and F.E. Hicks (2013b) “Characterizing suspended frazil ice in rivers using upward looking sonars”, Cold Regions Science and Technology, 86: 113–126.
- Gosink, J. P. and T. E. Osterkamp (1983) “Measurements and analyses of velocity profiles and frazil ice-crystal rise velocities during periods of frazil-ice formation in rivers”, Annals of Glaciology, 79–84.
- Gray, D. M. (editor) (1970) Principles of Hydrology, Secretariat, Canadian National Committee for the International Hydrologic Decade.
- Hancu, S. (1967) “Modelarea hidraulica in curenti de aer sub presiune”, (in Romanian), Editura Academiei Republicii Socialiste Romania.
- Hanjalic, K. and B.E. Launder (1972) “Fully developed asymmetric flow in a plane channel”, Fluid Mechanics, 51(2): 301-335.
- Healy, D. and Hicks, F. (1997) “A Comparison of the ICEJAM and RIVJAM Ice Jam Profile Models”, Water Resources Engineering Report No. 97-H1, Department of Civil and Environmental Engineering, University of Alberta, Edmonton, 182 pp.

- Healy, D. and F. Hicks (1999a) “An assessment of the applicability of steady flow ice jam profile models”, Proc. 10th CGU-HS CRIPE Workshop on River Ice, 185-195.
- Healy, D. and F. Hicks (1999b) “A comparison of the ICEJAM and RIVJAM ice jam profile models”, ASCE Journal of Cold Regions Engineering, 13(4): 180-198.
- Healy, D. and F. Hicks (2001) “Experimental study of ice jam formation” Proc. 11th CGU-HS CRIPE Workshop on River Ice, 126-144.
- Healy, D. and F. Hicks (2004) “Index velocity methods for winter discharge measurement”, Canadian Journal of Civil Engineering, 31:407-419.
- Henderson (1966) Open Channel Flow, MacMillan Publishing Co. Inc., NY, 522 pp.
- Henderson and R. Gerard (1981) “Flood waves caused by ice jam formation and failure”, Proc. 5th IAHR Ice Symposium, 1: 277-287.
- Hicks, F.E., X. Chen, and D. Andres (1995) “Effects of ice on the hydraulics of the Mackenzie River at the Outlet of Great Slave Lake, NWT: A Case Study”, Canadian Journal of Civil Engineering, 22(1): 43-54.
- Hicks, F. and P. Steffler (1996) *a discussion of* “Estimation of Mean Flow Velocity in Ice-Covered Channels”, by M. Teal and R. Ettema (Vol. 120, No. 12, pp.1385-1400), ASCE Journal of Hydraulic Engineering, 122(8): 475-476.
- Hicks, F.E., X. Chen, and D. Andres (1997a) “Modeling thermal breakup on the Mackenzie River at the outlet of Great Slave Lake, NWT”, Canadian Journal of Civil Engineering, 24: 570-585.
- Hicks, F., K. McKay and S. Shabayek (1997b) “Modelling an ice jam release surge on the St. John River, New Brunswick”, Proc. 9th CGU-HS CRIPE Workshop on River Ice, 303-314.
- Hicks, F. and D. Healy (2003) “Determining winter discharge based on hydraulic modeling”, Canadian Journal of Civil Engineering, 30(1): 101–112.
- Hicks, F., W. Cui and G. Ashton (2009) “Chapter 4 - Heat Transfer and Ice Cover Decay”, in River Ice Breakup (S. Beltaos, ed.), Water Resources Publications, LLC, 480 pp.

- Hutchison (nee Kowalczyk), T. and F. Hicks, (2007) “Observations of ice jam release events on the Athabasca River, AB”, *Canadian Journal of Civil Engineering*, 34(4): 473-484.
- Jasek, M. (1996) “Breakup on the Porcupine River, Yukon Territory”, *Proc. Hydro-Ecology Workshop, NHRI Symposium No. 16*, 95-113.
- Jasek M.J. (1998) “1998 break-up and flood on the Yukon River at Dawson – Did El Nino and climate change play a role?” *Proc. 14th IAHR Ice Symposium*, 2: 761-768.
- Jasek, M. (1999) “Analysis of ice jam surge and ice velocity data”, *Proc. of the 10th CGU-HS CRIPE Workshop on River Ice*, 174-184.
- Jasek, M. (2003) “Ice jam release surges, ice runs, and breaking fronts; field measurements, physical descriptions, and research needs”, *Canadian Journal of Civil Engineering*, 30: 951-953, plus discussion by S. Beltaos (2003 – 30: 949-950) and response by author (2003 – 30: 951-953).
- Jasek, M., F. Weber and J. Hurley (2003) “Ice thickness and roughness analysis on the Peace River using RADARSAT-1 SAR imagery”, *Proc. 12th CGU-HS CRIPE Workshop on River Ice*, 19 pp.
- Jasek, M., J. Marko, D. Fissel, M. Clarke, J. Buermans and K. Paslawski (2005) “Instrument for detecting freeze-up, mid-winter and break-up ice processes in rivers”, *Proc. 13th CGU-HS CRIPE Workshop on River Ice*, 151-183.
- Jasek, M. and J. Marko (2007) “Instrument for detecting suspended and surface ice runs in rivers”, *Proc. 14th CGU-HS CRIPE Workshop on River Ice*, 151-183.
- Jasek, M. and S. Beltaos (2009) “Chapter 8 – Ice-jam release: javes, ice runs and breaking fronts”, in River Ice Breakup (S. Beltaos, ed.), Water Resources Publications, LLC, 247-304.
- Kane, D. (1981) “Physical mechanics of aufeis growth”, *Canadian Geotechnical Journal* 8(2):186–195.
- Kempema E.W., E. Reimnitz, and P.W. Barnes (2001) “Anchor-ice formation and ice rafting in southwestern Lake Michigan, USA”, *Sedimentary Research* 71: 346-354.
- Kempema, E.W. and S.K. Konrad (2004) “Anchor ice and water exchange in the hyporheic zone”, *Proc. 17th IAHR Ice Symposium*, 251 – 257.

- Kempema, E.W., R. Ettema and B. McGee (2008a) “Insights from anchor ice formation in the Laramie River, Wyoming”, Proc. 19th IAHR Ice Symposium, Vol. 1: 113-126.
- Kempema, E.W., S. Daly and R. Ettema (2008b) “Fish protection, wedge-wire intake screens, and frazil ice”, Proc. 19th IAHR Ice Symposium, Vol. 1: 63-76.
- Kempema, E.W. and R. Ettema (2009) “Variations in anchor-ice crystal morphology related to river flow characteristics”, Proc. 15th CGU-HS CRIPE Workshop on River Ice, 159 – 168.
- Kempema, E.W. and R. Ettema, (2011) “Anchor ice rafting: observations from the Laramie River”, River Research and Applications 27: 1126-1135.
- Kempema, E.W., J.M. Shaha and A.J. Eisinger (2002) “Anchor-ice rafting of coarse sediment: observations from the Laramie River, Wyoming, USA”, Proc. 16th IAHR Ice Symposium, Vol. 1: 27-33.
- Lal, A.M.W. and H.T. Shen (1989) “A mathematical model for river ice processes (RICE)”, Report No. 89-4, Department of Civil and Environmental Engineering, Clarkson University, Potsdam, New York, 164 pp.
- Larsen, P.A. (1969) “Head losses caused by an ice cover on open channels”, Journal Boston Society of Civil Engineers, 56(1): 45-67.
- Leconte, R. and P.D. Klassen (1991) “Lake and river ice investigations in northern Manitoba using airborne SAR imagery”, Arctic, 44 (Supp.1): 153-163.
- Lever, J., S. Daly, J. R. and D. Furey (1992) “A frazil ice concentration meter”, Proc. of the 11th IAHR Ice Symposium, 1362-1376.
- Liu, L. and H.T. Shen (2004) “Dynamics of ice jam release surges”, Proc. of the 17th IAHR Ice Symposium, 244–250.
- Mahabir, C., F. Hicks, and A. Robinson Fayek (2007) “Transferability of a neuro-fuzzy river ice jam flood forecasting model”, Cold Regions Science and Technology, 48(3): 188-201.
- Mahabir, C., F. Hicks, and A. Robinson Fayek (2006) “Neuro-fuzzy river ice breakup forecasting system”, Cold Regions Science and Technology, 46(2): 100-112.

- Malenchak, J. and S. Clark (2013) “Chapter 5 – Anchor Ice”, in River Ice Formation, Beltaos, (S. Beltaos, ed.), CGU-HS CRIPE, Edmonton, Alberta, 135-158.
- McFarlane, V., M. Loewen and F. Hicks (2012) “Laboratory experiments to determine frazil properties”, Proc. of Canadian Society for Civil Engineering Annual Conference, Edmonton, AB, 10 pp.
- McFarlane, V., M. Loewen and F. Hicks (2014) “Laboratory measurements of the rise velocity of frazil ice particles”, Cold Regions Science and Technology 106-107: 120-130.
- McFarlane, V., M. Loewen, and F. Hicks (2015a) “Measurements of the evolution of frazil particle size distributions”, Journal of Cold Regions Science and Technology, 120, 45–55.
- McFarlane, V., M. Loewen, F. Hicks, F (2015b) “Field measurements of the size distribution of frazil ice particles”, Proceedings of the 18th CGU-HS CRIPE Workshop on River Ice, Quebec City, QC, Canada, 18 pp.
- Marko, J.R. and M. Jasek (2010a) “Sonar detection and measurements of ice in a freezing river I: methods and data characteristics”, Cold Regions Science and Technology, 63, 121-134.
- Marko, J.R. and M. Jasek (2010b) “Sonar detection and measurement of ice in a freezing river II: observations and results on frazil ice”, Cold Regions Science and Technology, 63, 135-153.
- Michel, B. (1971) “Winter regime of rivers and lakes”, US Army Cold Regions Research and Engineering Laboratory, Hanover, NH, Monograph III-B1a.
- Michel, B. (1978) Ice Mechanics, Les presses de l’Université Laval, Québec City, 499 pp.
- Michel, B. and M Drouin (1981) “Courbes de remous sous les couverts de glace de La Grande Riviere”, Canadian Journal of Civil Engineering, 8(3): 351-363.
- Morse, B., M. Hessami and C. Bourel (2003) “Characteristics of ice in the St. Lawrence River”, Canadian Journal of Civil Engineering, 30: 766-774.
- Morse, B. and K. Hamai and Y. Choquette (2005) “River discharge measurement using the velocity index method”, Proc. 13th CGU-HS CRIPE Workshop on River Ice, 159-168.

- Morse, B. and M. Richard (2009) "A field study of suspended frazil ice particles", *Cold Regions Science and Technology*, 55(1): 86-102.
- Nafziger, J., F. Hicks, P. Thoms, V. McFarlane, J. Banack, and R. Cunjak (2013) "Measuring supercooling prevalence on small regulated and unregulated streams in New Brunswick and Newfoundland, Canada", *Proc. 17th CGU-HS CRIPE Workshop on River Ice*, 23 pp.
- Newbury, R.W. (1968) Nelson River: A study of subarctic river processes, Ph.D. thesis, Johns Hopkins University, Baltimore, Maryland.
- Nezhikhovskiy, R.A. (1964) "Coefficients of roughness of bottom surface on slush-ice cover", *Soviet Hydrology*, Washington, American Geophysical Union, 127-150.
- Osterkamp, T.E. (1978) "Frazil ice formation", *ASCE Journal of Hydraulic Engineering*, 104(9): 1239-1255.
- Pariset, E., R. Hausser and A. Gagon (1966) "Formation of ice covers and ice jams in rivers", *ASCE Journal of Hydraulic Engineering*, 92(6): 1-23.
- Pelletier, K., F. Hicks, J. van der Sanden and Y. Du (2003) "Monitoring breakup development on the Athabasca River using RADARSAT-1 SAR imagery", *Proc. 12th CGU-HS CRIPE Workshop on River Ice*, 27 pp.
- Ponce, V.M. (1989) Engineering Hydrology, Prentice Hall, NJ, 640 pp.
- Richard, M., B. Morse, S.F. Daly and J. Emond (2010) "Quantifying suspended frazil ice using multi-frequency underwater acoustic devices", *River Research and Applications*, 27(9): 1106-1117.
- Rimsha, V.A. and R.V. Donchenko (1957) "The investigation of heat loss from free water surfaces in wintertime" (in Russian), *Trudy Lennigrad Gosud.Gidrol. Inst.*, 65: 58-83.
- Robert, S. (1979) Contribution to the study of nucleation in frazil (in French), M.S.A. thesis, Laval University, Quebec City.
- Robichaud, C. (2003) "Hydrometeorological factors influencing breakup ice jam occurrence at Fort McMurray, Alberta", MSc thesis, Dept. of Civil and Env. Engineering, Univ. of Alberta, Edmonton, 281 pp.
- She, Y., F. Hicks, P. Steffler, and D. Healy (2009a) "Constitutive model for internal resistance of moving ice accumulations and Eulerian

- implementation for river ice jam formation”, *Cold Regions Science and Technology*, 55: 286-294.
- She, Y., R. Andrishak, F. Hicks, B. Morse, E. Stander, C. Krath, D. Keller, N. Abarca, S. Nolin, F.N. Tanekou, C. Mahabir, (2009b) “Athabasca River ice jam formation and release events in 2006 and 2007”, *Cold Regions Science and Technology* 55: 249-261.
- She, Y., F. Hicks, P. Steffler, and D. Healy (2008) “Effects of unsteadiness and ice motion on river ice jam profiles”, *Proc. 19th IAHR Ice Symposium*, 1: 327-338.
- She, Y. and F. Hicks (2006) “Modeling ice jam release waves with consideration for ice effects”, *Cold Regions Science and Technology*, 45:137-147.
- She, Y. and F. Hicks (2005) “Incorporating ice effects in ice jam release surge models”, *Proc. 13th CGU-HS CRIPE Workshop on River Ice*, 470-484.
- Shen, H.T., J. Su, and L. Liu (2000) “SPH simulation of river ice dynamics”, *Computational Physics* 165: 752-770.
- Shen, H.T., Y.C. Chen, A. Wake, and R.D. Crissman (1993) “Lagrangian discrete parcel simulation of river ice dynamics”, *International Journal of Offshore and Polar Engineering*, 3 (4), 328-332.
- Stickler, M. and K.T. Alfredsen (2005) “Factors controlling anchor ice formation in two Norwegian rivers”, *Proc. 13th CGU-HS CRIPE Workshop on River Ice*, 14 pp.
- Stickler, M. and K.T. Alfredsen (2009) “Anchor ice formation in streams: a field study”, *Hydrologic Processes*, 23: 2307-2315.
- Tracy, B.T. and S.F. Daly (2003) “River ice delineation with RADARSAT SAR”, *Proc. 12th CGU-HS CRIPE Workshop on River Ice*, 11 pp.
- Tsang, G. (1982) Frazil and anchor ice: A monograph. National Research Council of Canada, Subcommittee on Hydraulics of Ice Covered Rivers, Ottawa, 90 pp.
- Tsang, G. (1984) “Concentration of frazil in flowing water as measured in laboratory and in the field”, *Proc. 7th IAHR Ice Symposium*, Vol. III: 99-869.
- Tsang, G. (1985) “An instrument for measuring frazil concentration”, *Cold Regions Science and Technology*, 10(3): 235-249.

- Tsang, G. (1986) "Preliminary report on field study at Lachine Rapids of cooling of river and formation of frazil and anchor ice", Proc. 4th CGU-HS CRIPE Workshop on River Ice, F5.1-5.51.
- Turcotte, B and B. Morse (2013) "A global river ice classification model", Journal of Hydrology, 507:134-148.
- Tuthill, A.M. and J. H. Lever (2006) "Design of breakup ice control structures", U.S. Army Cold Regions Research and Engineering Laboratory, Hanover, NH, CRREL Technical Report TR-06-7.
- Tuthill, A.M. (2005) "Breakup ice control structures: performance review", U.S. Army Cold Regions Research and Engineering Laboratory, Hanover, NH, ERCD/CRREL TN-05-5.
- Tuthill, A.M. (1995) "Structural ice control: Review of existing methods", U.S. Army Cold Regions Research and Engineering Laboratory, Hanover, NH, CRREL Special Report SR 95-18.
- Unterschultz K., J. van der Sanden and F. Hicks (2009) "Potential of RADARSAT-1 for the monitoring of river ice: results of a case study on the Athabasca River at Fort McMurray, Canada", Cold Regions Science and Technology, 55: 238-248.
- U.S. Army Corps of Engineers (USACE) (1959) "Snow Hydrology", North Pacific Region, Portland Oregon, 437 pp.
- U.S. Army Corps of Engineers (2010) "HEC-RAS River Analysis System – Hydraulic Reference Manual", HEC report CPD-69, 417 pp.
- Uzuner, M.S. (1975) "The composite roughness of ice covered streams", Journal of Hydraulic Research, 13(1): 79-102.
- Uzuner, M.S. and J.F. Kennedy (1976) "Theoretical model of river ice jams", ASCE Journal of Hydraulic Engineering, 102(9): 1365-1383.
- van der Sanden, J.J. and H. Drouin (2011) "Satellite SAR observations of river ice cover: a RADARSAT-2 (C-band) and ALOS PALSAR (L-band) comparison", Proc. 16th CGU-HS CRIPE Workshop on River Ice, 11 pp.
- Watson, D., F. Hicks, F., and R. Andrishak (2009) "Analysis of observed 2008 ice jam release events on the Hay River, NWT." Proc. 15th CGU-HS CRIPE Workshop on River Ice, 303-316.

- Weber, F., D. Nixon, and J. Hurley (2001) "Identification of river ice types on the Peace River using RADARSAT-1 imagery", Proc. 11th CGU-HS CRIPE Workshop on River Ice, 17 pp.
- White, K.D. (2003) "Review of prediction methods for breakup ice jams", Canadian Journal of Civil Engineering 30, 89-100.
- Wunderlich, W.O. (1972) "Heat and mass transfer between a water surface and the atmosphere", Tennessee Valley Authority Engineering Laboratory, Norris, Tenn., Report No. 14.
- Yankielun, N. and J. Gagnon (1999) "Laboratory tests of a time-domain reflectometry system for frazil ice detection", Canadian Journal of Civil Engineering, 26: 168-176.
- Zhao, L., F. Hicks and A. Robinson Fayek (2009) "Long lead forecasting of peak flow during breakup using fuzzy logic", Proc. 15th CGU-HS CRIPE Workshop on River Ice, 287-302.

INDEX

- acoustic Doppler velocity meter
 - ADV, 126
- active frazil, 8
- air bubbles and impurities, 55
- albedo, 36, 76
- anchor ice, 13
- anchor ice release, 17
- angle of internal friction, 92, 145
- aspect ratio, 60
- aufeis, 25
- bed roughness, 66
- border ice, 4
- Bowen's ratio, 79
- breakup, 35
- bridging, 19
- buttering, 12
- candled ice, 38
- cloud cover, 77
- coefficient of lateral thrust, 93
- cohesion, 93
- columnar ice, 24
- composite roughness, 63
- condensation, 78
- conduction, 80
- consolidation
 - consolidate, 46
- convective heat transfer, 79
- culvert icing, 28
- current meter, 127
- Dalton's Law, 78
- dam break, 104
- degree-day approach, 82
- degree-days of thaw. *See*
 - degree-day approach
- dikes, 116
- discontinuous ice cover, 71
- dynamic breakup, 38
- Effects of Streamflow
 - Regulation, 32
- emittance, 77, 145
- energy budget, 74
- equilibrium ice jam, 98
- equilibrium ice jam analysis, 99
- estimating ice growth, 83
- evaporation, 78
- explosives, 120
- floating ice jam, 89
- flood forecasting, 109
- flood proofing, 109
- flood risk zon, 108
- floodplain management, 108
- floodwalls, 116
- Frazil discs, 51
- frazil ice, 5
- Frazil pan thickness, 53
- frazil pans, 9
- frazil rafts, 11
- Frazil rise velocity, 53
- frazil slush porosity, 54
- frazil transport, 73
- freeboard, 116
- freeze-up, 3
- freezing degree-days. *See*
 - degree-day approach
- frontal progression, 21
- Geographic Information Systems
 - GIS, 135
- granular ice, 29
- ground penetrating radar
 - GPR, 138
- grounded ice jams, 89
- Grounding. *See* grounded ice jams
- hanging ice dam, 28
- head of ice jam, 91
- heat flux, 74
- heat transfer coefficient, 81
- hinge cracks, 39
- hummocky ice cover, 22
- hydraulic radius, 62, 144

hydraulic thickening, 20
hydro-peaking, 33
ice boom, 117
Ice clearing, 44
ice control structure, 117
ice control structures, 117
ice cutting, breaking, and
 blasting, 112
ice dams, 15
ice discharge capacity, 117
ice disks, 29
Ice Jam, 44
ice jam classification, 87
ice jam floods, 87
ice jam porosity, 93, 143
ice jam release, 100
Ice jam release, 46
ice jam release wave, 46
ice jam roughness, 69
ice profiling sonar, 133
ice roughness from velocity
 profiles, 66
ice runs, 105
Ice runs, 46
ice thickness, 137
icing. *See* aufeis
impeded ice jam release, 102
index-velocity method, 130
isoline of maximum velocity, 63
isothermal, 74
jam stability equation, 92
jave, 104. *See* ice jam release
 wave
juxtaposed ice cover, 20
latent heat of melting, 58
linear heat transfer approach, 80
logarithmic velocity
 distribution, 67
longwave radiation, 77
Manning's equation, 62
marble ice. *See* granular ice
mass transfer method, 78
measuring water level, 125
mechanical removal of ice, 119
mini-jam, 44
Mohr-Coulomb theory, 91
naled. *See* aufeis
open leads, 36
Overflow, 39
partial ice cover, 71
passive pressure coefficient, 92
phreatic surface, 62
polycrystalline, 55
rating curve, 129
reactive flood mitigation, 119
Relative density of ice, 57
remnant ice, 47
ridging, 42
ripples, 69
rubble breaking front, 102
satellite radar, 135
sediment rafting, 17
seed crystals, 6
seepage flow, 93
shear stress on the ice
 underside, 93, 146
shear wall, 47
shearing interface, 47
sheet breaking front, 102
sheet ice accumulation, 43
shorefast ice. *See* border ice
simple ice cover, 61
skim ice, 4
snow ice, 23
snow water equivalent, 123
snowmelt, 36, 49, 111
solar radiation, 75
specific heat of ice, 58
staff gauges, 140
stage-fall analysis, 129
Stefan equation, 83
streamflow measurement, 126
structural flood mitigation, 116
sunshine ball, 124

supercooling, 6
surface ice treatment, 113
surface ice velocity, 130
suspended concentrations of
 frazil ice, 51
SWE. *See* snow water
 equivalent
thalweg, 36
thawing degree-days. *See*
 degree-day approach
thermal breakup, 35
thermal conductivity of ice, 58
thermal diffusivity of ice, 59
thermal properties of river ice,
 50
thin sections, 24
time-lapse camera, 133
top of ice profile, 139
transverse cracks, 41
two-point measurement, 127
unimpeded ice jam release, 101
valley shading effects, 81
velocity distribution, 61
viscous-plastic constitutive
 models, 92
water temperature
 measurement, 131
wave peak attenuation, 105
zero shear interface, 63

ABOUT THE AUTHOR – FAYE HICKS, PhD



Dr. Hicks is a retired civil engineering researcher and educator with more than 30 years' experience in river engineering. For 26 years her research focused on advancing knowledge in river ice processes and hydraulics, through experimental, numerical and field studies. Together with her research colleagues and her superb graduate students, Dr. Hicks has conducted innovative and unprecedented studies investigating the dynamic aspects of river ice jam formation and release, frazil ice properties, ice cover stability, and the effects of streamflow regulation on river ice. Dr. Hicks is also the co-creator of the public domain *RiverID* hydraulics and ice process model.

In 2008 Dr. Hicks was awarded the Camille A. Dagenais Award from the *Canadian Society for Civil Engineering*, for outstanding contributions in hydrotechnical engineering. She has been awarded the *Canadian Geophysical Union - Committee on River Ice Processes and the Environment's* Gerard Medal five times and, in 2013, she was awarded their Michel Medal for outstanding and sustained contributions to the advancement of river ice science and engineering in Canada. Dr. Hicks was also awarded the Can-Am Civil Engineering Amity Award by the *American Society of Civil Engineers* in 2015.

Dr. Hicks also provides technical writing advice to university and college students through her academic blog: thesisstips.wordpress.com.